Title
Engineered nanomaterials for water treatment

ISBN
9780128224236

Authors
Han, Z
Adeleye, AS
Keller, AA

Publication Date
2023

DOI
10.1016/B978-0-12-822425-0.00041-5

00041 Nanomaterials for water treatment

Ziwei Han, and Adeyemi S Adeleye, Department of Civil and Environmental Engineering, University of California, Irvine, CA, United States

Arturo A Keller, Bren School of Environmental Science & Management, University of California, Santa Barbara, CA, United States and University of California Center for Environmental Implications of Nanotechnology, University of California, Santa Barbara, CA, United States

Abstract

The pressing need for advanced yet cost-effective water treatment has led to the development of a wide range of engineered nanomaterials (ENMs), from carbon-based to metal and metal oxide nanomaterials, and including novel structures such as metal oxide frameworks (MOFs) and covalent organic frameworks (COFs). ENMs have been developed to treat conventional water pollutants as well as emerging contaminants, and address new challenges. In this article we provide an overview of the current literature on a wide range of ENMs as well as several major classes of water contaminants.

Key Points

At the end of this article, readers should understand that:

- Nanomaterials can effectively treat many legacy and emerging water contaminants.
- Adsorption and/or degradation of contaminants are the main treatment mechanisms.
- Novel nanohybrids and nanocomposites can be tailored to enhance specificity and removal of contaminants.
- The largest barrier to general commercialization is cost of nanomaterials vs. conventional technology.

Introduction

Water is one of the most important resources for the survival and health of human and other organisms. However, according to a World Health Organization (WHO) report, about 29% (2.2 billion) of the world population lacked drinking water with adequate sanitation in 2017 (**World Health Organization, 2019**). The demand for clean water is rising with global population growth and increasing effects of environmental issues, such as drought, increasing temperatures, changing precipitation patterns, and water pollution (**Dos Santos *et al*., 2017**; **Mekonnen and Hoekstra, 2016**; **Vörösmarty *et al*., 2000**). Ecological stress is also increasing, as we divert more water for human consumption and impact water quality. Therefore, innovative water treatment is a necessity to address the scarcity of water resources and improve water quality (Mekonnen and Hoekstra, 2016; Kallis, 2010).

In wastewater treatment plants (WWTPs), most suspended solids and biodegradable organic matter can be removed by conventional technologies such as clarification and biological technologies (Sonune and Ghate, 2004; Daud *et al*., 2015; Sustarsic, 2009). However, WWTPs face several challenges, which threaten the possibility of direct and even indirect water reuse. First, there are emerging contaminants (such as pharmaceuticals and personal care products [PPCPs], flame retardants, and per- and polyfluoroalkyl substances [PFAS]) that cannot be effectively removed by traditional wastewater treatment technologies, (Radjenović *et al*., 2009; Radjenovic *et al*., 2007; Kim *et al*., 2020; Houtz *et al*., 2018) and the relevant health-based regulations are becoming more stringent (Zuo *et al*., 2014; Roberson, 2011). Second, a mixed waste stream from industrial, commercial, and residential activities increases the complexity of wastewater composition and the difficulty of wastewater treatment (Nödler and Scheurer, 2019; Xu *et al*., 2019). Additionally, remote and developing regions where decentralized wastewater treatment is commonly applied have increasingly higher requirements for affordability and reliability of treatment technologies (Boller, 1997; Qu *et al*., 2019). To achieve higher water quality from WWTPs, the effluent is usually purified with further treatment technologies, such as advanced oxidation process (AOP), (Monteoliva-García *et al*., 2020; Qin *et al*., 2015; Ahmed *et al*., 2020; Banks *et al*., 2020; Nzeribe *et al*., 2019) and reverse osmosis (RO), (Mastropietro *et al*., 2021; Abejón *et al*., 2015; Sahebi *et al*., 2020). However, these technologies have high operation and maintenance costs, high energy consumption, and poor selectivity, making them difficult to promote in smaller communities and developing countries (Ahmed *et al*., 2020; Mastropietro *et al*., 2021; Abejón *et al*., 2015; Brienza and Katsoyiannis, 2017; Kanakaraju *et al*., 2018).

Nanomaterials, with a size of 1–100 nm in at least one dimension, (**Ikhmayies, 2014**) have been applied in laboratory- or pilot-scale studies for environmental remediation (**Adeleye *et al*., 2016a**). The extremely small size of nanomaterials results in unique properties compared to larger-sized materials with a similar composition (Lin *et al*., 2008; Rahmani *et al*., 2011; Stanley-Wood and Lines, 2007). Nanomaterials have a much larger surface area that can contact more contaminants, leading to a higher adsorption or degradation capacity (Shaji and Zachariah, 2017; Virkutyte and Varma, 2014). Also, the increase of binding sites on the nanomaterial surface results in higher reactivity and, in some cases, can be used for water disinfection (Jiang *et al*., 2008; Huo *et al*., 2020; Zeng *et al*., 2017). Thus, with high surface area and reactivity, nanomaterials are considered a prospective technology to improve water quality (**Adeleye *et al*., 2016a**).

This article will introduce several different types of nanomaterials, as well as their latest applications in water treatment, including the removal of different types of pollutants and the mechanisms of remediation. Additionally, this article will discuss the outlook of

nanomaterials in water remediation, in addition to discussing a few case studies that capture the application of nanotechnology in water treatment.

Classification of Nanomaterials Used for Water Treatment

Carbonaceous Nanomaterials

Carbonaceous engineered nanomaterials (C-ENMs) are mainly composed of carbon atoms. Common C-ENMs include carbon nanotubes (CNTs), (Wang *et al*., 2019; Kumar *et al*., 2014; Onyancha *et al*., 2021) graphene and graphene-based materials, (Wang *et al*., 2013; Pan *et al*., 2020; Goodwin *et al*., 2018) graphene oxide (GO), (Wang *et al*., 2019; Pan *et al*., 2020; Pendolino and Armata, 2017) fullerene, (**Regulska *et al*., 2019**) and carbon nanofibers (Ding *et al*., 2018; Painuli *et al*., 2021). These materials have sp^2 or sp^3 (in GO or fullerene) hybrid carbon bonds and excellent physicochemical properties at the nanoscale (Goodwin *et al*., 2018; Shan *et al*., 2017). The large surface area and irregular morphology exhibited by C-ENMs provide a large number of binding sites for pollutants (**Abd-Elhamid *et al*., 2019**). Some C-ENMs, such as fullerene, have a closed cage structure that can capture contaminants (Shan *et al*., 2017; Kuganathan *et al*., 2019). In addition, the wide distribution of sp^2 hybrid carbon bonds results in high electron transport, which can increase reaction rates and efficiency (Ikram *et al*., 2020; Fan *et al*., 2012). Further modification of C-ENMs with different functional groups can take advantage of hydrophobic or electrostatic effects to improve the selectivity of specific pollutants (Chen *et al*., 2009; Ali *et al*., 2019b; Ma *et al*., 2017; Barrejón *et al*., 2019). Thus, C-ENMs and are widely considered for water purification based on mechanisms such as adsorption, (Liu *et al*., 2020a; Zhou *et al*., 2015; Lal *et al*., 2020; Huang *et al*., 2018b) filtration, (Matharu *et al*., 2020; Cheng *et al*., 2019b; Wang *et al*., 2016c) and transformation (Huang *et al*., 2018b; Yang *et al*., 2019b). More information about the classes, mechanisms, and applications of C-ENMs have been summarized in several reviews (Shan *et al*., 2017; Oyekunle *et al*., 2021; Nasrollahzadeh *et al*., 2021).

Metals and Metal Oxides

Metals and metal oxides (Me/MeO) are a class of nanomaterials composed of single or multiple metals and/or their oxides. Several nanomaterials, such as pristine and modified nanoscale zero-valent iron (nZVI), (Wang *et al*., 2016a; Černíková *et al*., 2020; Liu *et al*., 2019a) nano iron oxide (Fe_2O_3), (Nogueira *et al*., 2018; Mirbagheri and Sabbaghi, 2018; Khan and Lo, 2017) nano titanium dioxide (TiO_2), (Nogueira *et al*., 2018; Apopei *et al*., 2020; Chen *et al*., 2015; de S. Furtado *et al*., 2021; Franz *et al*., 2020) nano zinc oxide (ZnO), (Amde *et al*., 2020; Kamaraj *et al*., 2020; Sun *et al*., 2018) have been widely studied and applied for water treatment. The high remediation performance of Me/MeO not only relies on their large surface area, but also their redox properties, (Fang *et al*., 2020; Ou *et al*., 2020; Liu *et al*., 2021) or the promotion of co-precipitation and complexation (Liu *et al*., 2021; Wen *et al*., 2014; Okonji *et al*., 2020). Several reviews have discussed the mechanisms and applications of nano Me/MeO for water treatment (Santhosh *et al*., 2016; Pradeep, 2009; Ighalo *et al*., 2021; Stefaniuk *et al*., 2016; Lee and Park, 2013).

Nanohybrids and Nanocomposites

A nanohybrid combines two or more nanomaterials, while a nanocomposite is a combination of nanomaterials and other larger-size materials such as polymeric structures or activated carbon (**Aich *et al*., 2014**). Nanohybrids and nanocomposites often have the characteristics of their various constituent materials, which can make up for the shortcomings of using a single material (Mirbagheri and Sabbaghi, 2018; Nabi *et al*., 2020; Xu *et al*., 2018; Mehrabi *et al*., 2019; Nawaz *et al*., 2017). For example, doping nanoTiO_2 in a polymeric membrane provides reactive sites within a stable structure and can help collect and recycle the nanoparticles after treatment (**Nabi *et al*., 2020**). Modifying the ratio of different components in nanohybrids and nanocomposites may result in different properties and remediation performance (Sun *et al*., 2018; Mehrabi *et al*., 2019; Nawaz *et al*., 2017). For instance, in nanoTiO_2-nanoZnO hybrid material, when nanoTiO_2 is the main heterogeneous photocatalyst, its reaction activity will decrease with increasing nanoZnO. However, when nanoZnO is used as the main heterogeneous photocatalyst, the reaction activity increases with increasing nanoTiO_2 (**Sun *et al*., 2018**). This difference may be related to the migration direction of electrons and holes in the different materials (**Sun *et al*., 2018**). More information about the classes, mechanisms, and applications of nanohybrid/nanocomposite for water treatment was covered in several reviews (Kumar *et al*., 2021; Miculescu *et al*., 2016; Mardikar *et al*., 2021).

Organic Framework Nanostructures

In addition to considering the use of different chemicals, the performance of nanomaterials can also be improved by developing new nanostructures. At present, the emerging new nanostructured materials in the field of water treatment include covalent organic frameworks (COFs) and metal-organic frameworks (MOFs). MOFs are porous crystalline materials with an ordered honeycomb structure formed by combining metal elements as nodes and organic linkers (**Goetjen *et al*., 2020**). COFs are similar to MOFs, except that in COFs the metal nodes are replaced with non-metals (**Xia *et al*., 2021**). COFs and MOFs have high surface areas, and their inherent nano-pores can be used as channels for molecular transmission. In addition, they possess low mass and good heat resistance, which make them a popular choice for novel adsorption or filtration materials (Xia *et al*., 2021; Mon *et al*., 2018; Rego *et al*., 2021; Yuan *et al*., 2019). Some review papers also summarized the properties, mechanisms, and applications of COFs/MOFs-based nanomaterials for water treatment (Xia *et al*., 2021; Yuan *et al*., 2019; Li *et al*., 2019e).

Water Treatment Mechanisms

Adsorption

In terms of water treatment, adsorption is a technology that transfers and concentrates the contaminants of interest from the water phase to the surface of a solid (adsorbent). Due to the simplicity of operation, low cost, and high efficiency, adsorption is a widely preferred method for water treatment. Many C-ENMs, (Sun *et al*., 2020; Ahsan *et al*., 2019; Vajedi and Dehghani, 2019; Henriques *et al*., 2016; Ma *et al*., 2018) nano Me/MeO, (Vajedi and Dehghani, 2019; ElHussein *et al*., 2020; Clark *et al*., 2019; Irshad *et al*., 2019; Behjati *et al*., 2018; Rahdar *et al*., 2021) and new generation nanostructured materials (such as COFs and MOFs (**Ahsan *et al*., 2019**; **Liu *et al*., 2018**; **Ji *et al*., 2018**; **Liu *et al*., 2020b**; **Cui *et al*., 2020a**)) can adsorb contaminants, at times with particular specificity, depending on the adsorbent's chemical composition and surface characteristics.

C-ENMs, such as CNTs, graphene, and graphene-based nanomaterials, or the new generation of nanostructured materials (COFs or MOFs), have extremely high surface area and porosity, which promote interactions between the adsorbents and contaminants. They are particularly suited to remove a wide range of organic molecules, (Akinpelu *et al*., 2019; Ahlawat *et al*., 2020; Hashem *et al*., 2019; Zebardast *et al*., 2018; Wang *et al*., 2010) but can also be tailored to remove inorganic ions (Vajedi and Dehghani, 2019; Liu *et al*., 2020b; Samuel *et al*., 2019; Niu *et al*., 2021; Cui *et al*., 2019). The adsorption mechanisms include covalent bonds, ion exchange, π-electron coupling, hydrogen bonding, electrostatic interaction, and micropore filling (Ahlawat *et al*., 2020; Gupta *et al*., 2013; Jabbari *et al*., 2016). Further modification of nanomaterials with functional groups can enhance the adsorption capacity or contaminant selectivity by changing the properties of the adsorbents, such as hydrophobicity (Ahlawat *et al*., 2020; Yang *et al*., 2015; Norzilah *et al*., 2011).

Me/MeO ENMs, such as nZVI, (Fang *et al*., 2020; Han *et al*., 2021; Wei *et al*., 2018) nanoFe_3O_4, (Mahdavi *et al*., 2014; Liu *et al*., 2019c; Ali *et al*., 2019a; Zhang *et al*., 2019b) nanoTiO_2, (Vajedi and Dehghani, 2019; Irshad *et al*., 2019) nanoZnO, (Mahdavi *et al*., 2014; Gu *et al*., 2020; Sharma *et al*., 2019) are also widely used to adsorb many heavy metals, metalloids, and inorganic salts. The high adsorption capacity of Me/MeO ENMs is not only due to their large surface area, but also metallic elements or surface functional groups that enhance the interactions between the adsorbents and contaminants, such as metal displacement reactions, (Liang *et al*., 2021; Liang *et al*., 2020b; Lv *et al*., 2019) co-precipitation, (Su *et al*., 2015; Wen *et al*., 2014; Lv *et al*., 2019) and complexation (Liu *et al*., 2021; Liang *et al*., 2021). For instance, the adsorption capacity of nZVI for phosphate was enhanced by complexation between iron and phosphate (**Liu *et al*., 2021**). Also, the sulfidation of nZVI to produce sulfide-modified nZVI (SnZVI) made the surface of the nanoparticle irregular (which increased the specific surface area) and introduced sulfhydryl (-SH) groups (which co-precipitate metals), both of which increased the nanoparticle's cadmium (Cd) adsorption capacity (**Su *et al*., 2015**).

Nanocomposites, such as magnetic nanoparticles coated with a porous shell that can host ligands or surfactant micelles, have also been employed successfully to remove a wide range of contaminants, such as legacy organic pollutants, (Wang *et al*., 2009; Clark and Keller, 2012a) emerging contaminants, (Huang and Keller, 2013; Huang *et al*., 2016a) metals, (Huang and Keller, 2015; Huang *et al*., 2016b; Huang and Keller, 2016) natural organic matter (NOM), (**Wang *et al*., 2011**) and inorganic ions (**Clark and Keller, 2012b**). These interactions involve covalent bonds, electrostatic interactions, and other mechanisms to adsorb the target contaminants onto the outer shell. The magnetic nanoparticles can then be removed from the treated water using a simple magnetic field, with no pressure differential or clogging. Regeneration of the ligand or surfactant micelles is done off-line, and the functionalized magnetic nanoparticles are then reused for many cycles, reducing overall cost, and recovering the valuable nanomaterial.

When applying nanomaterials, many factors that affect the adsorption efficiency need to be considered, such as ionic strength, natural organic matter (NOM), pH, temperature, stirring speed (or flow speed), water-solubility, hydrophobicity and electrical properties of the target pollutants, and the isoelectric point of the nanomaterials (Ahsan *et al*., 2019; Clark *et al*., 2019; Norzilah *et al*., 2011; Samuel *et al*., 2018). Some metal-based nanomaterials, such as nZVI, can dissolve under acidic (low pH) conditions and reduce their effectiveness in water (**Bae and Hanna, 2015**). Also, a change of pH can result in different electrical properties of the adsorbate and the adsorbent, and affect the interactions occurring by electrostatic force (Ahsan *et al*., 2019; Clark *et al*., 2019; Norzilah *et al*., 2011). Therefore, finding suitable reaction conditions can improve adsorption efficiency. Given the finite number of sorption sites, the nanomaterial (adsorbent) needs to be regenerated or replaced on a regular interval (Tan *et al*., 2015; Aigbe and Osibote, 2020; Huang *et al*., 2018a).

Filtration

Filtration is a technology that uses porous materials, including membranes, to separate chemical or biological contaminants from water under pressure. Some nanostructures that have nanoscale pores can be directly applied for filtration (Apopei *et al*., 2020; Chen *et al*., 2020a; Yanez *et al*., 2017). Many nanomaterials, such as nanofibers, can be layered to generate a mesh for filtration (Chen *et al*., 2020b; Feng *et al*., 2013; Nalbandian *et al*., 2015). Nanofibers have been widely used in the nanofiltration (NF) step of water treatment plants and have proven to effectively remove contaminants that are equal or higher than the molecular weight cut-off (MWCO) (Zhang *et al*., 2019e; Ma *et al*., 2014; Han *et al*., 2020b). The main mechanisms of nanomaterials for filtration are size exclusion, hydrophobic interactions, and electrostatic interactions (Ganiyu *et al*., 2015; Dolar *et al*., 2013; Nghiem *et al*., 2006; Alturki *et al*., 2010). Size exclusion is often the most important filtration mechanism, (Auset and Keller, 2006; Sirivithayapakorn and Keller, 2003) and filtration capacity is often affected by the pore size and distribution of the material. Hydrophobic interactions also influence adsorption phenomena between contaminants and the membrane surface (Dolar *et al*., 2013; Alturki *et al*., 2010). Hydrophobic contaminants are more likely to adsorb to a C-ENM membrane surface. However, diffusion may also occur, and the adsorbed contaminant could desorb into the permeate (Dolar *et al*., 2013; Alturki *et al*., 2010). This phenomenon was observed when removing hydrophobic pharmaceuticals (log $K_{ow} > 2.0$), such as procaine (log $K_{ow} = 2.14$) (**Dolar *et al*., 2013**). Electrostatic interactions also play an important role in nanofiltration (Nghiem *et al*., 2006; Ozaki *et al*.,

2008; Verliefde *et al*., 2007). For example, ibuprofen and diclofenac (which are both negatively charged at pH 7) have higher removal than atenolol (which is positively charged at pH 7) if the NF membrane has a positive charge at pH 7 (**Verliefde *et al*., 2007**). Similarly, sulfamethoxazole was observed to possess the same charge (negative) as the nanofiltration membrane when pH was higher than its pK_a (pH 5.7), which resulted in a higher rejection rate (**Nghiem *et al*., 2006**).

Many factors need to be considered in the application of NF, such as the size and hydrophobicity of the target pollutants, the pore size of the nanomaterials, the hydrophilicity and the functional groups contained, and the characteristics of the water (such as pH, ionic strength, NOM concentration, temperature) (Ganiyu *et al*., 2015; Dolar *et al*., 2013; Nghiem *et al*., 2006; Alturki *et al*., 2010). In addition, after a certain operation time, the filtration sites of porous materials and membranes become saturated, increasing the pressure differential across the membrane, and reducing water flow (Xu *et al*., 2019; Nghiem and Hawkes, 2009). Given the nanoscale pore size and high operating pressure, the quality requirement of the influent water should be high enough to avoid fouling and blocking. Thus, before nanofiltration, the influent is often pretreated with adsorption and/or microfiltration to remove larger particles and improve the service life and energy efficiency of the NF membranes (Xu *et al*., 2015; Kim *et al*., 2011; Davood Abadi Farahani *et al*., 2016).

Oxidation-Reduction

Applying redox reactions in water treatment has attracted widespread attention because of fundamental transformation or elimination of the target contaminants. The extremely high specific surface area of nanomaterials, arising from small size, leads to high reactivity and reaction kinetics. Nanomaterials may play different roles in redox reactions (such as reducing agents, (Meng *et al*., 2021; Xu *et al*., 2020; Lin *et al*., 2018; Wang *et al*., 2020b) oxidizing agents, (Babuponnusami and Muthukumar, 2012; Zha *et al*., 2014; Mikhailov *et al*., 2017) precursors, (Wang *et al*., 2020e; Angamuthu *et al*., 2017) or catalysts, (**de S. Furtado *et al*., 2021**; **Franz *et al*., 2020**; **Ran *et al*., 2020**; **Pirsaheb *et al*., 2020**)) in the treatment of pollutants. Some nanomaterials may also transform contaminants by producing free radicals with strong oxidizing properties (indirect oxidation). For example, the dissolved iron from nZVI can lead to Fenton-like reactions in water and generate hydroxyl radical that has a strong oxidation potential (Babuponnusami and Muthukumar, 2012; Zha *et al*., 2014; Mikhailov *et al*., 2017). By modifying nanomaterials to improve their electron transport efficiency, their redox ability can be further improved (Lin *et al*., 2017; Nguyen *et al*., 2021; Deng *et al*., 2018; Su *et al*., 2018a). Nanomaterials such as nZVI exhibit reducing properties which may be employed for water treatment (Černíková *et al*., 2020; Liu *et al*., 2019a; Han *et al*., 2021; Němeček *et al*., 2016). Reduction can be used to immobilize heavy metals (e.g., lead [Pb], chromium [Cr]) and metalloids (e.g., arsenic [As]), (Černíková *et al*., 2020; Liu *et al*., 2019a; Han *et al*., 2021; Němeček *et al*., 2016; Su *et al*., 2014a; Stevenson *et al*., 2017) or for dehalogenation of solvents (e.g., tetrachloroethylene, trichloroethylene) (Meng *et al*., 2021; Xu *et al*., 2020; Lin *et al*., 2018; Wang *et al*., 2020b; Cao *et al*., 2017).

In addition, nanomaterials can also act as photocatalysts in redox reactions. NanoTiO_2, nanoZnO, and to an extent, GO, are commonly used nanomaterials in water treatment-based photocatalysis. They generate hydroxyl radicals in water under light excitation, and have been used to effectively degrade several organic compounds in water (de S. Furtado *et al*., 2021; Franz *et al*., 2020; Ran *et al*., 2020; Pirsaheb *et al*., 2020; Adeleye *et al*., 2018). Although ultraviolet (UV) light has become a commonly used excitation light source because of its high energy photons, it increases operation and maintenance costs, requires a high energy to water ratio, with potentially additional environmental impacts from high energy use (e.g., generation of greenhouse gases and ozone-depleting substances) (Lee *et al*., 2017; Bahnemann, 2004; Chong *et al*., 2010). Therefore, recent research has focused on the development of nanomaterials with lower energy band gap to achieve photodegradation using visible light (or sunlight) (Chong *et al*., 2010; Cui *et al*., 2020b; Yentür and Dükkancı, 2020). A recent study successfully used a MoS_2/rGO/WO_3 nanohybrid to degrade 80% of carbamazepine in 20 min under visible light, (**Cui *et al*., 2020b**) making it more competitive in real applications.

Disinfection

Conventional disinfection technologies, such as chlorination, ozonation, and ultraviolet (UV) irradiation, have been successfully applied in water treatment, (Song *et al*., 2016; Ghernaout, 2017; Ghernaout, 2020) but they have some disadvantages such as generation of disinfection by-products, low disinfection efficiency, high energy consumption, and high cost of operation and maintenance (Ghernaout, 2017; Du *et al*., 2017; Gude, 2015; Pichel *et al*., 2019). High adsorption capacity and reactivity make nanomaterials a potentially viable option for inactivating microorganisms. The mechanisms of inactivation could be physical, such as filtration and adsorption, (Matharu *et al*., 2020; Kim *et al*., 2007; Ojha, 2020) or chemical, such as oxidation, (Ojha, 2020; Khalil *et al*., 2011; Panchal *et al*., 2020) or compromising cell membranes (Ojha, 2020; Arshad *et al*., 2017). For example, nanoTiO_2 and nanoZnO are photocatalytic, and can generate hydroxyl radicals and weaken the activity of microorganisms under sunlight or ultraviolet light (Ojha, 2020; Khalil *et al*., 2011; Panchal *et al*., 2020). Nanomaterials can also achieve disinfection by biological inhibition (Ojha, 2020; Arshad *et al*., 2017). For instance, nano-silver (Ag) is considered for disinfection because the Ag ions released by nano-Ag can damage cell membrane and inhibit DNA replication, thereby preventing the growth of microorganisms (**Ojha, 2020**).

Multifunctionality

Since some nanomaterials are used for water treatment based on multiple mechanisms that may occur simultaneously. For example, reduction and adsorption may occur during the removal of hexavalent Cr (Cr (VI)) or pentavalent As (As (V)) by nZVI (Černíková *et al*., 2020; Han *et al*., 2021; Němeček *et al*., 2016). Some nanohybrids or nanocomposites that include multiple materials may also show multifunctionality and better remediation performance than a single nanomaterial (Liu *et al*., 2019a; Ahmad *et al*., 2018; Gu *et al*., 2018; Zhou *et al*., 2021). For example, doping magnetic Zirconium (Zr) to MOFs can effectively remove Cr (VI) by adsorption, reduction, and chelation (the capacity is 259.1 mg/g) (**Zhou *et al*., 2021**). Also, the introduction of β-FeOOH with photocatalytic activity into the

nanofiltration membrane can simultaneously improve the self-cleaning ability of the filter membrane (Lv *et al*., 2017; Wang *et al*., 2020c; Chen *et al*., 2020c).

Nanomaterials in Water Treatment

The following section presents examples of the use of diverse nanomaterials presented in "**Classification of Nanomaterials Used for Water Treatment**", for the treatment of common classes of contaminants, applying the mechanisms presented in "**Water Treatment Mechanisms**". For ease of reference, we summarize the studies in **Table 1** (emerging contaminants), **Table 2** (inorganic contaminants), **Table 3** (organic contaminants) and **Table 4** (disinfection by-products).

Emerging Contaminants

Microplastic

Use of carbonaceous nanomaterials (C-ENMs)

C-ENMs such as CNTs and GO have a high surface area and can adsorb onto microplastics (MPs), which increases the size of heteroagglomerates formed and the potential to remove microplastics from the aqueous phase. Large C-ENMs-based structures can also act as adsorbents for microplastics. For instance, a sponge-like GO modified with chitin was recently employed to remove polystyrene (PS), with an adsorption capacity of 5.9–8.5 mg/g (**Sun *et al*., 2020**). The removal efficiency reported in the study (72.4–89.8%) was higher than that of granular activated carbon (GAC) adsorption technology (56.9–60.9%) in traditional drinking water treatment plants (DWTPs) (**Wang *et al*., 2020a**). Both C-ENMs and microplastics can be attracted to each other in water via hydrophobic interactions. Only a few studies have considered enhancing the removal of MPs with C-ENMs, and all of them were based on the adsorption (see **Table 1** and **Fig. 1**(a)).

Use of metals and metal oxides (Me/MeO)

Given the high electron transport efficiency of many nano-Me/MeO, researchers have applied Me/MeO for degradation of MPs (see **Fig. 1**(a) and **Table 1** for the examples), especially photodegradation with nanoTiO_2 or nanoZnO (Nabi *et al*., 2020; Tofa *et al*., 2019). The photocatalytic activities of nanoTiO_2 degraded PS, with a removal efficiency up to 98.4% in 12 h (**Nabi *et al*., 2020**). Also, platinum (Pt)-doped nanoZnO achieved 94% removal of polyethylene (PE) within 90 min (**Tofa *et al*., 2019**).

Use of nanohybrids/nanocomposites

Nanohybrids and nanocomposites usually take advantage of several mixed materials and result in higher treatment performance or simpler operation than single nanomaterials (Chen *et al*., 2020a; ELMACI, 2020; Tang *et al*., 2021). A nanocomposite made up of nanoFe_3O_4 and activated carbon adsorbed 100% of PS within 30 min which is a higher efficiency than that exhibited by most GAC-based adsorption (56.9%–60.9%) and coagulation technologies (44.5%–99%) (**Wang *et al*., 2020a**). The adsorption capacity of Fe_3O_4-CNTs nanohybrids for PE, polyethylene terephthalate (PET), and polyamide (PA) reached 1650, 1400, and 1100 mg/g, respectively (**Tang *et al*., 2021**). The Fe_3O_4 in the nanocomposite helped to recover the MP-adsorbed nanocomposite with an external magnetic field. More so, the recovered Fe_3O_4-CNTs could be recycled through thermal treatment (at 600°C) (**Tang *et al*., 2021**).

Use of organic framework nanostructures

COFs and MOFs have a large number of nanopores and strong plasticity, which make them ideal materials for adsorption and filtration (Xia *et al*., 2021; Mon *et al*., 2018; Rego *et al*., 2021; Yuan *et al*., 2019). Some recent studies related to the applications of COF/MOFs for MPs removal were listed in **Table 1**. Also, adsorption is the main mechanism used to treat MPs (**Fig. 1**(a)). A recent study fabricated Zr-MOFs-based foam, which successfully adsorbed and filtered more than 80% of PS, polyvinylidene difluoride (PVDF), and poly (methyl methacrylate) (PMMA) in water (**Chen *et al*., 2020a**).

Pharmaceutical and personal care products (PPCPs), and endocrine-disrupting chemicals (EDCs)

Use of carbonaceous nanomaterials (C-ENMs)

The main mechanisms for removing PPCPs and endocrine-disrupting chemicals (EDCs) with C-ENMs are adsorption and degradation (see **Fig. 1**(b), with some examples in **Table 1**). The photoactivity of GO leads to the degradation of bisphenol A (BPA) (**Adeleye *et al*., 2018**). The most commonly used sorbents are CNTs, including single-walled (SWCNTs) (Kim *et al*., 2014; Balarak *et al*., 2016; Xu *et al*., 2017a) or multi-walled carbon nanotubes (MWCNTs) (Kim *et al*., 2014; Xu *et al*., 2017a; Wang *et al*., 2016b). Due to the graphite layer present in CNT, they have a very high van der Waals force index (Liu *et al*., 2013; Ji *et al*., 2009). Also, CNTs are composed of fused benzene rings with strong polar sp^2 hybrid carbon atoms, which have a good affinity for aromatic or hydrophobic pollutants (Liu *et al*., 2013; Lin and Xing, 2008; Das *et al*., 2014). Studies have confirmed that the adsorption capacity of CNTs for BPA is as high as 82.9 mg/g (**Ahsan *et al*., 2019**). Additionally, C-ENMs have abundant modifiable sites, and by adding appropriate functional groups, the adsorption capacity and the selectivity for the contaminants can be enhanced (Wang *et al*., 2016b; Jung *et al*., 2015; Piao *et al*., 2008; Lee *et al*., 2016).

Table 1 Recent studies about applying nanomaterials for emerging contaminants removal

Contaminant	*Technology*	*Method*	*Mechanisms*	*Efficiency (time)*	*Capacity (mg/g)*	*Referen*
Microplastics (MPs)						
Polystyrene (PS)	Me/MeO	TiO_2 + UV	Photodegradation	98.4% (12 h)		(Nabi *e*
	Nanohybrid	Zr-MOF	Adsorption	85.7%		(Chen 2020
	Nanohybrid	Carbon@Fe_3O_4	Adsorption	100 (30 min)		(ELMA
	Nanocomposite	Chitin-GO sponge	Adsorption	72.4%–89.8%	5.898–8.461	(Sun *et*
Polyethylene (PE)	Me/MeO	TiO_2 + UV	Photodegradation	100% (36 h)		(Nabi *e*
	Nanohybrid	Fe_3O_4-CNT	Adsorption		1650	(Tang
	Nanohybrid	ZnO-Pt	Photodegradation	94% (90 min)		(Tofa *e*
Polyethylene terephthalate (PET)	Nanohybrid	Fe_3O_4-CNT	Adsorption		1400	(Tang
Polyamide (PA)	Nanohybrid	Fe_3O_4-CNT	Adsorption		1100	(Tang
Polyvinylidene difluoride (PVDF)	Nanohybrid	Zr-MOF	Adsorption	90.1%		(Chen 2020
Poly (methyl methacrylate) (PMMA)	Nanohybrid	Zr-MOF	Adsorption	88.2%		(Chen 2020
Pharmaceuticals						
Carbamazepine	Me/MeO	TiO_2 + UV	Photodegradation	100% (1 h)		(Ran *et*
	Me/MeO	TiO_2 + UV	Photodegradation	99% (55 min)		(Franz
	Me/MeO	UiO-66	Adsorption		16.69	(ElHus 2020
	Nanohybrid	CoMgFe-layered double oxides (LDO)	Redox	100% (20 min)		(Hong 2020
	Nanohybrid	UiO-66/graphene	Adsorption		51.17	(ElHus 2020
	Nanohybrid	MoS_2/rGO/WO_3 +visible light	Photodegradation	79.67% (20 min)		(Cui *et*
	Nanohybrid	Ag/AgCl/$BiVO_4$ +visible light	Photodegradation	70.6% (4 h)		(Yentü Dükl
	Nanocomposite	Fe_3O_4-black carbon	Adsorption		33.6	(He *et*
	Nanocomposite	CuO/Cu_2O/Cu-biochar composite	Adsorption	93.02% (3.5 h)	4.9	(Liang 2020
Diclofenac	Me/MeO	$ZnFe_2O_4$	Redox	90% (2 min)		(Al-An 2020
	Me/MeO	Sulfide-modified nZVI (SnZVI)	Adsorption + oxidation	73.6% (2 h)		(Su *et*

Table 1 (Continued)

Contaminant	*Technology*	*Method*	*Mechanisms*	*Efficiency (time)*	*Capacity (mg/g)*	*Reference*
	Nanohybrid	Co_3O_4-CeO_2	Photodegradation	90% (15 min)		(**Xian *et al.*, 2019**)
	Nanohybrid	ZnO/SnO_2 + UV	Photodegradation	100% (1 h)		(**Novakovic *et al.*, 2020**)
	Nanohybrid	ZnO/TiO_2 + UV	Photodegradation	100% (1 h)		(**Novakovic *et al.*, 2020**)
	Nanohybrid	ZnO/In_2O_3 + UV	Photodegradation	100% (1 h)		(**Novakovic *et al.*, 2020**)
	Nanohybrid	GO@$CoFe_2O_4$	Adsorption		32.4	(**Tran *et al.*, 2020**)
	Nanohybrid	Fe_3O_4 - COF	Adsorption		40.4	(**Zhuang *et al.*, 2020**)
	Nanohybrid	MWCNTs- Fe_3O_4	Redox	98.52% (82.24 min)		(**Pourzamani *et al.*, 2018**)
	Nanocomposite	CuO/Cu_3O/Cu-biochar composite	Adsorption	88.96% (3.5 h)	4.2	(**Liang *et al.*, 2020a**)
	Nanocomposite	GAC-TiO_2N	Filtration	80%		(**Apopei *et al.*, 2020**)
Endocrine-Disrupting Chemicals (EDCs)						
Bisphenol A (BPA)	Carbonaceous	GO	Adsorption		99.7	(**Ahsan *et al.*, 2019**)
	Carbonaceous	CNT	Adsorption		82.9	(**Ahsan *et al.*, 2019**)
	Me/MeO	nZVI	Redox	96.4% (2.5 h)		(**Guo *et al.*, 2020b**)
	Me/MeO	amino-functionalized magnetic Fe_3O_4	Redox	87.3% (11 h)		(**Sadeghzadeh *et al.*, 2020**)
	Me/MeO	$CoFe_2O_4$	Redox	97% (40 min)		(**Long *et al.*, 2021**)
	Me/MeO	Peroxymonosulfate (PMS)-modified CoS	Redox	90% (10 min)		(**Ding *et al.*, 2020**)
	Nanohybrid	Cu@GO	Adsorption		182.2	(**Ahsan *et al.*, 2019**)
	Nanohybrid	Cu@CNT	Adsorption		164.1	(**Ahsan *et al.*, 2019**)
	Nanohybrid	Fe@Nitrogen-doped CNT-rGO	Redox		~280	(**Sridhar and Park, 2020**)
	Nanohybrid	TiO_{2-x}/rGO	Photodegradation	~95% (60 min)		(**Xu *et al.*, 2018**)
	Nanocomposite	Polysulfone/GO membrane	Filtration	93%		(**Nasseri *et al.*, 2018**)
	Nanocomposite	kaolin-based Ag@TiO_2	Photodegradation	93.22% (3 h)		(**Shareef *et al.*, 2020**)
	Organic framework nanostructures	COF	Adsorption		61.3	(**Liu *et al.*, 2018**)
Per- and polyfluoroalkyl substances (PFASs)						

Table 1 (Continued)

Contaminant	*Technology*	*Method*	*Mechanisms*	*Efficiency (time)*	*Capacity (mg/g)*	*Reference*
Perfluoro-n-hexanoic acid (PFHxA)	Organic framework nanostructures	$[NH_2]$-COF	Adsorption	90% (0.5 h)		(**Ji *et al.*, 2018**)
	Nanocomposite	Ag-activated carbon	Adsorption	81.5%–83% (24 h)		(**Omo-Okoro *et al.*, 2021**)
Perfluoro-n-heptanoic acid (PFHpA)	Organic framework nanostructures	$[NH_2]$-COF	Adsorption	94% (0.5 h)		(**Ji *et al.*, 2018**)
	Nanocomposite	Ag-activated carbon	Adsorption	82.2%–83% (24 h)		(**Omo-Okoro *et al.*, 2021**)
Perfluoro-n-octanoic acid (PFOA)	Carbonaceous	CNT	Electrochemical oxidation	> 90% (3 h)		(**Xue *et al.*, 2015**)
	Me/MeO	Zr-PbO_2	Electrocatalysis	81.8% (1.5 h)		(**Xu *et al.*, 2017b**)
	Me/MeO	Fe-TiO_2, Cu-TiO_2	Photodegradation	91% (12 h)		(**Chen *et al.*, 2015**)
	Me/MeO	M-TiO_2 (Pt, Pd, Ag)	Photodegradation	57.7%–100% (7 h)		(**Li *et al.*, 2016**)
	Nanohybrid	TiO_2-MWCNT	Photodegradation	~100% (8 h)		(**Song *et al.*, 2012**)
	Nanohybrid	In_2O_3-Graphene \	Photodegradation	~90% (3 h)		(**Li *et al.*, 2013**)
	Nanohybrid	Pb-$BFeO_3$/rGO	Redox	~90% (5 min)		(**Li *et al.*, 2017**)
	Nanohybrid	SiC/graphene	Photodegradation	40.5%–58.5% (8 h)		(**Huang *et al.*, 2016c**)
	Nanohybrid	Zr-$MnFe_2O_4$ @rGO	Adsorption		10.1	(**Elanchezhiyan *et al.*, 2020**)
	Nanohybrid	nZVI-rGO	Redox	39% (10 min)		(**Masud *et al.*, 2021**)
	Nanohybrid	CeO_2/In_2O_3	Photodegradation	> 90% (1 h)		(**Jiang *et al.*, 2016**)
	Nanocomposite	Phosphorene nanocomposite membrane	Filtration	99%		(**Eke *et al.*, 2021**)
	Nanocomposite	Ag-activated carbon	Adsorption	82.4%–83% (24 h)	321.2	(**Omo-Okoro *et al.*, 2021**)
	Nanocomposite	SnO_2-Sb/carbon aerogel	Electrochemical oxidation	91% (5 h)		(**Zhao *et al.*, 2013**)
	Organic framework nanostructures	$[NH_2]$-COF	Adsorption	95% (0.5 h)		(**Ji *et al.*, 2018**)
	Organic framework nanostructures	MOF	Adsorption	84.53%		(**Guo *et al.*, 2020a**)

Table 1 (Continued)

Contaminant	*Technology*	*Method*	*Mechanisms*	*Efficiency (time)*	*Capacity (mg/g)*	*Reference*
Perfluoro-n-nonanoic acid (PFNA)	Organic framework nanostructures	$[NH_2]$-COF	Adsorption	96% (0.5 h)		(**Ji *et al.*, 2018**)
	Nanocomposite	Ag-activated carbon	Adsorption	82.7%–83% (24 h)		(**Omo-Okoro *et al.*, 2021**)
Perfluoro-n-pentanoic acid (PFPeA)	Nanocomposite	Ag-activated carbon	Adsorption	82.3%–82.9% (24 h)		(**Omo-Okoro *et al.*, 2021**)
	Nanohybrid	nZVI-rGO	Redox	18% (10 min)		(**Masud *et al.*, 2021**)
Perfluoro-n-decanoic acid (PFDA)	Organic framework nanostructures	$[NH_2]$-COF	Adsorption	97% (0.5 h)		(**Ji *et al.*, 2018**)
	Nanocomposite	Ag-activated carbon	Adsorption	82.8%–83% (24 h)		(**Omo-Okoro *et al.*, 2021**)
Perfluoro-n-undecanoic acid (PFUA)	Organic framework nanostructures	$[NH_2]$-COF	Adsorption	97% (0.5 h)		(**Ji *et al.*, 2018**)
Perfluoro-n-dodecanoic acid (PFDoA)	Organic framework nanostructures	$[NH_2]$-COF	Adsorption	97% (0.5 h)		(**Ji *et al.*, 2018**)
Perfluoro-n-tridecanoic acid (PRTrDA)	Organic framework nanostructures	$[NH_2]$-COF	Adsorption	100% (0.5 h)		(**Ji *et al.*, 2018**)
Perfluoro-n-butanoic acid (PFBA)	Organic framework nanostructures	$[NH_2]$-COF	Adsorption	62% (0.5 h)		(**Ji *et al.*, 2018**)
	Nanocomposite	Ag-activated carbon	Adsorption	81%–82.6% (24 h)		(**Omo-Okoro *et al.*, 2021**)
Perfluorobutane sulfonate (PFBS)	Organic framework nanostructures	$[NH_2]$-COF	Adsorption	88% (0.5 h)		(**Ji *et al.*, 2018**)
	Nanocomposite	Ag-activated carbon	Adsorption	81.8%–83% (24 h)		(**Omo-Okoro *et al.*, 2021**)
Perfluorohexane sulfonate (PFHxS)	Organic framework nanostructures	$[NH_2]$-COF	Adsorption	96% (0.5 h)		(**Ji *et al.*, 2018**)
	Nanocomposite	Ag-activated carbon	Adsorption	82.4%–83% (24 h)		(**Omo-Okoro *et al.*, 2021**)
Perfluorooctane sulfonate (PFOS)	Me/MeO	UiO-66	Adsorption		1.24	(**Clark *et al.*, 2019**)
	Me/MeO	MnO_2 + H_2O_2	Redox	~99% (15 min)		(**Chang *et al.*, 2020**)
	Me/MeO	TiO_2/UV	Photodegradation	83% (8 h)		(**de S. Furtado *et al.*, 2021**)

Table 1 (Continued)

Contaminant	*Technology*	*Method*	*Mechanisms*	*Efficiency (time)*	*Capaci (mg/g)*
	Nanohybrid	Pd/nZVI	Adsorption	35% (6 d)	
	Nanohybrid	Ni/nZVI	Adsorption & defluorination	94% (120 h)	
	Nanohybrid	Zr-$MnFe_2O_4$ @rGO	Adsorption		12.6
	Nanohybrid	nZVI-rGO	Redox	84% (10 min)	
	Nanocomposite	Ag-activated carbon	Adsorption	82.9%–83% (24 h)	454.1
	Organic framework nanostructures	$[NH_2]$-COF	Adsorption	97% (0.5 h)	
	Organic framework nanostructures	biphenyl-4,4′-dicarboxylic acid (BPDC)-modified MOF	Adsorption		304.9
Perfluoropentane sulfonic acid (PFPeS)	Nanohybrid	nZVI-rGO	Redox	19% (10 min)	
Perfluoro-2-propoxypropanoic acid (GenX)	Organic framework nanostructures	$[NH_2]$-COF	Adsorption	91% (0.5 h)	

Use of metal and metal oxides (Me/MeO)

Like C-ENMs, Me/MeO nanomaterials are often able to adsorb, and degrade PPCPs and EDCs through redox reactions (**Fig. 1**(b), with some examples in **Table 1**) (Franz *et al*., 2020; Ran *et al*., 2020; Novakovic *et al*., 2020; Hong *et al*., 2020b; Al-Anazi *et al*., 2020; Xian *et al*., 2019). nanoTiO_2 and nanoZnO are the most popular choices for photocatalytic degradation of PPCPs and EDCs (Franz *et al*., 2020; Ran *et al*., 2020; Novakovic *et al*., 2020). In the presence of UV, TiO_2 removed 100% of carbamazepine (which is hard to biodegrade) within 1 h (**Ran *et al*., 2020**). In addition to nanoTiO_2 and nanoZnO, there are studies considering the use of iron-containing nanomaterials, such as nano$ZnFe_2O_4$ and SnZVI, to degrade other persistent PPCPs such as diclofenac (Su *et al*., 2018a; Al-Anazi *et al*., 2020). One study found that both oxidation and adsorption occurred when SnZVI is used for diclofenac removal (**Su *et al*., 2018a**).

Use of nanohybrids/nanocomposites

At present, researchers are exploring new nanohybrids or nanocomposites to improve the efficiency of PPCPs and EDCs removal by nanostructures (Apopei *et al*., 2020; ElHussein *et al*., 2020; Cui *et al*., 2020b; Liang *et al*., 2020a; Pourzamani *et al*., 2018; Masud *et al*., 2020). For example, Fe_3O_4-COFs or $CoFe_2O_4$@GO exhibited a significant improvement in the adsorption of diclofenac (Tran *et al*., 2020; Zhuang *et al*., 2020). The adsorption capacity of Fe@CNT-rGO for BPA was as high as 280 mg/g (**Sridhar and Park, 2020**). In addition, studies found that the hybrids of different metallic nanomaterials can result in improved reactivity and photocatalytic ability by changing the crystal structure of the metals (Novakovic *et al*., 2020; Tobaldi *et al*., 2010; Wang *et al*., 2005). For example, the hybridizing of nanoTiO_2 by nanoZnO improved electron transport efficiency of nanoTiO_2, which result in 100% photodegradation of diclofenac within 1 h (**Novakovic *et al*., 2020**). Magnetic permanently confined micelle arrays (Mag-PCMA), which contain a magnetic core with silica shell bonded with surfactant micelles, (**Wang *et al*., 2009**) showed a fast and high adsorption ability for several PPCPs, including atenolol, gemfibrozil, and sulfamethoxazole (Huang and Keller, 2013; Huang *et al*., 2016a). The remediation performance can be optimized by adding a micelle swelling agent to increase the surface area and pore volume of Mag-PCMA (**Huang *et al*., 2016a**). Other studies that applied nanohybrids or nanocomposites were listed in **Table 1**.

Use of organic framework nanostructures

Current research on the use of new generation nanostructure materials for PPCPs and EDCs mainly focuses on adsorption (**Fig. 1**(b), some examples were listed in **Table 1**) (Liu *et al*., 2018; Zhuang *et al*., 2020). A recent study showed that the adsorption capacity of COFs for BPA was up to 61.3 mg/g (**Liu *et al*., 2018**). while Fe_3O_4-COF, a nanohybrid, had an adsorption capacity of 40.4 mg/g for diclofenac (**Zhuang *et al*., 2020**).

Table 2 Recent studies about applying nanomaterials for inorganic contaminants removal

Contaminant	*Technology*	*Method*	*Mechanisms*	*Efficiency*	*Capacity (mg/g)*	*References*
Metal						
Cadmium	Carbonaceous	Poly (2-hydroxyethyl methacrylate) grafted graphene oxide	Adsorption	89% (30 min)	10.667	(**Salawudeen *et al*., 2020**)
	Carbonaceous	Sawdust-derived cellulose nanocrystals (CNC)	Adsorption		2207	(**Oyewo *et al*., 2019**)
	Carbonaceous	rGO	Adsorption		8.5	(**Vajedi and Dehghani, 2019**)
	Me/MeO	FeS	Adsorption & co-precipitation	98.5%		(**Shahryari *et al*., 2019**)
	Me/MeO	FeS (stabilized with sodium carboxymethyl cellulose)	Adsorption & co-precipitation	93% (240 min)	497.5	(**Tian *et al*., 2020**)
	Me/MeO	SnZVI	Adsorption & co-precipitation		85–120	(**Su *et al*., 2015**)
	Me/MeO	TiO_2	Adsorption		9.7	(**Vajedi and Dehghani, 2019**)
	Me/MeO	TiO_2	Adsorption	89.45% (120 min)	45.1	(**Irshad *et al*., 2019**)
	Nanohybrid	Poly (vinyl alcohol)/chitosan on nanofibers membranes	Adsorption		148.79	(**Karim *et al*., 2019**)
	Nanohybrid	Polylactic acid/nano chitosan composite fibers	Adsorption	75% (180 min)		(**Thomas *et al*., 2020**)
	Nanohybrid	Chitosan/phosphorylated nanocellulose	Adsorption		232.55	(**Brandes *et al*., 2019**)
	Nanohybrid	Polyvinylpyrrolidone-Fe_3O_4	Adsorption		43.92	(**Hong *et al*., 2020a**)
	Nanohybrid	Fe_3O_4/GO	Adsorption		52.083	(**Thy *et al*., 2019**)
	Nanohybrid	TiO_2/rGO	Adsorption		9.5	(**Vajedi and Dehghani, 2019**)
	Nanohybrid	Activated carbon/ZrO_2	Adsorption		166.7	(**Sharma and Naushad, 2020**)
	Nanohybrid	EDTA-functionalized Fe_3O_4	Adsorption & complexation		79.4	(**Huang and Keller, 2015**)
	Nanocomposite	γ-cyclodextrin-MOF-based nanoporous carbon	Adsorption		140.85	(**Liu *et al*., 2019b**)
	Organic framework nanostructures	COF	Adsorption		116	(**Liu *et al*., 2020b**)
Chromium (VI)	Carbonaceous	carbon nano-rods (functionalized with 2, 2′-(ethylenedioxy)bis (ethylamine))	Adsorption & reduction (under natural light)	~99% (180 min)		(**Anand *et al*., 2019**)
	6 Me/MeO	Boehmite (γ-AlO)	Adsorption & reduction		64.7	(**Li *et al*., 2019c**)

Table 2 (Continued)

Contaminant	*Technology*	*Method*	*Mechanisms*	*Efficiency*	*Capacity (mg/g)*	*References*
	Nanohybrid	Fe/Al bimetallic nanoparticle	Adsorption & reduction		1470	(**Ou *et al*., 2020**)
	Nanohybrid	Polyvinylpyrrolidone-Fe_3O_4	Adsorption		25.52	(**Hong *et al*., 2020a**)
	Nanohybrid	$MgFe_2O_4$ @multi-walled carbon nanotubes (MWCNTs)	Adsorption		175.43	(**Verma and Balomajumder, 2020**)
	Nanohybrid	Magnetic Zr-based MOF	Adsorption & reduction & chelation		259.1	(**Zhou *et al*., 2021**)
	Nanohybrid	nZVI@MOF	Adsorption & reduction		226.5	(**Fang *et al*., 2020**)
	Nanocomposite	Chitosan-GO	Adsorption		104.16	(**Samuel *et al*., 2019**)
	Nanocomposite	Chitosan@Ag	Adsorption	90% (300 min)	0.60	(**Ekambaram *et al*., 2020**)
	Nanocomposite	ZnO-tetrapods/activated carbon	Adsorption & reduction	97% (360 min)	1.016	(**Sharma *et al*., 2019**)
	Nanocomposite	Zn-MOF/chitosan	Adsorption		225	(**Niu *et al*., 2021**)
	Organic framework nanostructures	COF	Adsorption		384	(**Cui *et al*., 2019**)
Copper	Carbonaceous	Carbon nanotubes (CNTs) (made by orange peel)	Adsorption	94% (75 min)	16.64	(**Safari *et al*., 2019**)
	Carbonaceous	rGO	Adsorption		6.1	(**Vajedi and Dehghani, 2019**)
	Me/MeO	TiO_2	Adsorption		4.2	(**Vajedi and Dehghani, 2019**)
	Me/MeO	Fe_3O_4	Adsorption		124.8	(**Liu *et al*., 2019c**)
	Nanohybrid	TiO_2/rGO	Adsorption		7.8	(**Vajedi and Dehghani, 2019**)
	Nanohybrid	Fe_3O_4 @MOF@COF	Adsorption		37.29	(**Li *et al*., 2020**)
	Nanohybrid	Fe_3O_4/triethanolamine/GO	Adsorption		68.7	(**Ren *et al*., 2019**)
	Nanocomposite	Polyetherimide based polyhedral oligomeric silsesquioxane (POSS) nanofiltration membrane	Filtration & adsorption	86%		(**Bandehali *et al*., 2019**)
	Nanocomposite	Fe_3O_4 @activated carbon	Adsorption		23.61	(**Shahrashoub and Bakhtiari, 2021**)
	Nanocomposite	Chitosan-coated carbon nanotubes (CNTs)	Adsorption		115.48	(**Dou *et al*., 2019**)
	Organic framework nanostructures	Polydopamine-COF	Adsorption		109.2 (10 min)	(**Xiao *et al*., 2021**)
Lead	Carbonaceous	Multi-walled carbon nanotubes (MWCNTs) functionalized by selenophosphoryl groups	Adsorption		156.25 (60 min)	(**Kończyk *et al*., 2019**)

Table 2 (Continued)

Contaminant	*Technology*	*Method*	*Mechanisms*	*Efficiency*	*Capacity (mg/g)*	*References*
	Carbonaceous	rGO	Adsorption		8.6	(**Vajedi and Dehghani, 2019**)
	Me/MeO	TiO_2	Adsorption		7.4	(**Vajedi and Dehghani, 2019**)
	Nanohybrid	TiO_2/rGO	Adsorption		9.1	(**Vajedi and Dehghani, 2019**)
	Nanohybrid	Fe_3O_4/triethanolamine/GO	Adsorption		121.5	(**Ren *et al*., 2019**)
	Nanohybrid	Polyvinylpyrrolidone-Fe_3O_4	Adsorption		61.67	(**Hong *et al*., 2020a**)
	Nanohybrid	EDTA-functionalized Fe_3O_4	Adsorption & complexation		100.2	(**Huang and Keller, 2015**)
	Nanocomposite	poly (vinyl alcohol)/chitosan@Nanofibers membranes	Adsorption		266.12	(**Karim *et al*., 2019**)
	Nanocomposite	nZVI/activated carbon	Adsorption & reduction & precipitation	95% (5 min)	59.35	(**Liu *et al*., 2019a**)
	Nanocomposite	Polyetherimide based polyhedral oligomeric silsesquioxane (POSS) nanofiltration membrane	Filtration (adsorption)	85%		(**Bandehali *et al*., 2019**)
	Nanocomposite	poly (2-acrylamido-2-methylpropanesulfonic acid) graft-$Ni_3Si_2O_5$ $(OH)_4$-MWCNT	Adsorption		153.3	(**Xiao and Lin, 2020**)
	Nanocomposite	CeO_2-MoS_2 hybrid biochar	Adsorption		263.6	(**Li *et al*., 2019a**)
	Organic framework nanostructures	Sulfhydryl functionalized COF (SH-COF)	Adsorption		239	(**Cao *et al*., 2020**)
	Organic framework nanostructures	Amide-based COF	Adsorption		185.7	(**Li *et al*., 2019d**)
Mercury	Carbonaceous	GO foam	Adsorption	96% (1440 min)	35	(**Henriques *et al*., 2016**)
	Carbonaceous	SWCNTs	Adsorption		41.66	(**Alijani and Shariatinia, 2018**)
	Me/MeO	Fe_3O_4 (modified with tetraethylenepentamine)	Adsorption		109.5	(**Behjati *et al*., 2018**)
	Nanohybrid	GO-Fe_3O_4	Adsorption		16.6	(**Diagboya *et al*., 2015**)
	Nanohybrid	Fe_3O_4 @ZrP	Adsorption		181.8	(**Ahamad *et al*., 2017**)
	Nanohybrid	COF-supported Ag	Adsorption	99% (30 min)	113	(**Wang *et al*., 2020d**)
	Nanohybrid	Se@ZnO-nanorods	Adsorption		1110	(**Amde *et al*., 2020**)
	Nanohybrid	Magnetic single walled carbon nanotubes (SWCNTs)-CoS	Adsorption		1660	(**Alijani and Shariatinia, 2018**)

Table 2 (Continued)

Contaminant	*Technology*	*Method*	*Mechanisms*	*Efficiency*	*Capacity (mg/g)*	*References*
	Nanocomposite	Cellulose nanofibrils (CNFs) @ bio-sorbent films	Adsorption	99% (1440 min)		(**Silva *et al*., 2020**)
	Nanocomposite	MoS_2 @fiber	Adsorption		6258.7	(**Fausey *et al*., 2020**)
	Organic framework nanostructures	Pyrene-based COF	Adsorption		232 (Hg^0), 738 (Hg^{2+})	(**Cui *et al*., 2020a**)
	Organic framework nanostructures	Sulfonated COF	Adsorption	99.8% (30 min)	98.42	(**Panda *et al*., 2020**)
Non-metal						
Arsenic	Carbonaceous	SWCNTs	Adsorption		49.65	(**Ma *et al*., 2018**)
	Me/MeO	Maghemite (γ-Fe_2O_3 functionalized by starch)	Adsorption		8.67	(**Siddiqui *et al*., 2020**)
	Nanohybrid	GO-$CuFe_2O_4$	Adsorption		51.64 (As (III)), 124.69 (As (V))	(**Wu *et al*., 2018**)
	Nanohybrid	GO-Gd_2O_3	Adsorption		216.7	(**Lingamdinne *et al*., 2021**)
	Nanocomposite	Fe_3O_4 @activated carbon	Adsorption		6.69	(**Joshi *et al*., 2019**)
	Nanocomposite	Fe_3O_4 @Al_2O_3 @Zn-Fe layered double hydroxides (LDH)	Adsorption		67.57	(**Adlnasab *et al*., 2019**)
	Nanocomposite	Nano-CeO_2 @ceramic filter	Filtration & adsorption	94.27%		(**Yang *et al*., 2021**)
	Nanocomposite	TiO_2 @activated carbon	Adsorption		13.38 (As (III)), 15.18 (As (V))	(**Luo *et al*., 2020**)
	Nanocomposite	Fe-Ti-Mn composite oxide	Adsorption		122.3 (As (III)), 74.4 (As (V))	(**Zhang *et al*., 2019a**)
	Organic framework nanostructures	Zn-MOF-74	Adsorption		211 (As (III)), 325 (As (V))	(**Yu *et al*., 2019**)
	Organic framework nanostructures	ethidium bromide modified-COF	Adsorption		53.1	(**Yang *et al*., 2020**)
Nitrate	Me/MeO	CuO	Adsorption		71.56	(**Rahdar *et al*., 2021**)
	Me/MeO	Boehmite (γ-AlO)	Adsorption		378.5	(**Li *et al*., 2019c**)
	Me/MeO	nZVI	Reduction	32.8% (30 min)		(**Wei *et al*., 2018**)
	Nanocomposite	nZVI@biochar	Reduction	78.2% (30 min)		(**Wei *et al*., 2018**)
	Nanocomposite	nanochitosan/clinoptilolite@ pentaethylenehexamine	Adsorption		277.77	(**Yazdi *et al*., 2019**)

Table 2 (Continued)

Contaminant	*Technology*	*Method*	*Mechanisms*	*Efficiency*	*Capacity (mg/g)*	*References*
	Nanocomposite	Chitosan nanobiopolymer@polyethersulfone (PES) membrane	Filtration	100%		**(Ghaemi *et al*., 2018)**
	Organic framework nanostructures	Fe supported MOF	Adsorption & complexation		92.59	**(Pandi and Choi, 2021)**

Table 3 Recent studies about applying nanomaterials for organic contaminants removal

Contaminant	*Technology*	*Method*	*Mechanisms*	*Efficiency*	*Capacity (mg/g)*	*References*
Chlorinated compounds						
Trichloroethylene (TCE)	Carbonaceous	CNT	Filtration	74%		(**Yanez *et al*., 2017**)
	Carbonaceous	GO	Adsorption		137.5	(**Rohaizad *et al*., 2020**)
	Me/MeO	nZVI	Redox	3.38% (420 min)		(**Meng *et al*., 2021**)
	Me/MeO	nZVI-alternating current electromagnetic field (AC EMF)	Dichlorination	~100% (30 min)		(**Phenrat *et al*., 2016**)
	Nanohybrid	nZVI-rGO	Oxidation	~100% (30 min)		(**Gu *et al*., 2018**)
	Nanohybrid	Me-GO (Me = Ag, Co, Pt)	Adsorption		171.8–365	(**Nas *et al*., 2019**;**Rohaizad *et al*., 2020**)
	Nanohybrid	Fe-CNTs	Redox, filtration	97%		(**Yanez *et al*., 2017**)
	Nanohybrid	polyethylenimine surface-modified nZVI (PEI-nZVI)	Reduction	99% (120 min)		(**Lin *et al*., 2018**)
	Nanocomposite	Fe-biochar	Redox	98.5% (420 min)		(**Meng *et al*., 2021**)
	Nanocomposite	polyvinyl alcohol coated calcium peroxide nanoparticles/FeS (PVA@nCaO_2/FeS)	Redox	58.9%– 99.7 (360 min)		(**Ali *et al*., 2020**)
Tetrachloroethylene (PCE)	Nanocomposite	polyethylenimine surface-modified nZVI (PEI-nZVI)	Reduction	99% (120 min)		(**Lin *et al*., 2018**)
	Nanocomposite	nZVI-layered double hydroxide (LDH)	Reduction & adsorption	100% (4 days)		(**Wang *et al*., 2020b**)
Non-chlorinated compounds						
Naphthalene	Carbonaceous	Multiwall carbon nanotubes (MWCNT-OH)	Adsorption		0.38	(**Akinpelu *et al*., 2019**)
	Nanohybrid	ZnO/Ag/GO	Photodegradation	92% (50 min)	500	(**Mukwevho *et al*., 2020**)
	Nanohybrid	Fe-ZnO nanofiber	Photodegradation	96% (240 min)		(**Sekar *et al*., 2018**)
	Nanocomposite	Mag-PCMA	Adsorption	95% (200 min)		(**Wang *et al*., 2009**)
	Nanocomposite	FeMn/biochar/H_2O_2	Photodegradation	82.2% (148 min)		(**Li *et al*., 2019b**)
	Nanocomposite	Kaolin/ Fe_3O_4	Adsorption	97% (66 min)		(**Arizavi *et al*., 2019**)
Methyl orange	Carbonaceous	MWCNTs	Adsorption		106.3	(**Ahlawat *et al*., 2020**)
	Carbonaceous	MWCNTs/activated carbon	Adsorption		196.1	(**Ahlawat *et al*., 2020**)
	Me/MeO	Co_3O_4	Adsorption		46.082	(**Uddin and Baig, 2019**)
	Me/MeO	MgO_2	Adsorption	97.4% (50 min)	2.01 (10 min)	(**El-Shamy, 2020**)
	Me/MeO	TiO_2	Photodegradation	45.9% (UV) 26.7% (sunlight), (45 min)		(**Pirsaheb *et al*., 2020**)

Table 3 (Continued)

Contaminant	*Technology*	*Method*	*Mechanisms*	*Efficiency*	*Capacity (mg/g)*	*References*
	Me/MeO	Fe_3O_4	Oxidation	43% (30 min)		(**Arshad *et al*., 2018**)
	Me/MeO	L-arginine-coated Fe_3O_4	Adsorption		338.98	(**Guo *et al*., 2018b**)
	Nanohybrid	Scoria-Ni/TiO_2	Photodegradation	95.89% (UV), 93.97% (sunlight) (45 min)		(**Pirsaheb *et al*., 2020**)
	Nanohybrid	SiO_2-Al_2O_3 @Ni-$H_3PW_{12}O_{40}$	Photodegradation	86% (180 min)		(**Shalaby *et al*., 2018**)
	Nanohybrid	Graphene/Fe_3O_4	Redox (oxidation)	99.24% (30 min)		(**Arshad *et al*., 2018**)
	Nanohybrid	UiO-66-NH_2 MOF	Filtration	84.5%		(**Hashem *et al*., 2019**)
Methylene blue	Carbonaceous	MWCNTs	Adsorption		185.1	(**Ahlawat *et al*., 2020**)
	Me/MeO	CuO	Adsorption	98.89% (210 min)	95.5	(**Thakur and Kumar, 2019**)
	Nanohybrid	GO/nZVI	Adsorption	99.1% (5 min)		(**Mehrabi *et al*., 2019**)
	Nanohybrid	Pt-Co@GO	Adsorption		273.6	(**Nas *et al*., 2019**)
	Nanohybrid	Ni/Zn-MOF-5	Photodegradation, adsorption	90% (100 min)		(**Zebardast *et al*., 2018**)
	Nanohybrid	Co/Zn-MOF-5	Photodegradation, adsorption	90% (100 min)		(**Zebardast *et al*., 2018**)
	Nanocomposite	Fe_3O_4-Si-COOH (silica gel)	Adsorption		246.31	(**Guo *et al*., 2018a**)
	Nanocomposite	MWCNTs/activated carbon	Adsorption		232.5	(**Ahlawat *et al*., 2020**)
	Nanocomposite	ZnO-activated carbon	Adsorption	> 99% (60 min)		(**Kamaraj *et al*., 2020**)

Table 4 Recent studies about applying nanomaterials for disinfection byproducts removal

Contaminant	*Technology*	*Method*	*Mechanisms*	*Efficiency*	*Capacity (mg/g)*	*References*
Disinfection byproducts						
Trichloromethane (TCM)	Carbonaceous	MWCNTs	Adsorption		10.98	(**Dehghani *et al*., 2016**)
	Carbonaceous	GO	Adsorption & photodegradation	70.6% (dark) 98% (visible light) (30 min)		(**Ulucan-Altuntas *et al*., 2020**)
	Me/MeO	$Fe_{3-x}Co_{x4}$	Redox	90% (5 min)		(**Silva *et al*., 2019**)
Bromodichloromethane (BDCM)	Carbonaceous	MWCNTs	Adsorption		6.85	(**Dehghani *et al*., 2016**)
	Me/MeO	$Fe_{3-x}Co_{x4}$	Redox	90% (5 min)		(**Silva *et al*., 2019**)
Dibromochloromethane (DBCM)	Carbonaceous	MWCNTs	Adsorption		6.57	(**Dehghani *et al*., 2016**)
	Me/MeO	$Fe_{3-x}Co_{x4}$	Redox	87% (5 min)		(**Silva *et al*., 2019**)
Tribromomethane (TBM)	Carbonaceous	MWCNTs	Adsorption		5.95	(**Dehghani *et al*., 2016**)
	Me/MeO	$Fe_{3-x}Co_{x4}$	Redox (oxidation)	86% (5 min)		(**Silva *et al*., 2019**)
Trichloronitromethane	Nanohybrid	Graphene-nZVI	Adsorption & redox	99% (120 min)		(**Chen *et al*., 2016**)
Monochloroacetic acid (MCAA)	Carbonaceous	GO	Adsorption	31.6% (2 min)		(**Liu *et al*., 2020c**)
Dibromoacetic acid (DCAA)	Carbonaceous	GO	Adsorption	27.1% (2 min)		(**Liu *et al*., 2020c**)
	Me/MeO	Ti_4O_7	Reduction	73% (11 s)		(**Almassi *et al*., 2020**)
	Me/MeO	CuO+UV	Photodegradation	99.79% (75 min)		(**Alavi *et al*., 2021**)
	Nanohybrid	MWCNT-Ti_4O_7	Reduction	96% (11 s)		(**Almassi *et al*., 2020**)
	Nanocomposite	Powder activated carbon-Ti_4O_7	Reduction	94% (11 s)		(**Almassi *et al*., 2020**)
Trichlorocetic acid (TCAA)	Carbonaceous	GO	Adsorption	30.2% (2 min)		(**Liu *et al*., 2020c**)
	Me/MeO	CuO+UV	Photodegradation	99.22% (75 min)		(**Alavi *et al*., 2021**)

Per- and polyfluoroalkyl substances (PFAS)

Use of carbonaceous nanomaterials (C-ENMs)

Research on the removal of PFAS by C-ENMs include adsorption, and redox reaction (see **Fig. 1**(c) and examples in **Table 1**) (Xue *et al*., 2015; Elanchezhiyan *et al*., 2020; Masud *et al*., 2021; Du *et al*., 2014; Zhang *et al*., 2019c). The high electron transport efficiency in C-ENMs enables them to act as precursors in redox reactions (Masud *et al*., 2021; Li *et al*., 2017). A recent study applied electrochemical oxidation process with CNTs to degrade perfluorooctanoic acid (PFOA), with a removal efficiency of 90% in 3 h (**Xue *et al*., 2015**). Due to the hydrophobicity of most PFASs, adsorption based on hydrophobic interactions is another possible mechanism of PFAS removal by C-ENMs (Du *et al*., 2014; Zhang *et al*., 2019d).

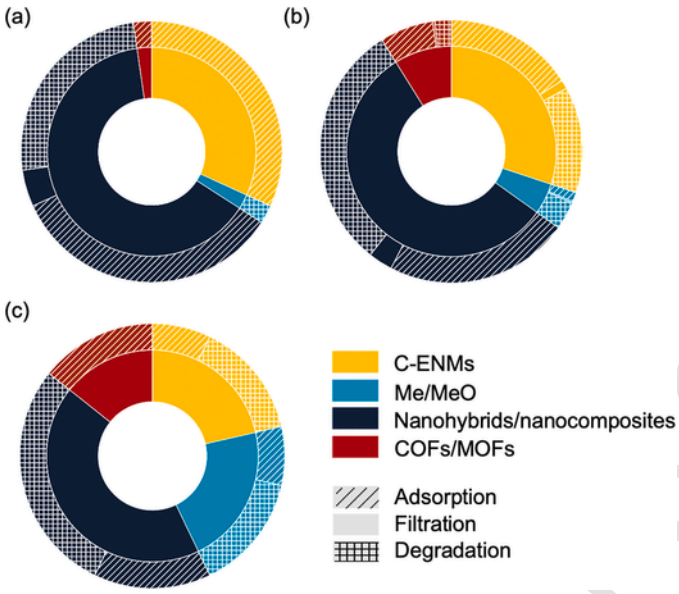

Fig. 1 Studies considering different nanomaterials to remove emerging contaminants from water based on different mechanisms. (a) Microplastics; (b) Pharmaceuticals and Personal Care Products (PPCPs) and Endocrine Disrupting Compounds (EDCs); and (c) Per- and Polyfluoroalkyl Substances (PFASs). The inner circle refers to four classes of nanomaterials (with different colors). The outer circle displays the mechanisms applied for treatment (with different textures). The definitions of acronyms in the figure: C-ENMs: carbonaceous-engineered nanomaterials; Me/MeO: nano metal/metal oxides; COFs: covalent organic frameworks; MOFs: metal-organic frameworks. The data was collected from the Web of Science considering the last 5 years (2016–2021).

Use of metal and metal oxides (Me/MeO)

There are quite a few studies related to adsorbing PFASs with nano Me/MeO (Clark *et al*., 2019; Park *et al*., 2018). For example, the adsorption capacity of UiO-66 for perfluorooctane sulfonate (PFOS) was 1.24 mg/g (**Clark *et al*., 2019**). Compared with adsorption and filtration, degradation of PFAS appears more promising since it can destroy the chemicals and actually remove them from the water cycle. Me/MeO nanomaterials with high electron transport efficiency and reactivity have been widely studied for PFAS degradation (Chen *et al*., 2015; de S. Furtado *et al*., 2021; Xu *et al*., 2017b; Li *et al*., 2016). NanoTiO_2 is a very promising candidate for degrading PFAS by photocatalysis. Doping with high conductive metals, such as gold (Au), Ag, and copper (Cu), can improve the removal of PFAS (Chen *et al*., 2015; Li *et al*., 2016). For example, Cu-nanoTiO_2 photodegraded 91% of PFOA within 12 h (**Chen *et al*., 2015**). In addition to photodegradation, PFOS can be oxidized and degraded by mixing MnO_2 and H_2O_2, and about 99% of pollutants can be removed in only 15 min (**Chang *et al*., 2020**).

Use of nanohybrids/nanocomposites

There is considerable interest in employing nanohybrid and nanocomposite materials for removing PFAS (see **Table 1**), specifically designing the nanomaterials to improve degradation reaction efficiency (**Fig. 1**(c)) (Masud *et al*., 2021; Zhao *et al*., 2013; Li *et al*., 2013; Huang *et al*., 2016c; Jiang *et al*., 2016). For example, Pb-$BFeO_3$/rGO can remove 90% of PFOA through Fenton reaction within 5 min (**Li *et al*., 2017**). nZVI-rGO can remove 84% of PFOS within 10 min (**Masud *et al*., 2021**). Also, nickel (Ni)-doped nZVI loaded on activated carbon was used to defluorinate PFOS (**Zenobio *et al*., 2020**). About 94% of PFOS was decomposed in water at 50°C (**Zenobio *et al*., 2020**). The doping of nZVI with the Ni catalyst enhanced the degradation PFOS, rather than mere adsorption without the catalyst (**Zenobio *et al*., 2020**). Some nanohybrid materials have also been used in adsorbing PFAS (Elanchezhiyan *et al*., 2020; Omo-Okoro *et al*., 2021). For example, Ag-activated carbon materials exhibited an adsorption efficiency of more than 80% for 10 different PFASs, and the adsorption capacity for PFOS (454.1 mg/g) was much higher than using traditional particulate activated carbon (PAC) technology (0.64 mg/g) (Clark *et al*., 2019; Omo-Okoro *et al*., 2021). Also, a Pb/nZVI hybrid had good PFOS removal efficiency (~35%) under acidic conditions (pH = 3.6) and 70°C. Complexation between PFOS and the dissolved Fe (III) from nanoparticles led to a better remediation performance (**Park *et al*., 2018**).

Use of organic framework nanostructures

Although there are only a few studies on the use of emerging nanostructured materials for removing PFAS, the high surface area and porosity of COFs and MOFs are amenable for removing PFAS from water via adsorption (**Fig. 1**(c)) (Ji *et al*., 2018; Guo *et al*., 2020a). For example, [NH_2]-COFs achieved an adsorption efficiency of more than 90% for 13 PFAS compounds within 0.5 h (**Table 1**), which is very promising (**Ji *et al*., 2018**). Additionally, a study found that the adsorption capacity of PFOS by organic ligand (biphenyl-4,4′-

dicarboxylic acid, BPDC)-modified MOFs could reach 304.9 mg/g, which was significantly higher than unmodified MOFs (66.2 mg/g) and the traditional PAC adsorption (0.64 mg/g) (Clark *et al*., 2019; Zhao *et al*., 2021).

Inorganic Chemicals

Metals

Use of carbonaceous nanomaterials (C-ENMs)

Given their high efficiency as adsorbents, C-ENMs have been widely used for removing metals in laboratory-scale studies (see **Fig. 2**(a) and some examples in **Table 2**). CNTs and GO can effectively remove metals such as Cu, (Dou *et al*., 2019; Safari *et al*., 2019; Bai *et al*., 2019) Cd, (Vajedi and Dehghani, 2019; Salawudeen *et al*., 2020) Cr, (**Samuel *et al*., 2019**) and Pb (**Vajedi and Dehghani, 2019**) in water. The adsorption capacities of C-ENMs for heavy metals without modification are usually about 5–50 mg/g (see **Table 2**). Further modification of carbon nanomaterials can improve the remediation performance by increasing their adsorption capacity or via other mechanisms. For example, chitosan-coated CNTs absorbed Cu up to 115.5 mg/g, which is significantly higher than using the pristine CNTs (16.6 mg/g) (Dou *et al*., 2019; Safari *et al*., 2019). The increased capacity for Cu removal was due to the abundant amino and hydroxyl groups present in chitosan. In addition, modified carbon nanorods with 2,2′- (ethylenedioxy)bis (ethylamine) (EDEA) could adsorb and reduce Cr (VI), and 99% removal efficiency was achieved within 3 h (**Anand *et al*., 2019**).

Use of metal and metal oxides (Me/MeO)

Removal of dissolved metals by Me/MeO using adsorption and redox reaction has been reported (see **Fig. 2**(a)). The toxicity, and thus, health risk of Cr (VI) can be decreased by reducing it to a lower valent state, Cr (III) (Barrera-Díaz *et al*., 2012; Jin *et al*., 2016). Iron-based nanomaterials, such as nZVI, have been applied for Cr (VI) reduction (Černíková *et al*., 2020; Němeček *et al*., 2016). Similar results can be achieved by using nano boehmite (γ-AlO), which had a adsorption capacity of 64.7 mg/g for Cr (VI) (**Li *et al*., 2019c**). nZVI can also adsorb metals such as Cd, Ni, molybdenum (Mo), cobalt (Co), and Zn (see **Table 2**) (Su *et al*., 2014a, 2015, 2018b, 2020, 2016). Sulfidation of nZVI and different ratios of sulfur to iron (S/Fe ratio) can impact metal removal due to the possibility of co-precipitation or ion exchange with FeS within SnZVI (Su *et al*., 2015, 2020, 2016).

Use of nanohybrids/nanocomposites

Since nanohybrids/nanocomposites combine the characteristics of several materials, the mechanisms used for heavy metal removal include adsorption, filtration, and reactions (see **Fig. 2**(a), and some latest examples were listed in **Table 2**). After doping cobalt sulfide (CoS) on SWCNT, the adsorption capacity of the nanohybrid for mercury (Hg) was as high as 1660 mg/g (**Alijani and Shariatinia, 2018**). A nano-MoS_2@fiber composite had an adsorption capacity of 6258.7 mg/g for Hg (**Fausey *et al*., 2020**). Nanocomposite materials have also been considered for filtration of metals. A polyetherimide based polyhedral oligomeric silsesquioxane (POSS) nanofiltration membrane filtered 85% of Cu and 86% of Pd (**Bandehali *et al*., 2019**). In addition, many recent studies also explored nanohybrid/nanocomposite materials for enhanced redox-based treatment (Mohagheghian *et al*., 2018; Nasiri *et al*., 2018; Zhao *et al*., 2019). For instance, WO_3-Fe_3O_4 nanocomposite could remove 99.96% of Cr (VI) in 5 h through photocatalytic reduction under visible light. The addition of Fe_3O_4 enhanced the electron transport efficiency and made it easy to recover the nanocomposite via external magnetic field (**Mohagheghian *et al*., 2018**). Compared with traditional photocatalytic technology, the improved photodegradation performance of the nanocomposite was due to a smaller energy band gap, resulting in the lower light frequency required to excite electrons.

Additionally, ligand-functionalized nanoparticle sorbents (such as Mag-Ligand, which is functionalized with ethylenediaminetetraacetic acid (EDTA)) is efficient for removing several metals such as Pb, Hg, and Cd (Huang and Keller, 2015; Huang and Keller, 2016). The complexation reaction between the metals and the ligand on the particle surface enhanced the adsorption capacity (**Huang and Keller, 2016**).

Use of organic framework nanostructures

Several studies have explored the ability of MOFs and COFs to remove heavy metals, mostly based on adsorption (see **Fig. 2**(a) and some examples in **Table 2**). An amide-based COF had an adsorption capacity of 185.7 mg/g for Pd (II) (**Li *et al*., 2019d**). The adsorption

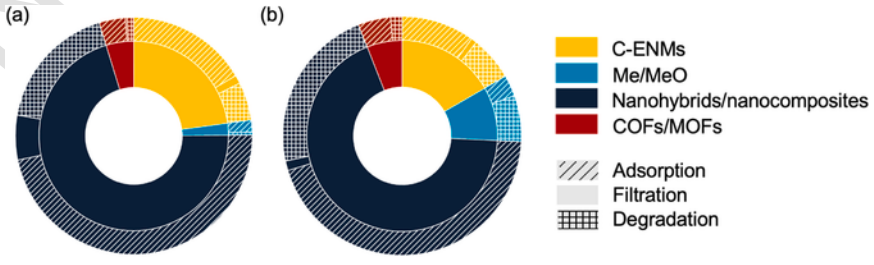

Fig. 2 Studies considering different nanomaterials to remove inorganic contaminants from water based on different mechanisms. (a) metals; (b) non-metals. The inner circle refers to four classes of nanomaterials (with different colors). The outer circle displays the mechanisms applied for treatment (with different textures). The data was collected from the Web of Science considering the last 5 years (2016–2021).

capacity of dual-porous COFs for Cr (VI) was as high as 384 mg/g, (**Cui *et al*., 2019**) which is higher than the adsorption capacity of most other adsorbents for Cr (VI). Similarly, efficient removal of Cd (116 mg/g) by COFs (**Liu *et al*., 2020b**) and Cr (225–259.1 mg/g) by MOFs (Fang *et al*., 2020; Niu *et al*., 2021; Zhou *et al*., 2021) were also reported. These studies demonstrate that COF/MOFs exhibited better adsorption capacities than traditional GAC adsorption technology (the adsorption capacities for Pb (II), Cr (VI), and Cd (II) were 13.3 mg/g, 2.8 mg/g, and 10.3 mg/g, respectively) (Sulaymon *et al*., 2009; Hydari *et al*., 2012).

Metalloids and other non-metallic contaminants

Use of carbonaceous nanomaterials (C-ENMs)

Several studies have demonstrated that C-ENMs have good adsorption capacity for metalloids and other non-metal contaminants. A recent study an adsorption capacity of SWCNTs to be 49.65 mg/g for As (**Ma *et al*., 2018**). In addition, several studies also explored the use of C-ENMs to remove nitrate (**Table 2**) (Ahmadzadeh Tofighy and Mohammadi, 2012; Alimohammadi *et al*., 2016). The functionalization of oxidized-CNT with nitrogen-containing groups increased nitrate adsorption (from 90.9 mg/g to 142.9 mg/g) by enhancing the basicity of the material surface and diffusion driving force (**Ahmadzadeh Tofighy and Mohammadi, 2012**).

Use of metal and metal oxides (Me/MeO)

Me/MeO remove non-metal contaminants via adsorption and reduction (see **Fig. 2**(b) and **Table 2**). Some iron-based nanomaterials, such as nZVI and Fe_2O_3, have been reported to efficiently remove As, nitrate, and phosphate (Wen *et al*., 2014; Han *et al*., 2021; Wei *et al*., 2018). Other Me/MeO nanomaterials, such as nanoCuO, nano γ-AlO, were also observed to possess high adsorption capacities for nitrate (**Table 2**) (Rahdar *et al*., 2021; Li *et al*., 2019c). Although nZVI is able to remove nitrate via reduction, a study found that the Pb adsorption by nZVI could be affected when nitrate is also present (**Su *et al*., 2014b**). Initially, the formation of ferrite during nitrate reduction led to higher Pb adsorption. However, the excess of nitrate could further consume ferrite and cause the desorption of Pb from nZVI.

Use of nanohybrids/nanocomposites

Several studies have explored the use of C-ENMs combined with nanosized Me/MeO (nanohybrids), or nanocomposites of Me/MeO nanomaterials and activated carbon or polymers to remove non-metallic contaminants (**Table 2**). The main mechanism of removal of non-metals by C-ENMs is adsorption, but when combined with other materials, additional mechanisms, such as reduction, may become dominant (**Fig. 2**(b)) (Han *et al*., 2020a; Motamedi *et al*., 2014). For example, a study revealed that the introduction of GO onto the nZVI's oxide shell increased nitrate removal efficiency from 40% (when treated with nZVI only) to 80% within 0.5 h by improving the adsorption ability and electron transport efficiency (**Han *et al*., 2020a**). Another study found that the removal rate of nitrate by nZVI increased from 32.8% to 78.2% after doping with biochar (**Wei *et al*., 2018**). Also, a nanocomposite made up of chitosan and nano-biopolymer adsorbed 100% of nitrate (**Ghaemi *et al*., 2018**).

Mag-PCMA was effective for the adsorption of several anions (including perchlorate, phosphate, nitrate, and sulfate) due to the abundance of cationic sites on the particle surface (**Clark and Keller, 2012b**). Nanomaterials combined with polymers are also promising for filtration of non-metals. For instance, CeO_2 and ceramic fiber nanocomposite achieved 94.3% removal of As due to both adsorption and filtration (**Yang *et al*., 2021**).

Use of organic framework nanostructures

Adsorption is the most common mechanism for COFs and MOFs to remove non-metallic pollutants (see **Fig. 2**(b) with some studies summarized in **Table 2**). A recent study determined the adsorption capacity of Zr-MOFs for As (III) and As (V) was 211 and 325 mg/g, respectively, (**Yu *et al*., 2019**) which are higher than that of GAC adsorption technology (38.8 mg/g and 51.3 mg/g for As (III) and As (V), respectively) (**Chen *et al*., 2007**). In addition, COFs modified with ethidium bromide was also efficient for As removal, with an adsorption capacity of 53.1 mg/g (**Yang *et al*., 2020**). A recent study indicated that the adsorption and chelation between Fe-MOFs and nitrate resulted in a high adsorption capacity of 92.6 mg/g (**Pandi and Choi, 2021**).

Organic Compounds

Halogenated organics

Use of carbonaceous nanomaterials (C-ENMs)

Several studies have applied C-ENMs for adsorption of halogenated organics (**Fig. 3**(a)), and high adsorption capacity was reported for trichloroethylene (TCE) and tetrachloroethylene (PCE) (**Table 3**). In a recent study, CNTs was used to filter TCE in water, with a removal rate of up to 74% (**Yanez *et al*., 2017**). Another study investigated the interaction energy (IE) between chlorobenzenes and two C-ENMs (SWCNT and graphene) based on density functional theory (DFT) and electronic structure calculations. The authors found that the IE was higher with higher number of chlorine atoms in the contaminants, which suggests that adsorption capacity would increase with chlorination of the organic compounds (**Balamurugan and Subramanian, 2013**).

Use of metal and metal oxides (Me/MeO)

Some Me/MeO nanomaterials are likely used to degrade halogenated organics (**Fig. 3**(a)), due to the nanomaterials' high electron transport efficiency and low energy band gap. Among others, nanoTiO_2 and nZVI have been widely employed to degrade halogenated organic compounds (Meng *et al*., 2021; Phenrat *et al*., 2016; Shiraishi *et al*., 2011). nZVI has a high reduction potential, but the efficiency of TCE degradation was very limited (3.38% in 420 min) (**Meng *et al*., 2021**). Another study indicated that sulfidation of nZVI

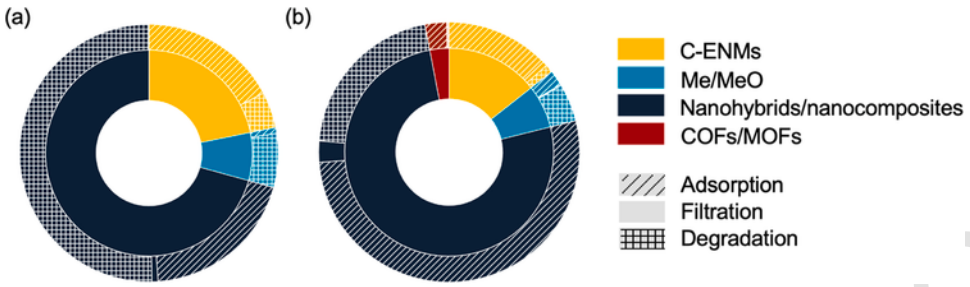

Fig. 3 Studies considering different nanomaterials to remove organic contaminants from water based on different mechanisms. (a) halogenated organics (b) non-halogenated organics. The inner circle refers to 4 types of nanomaterials (with different colors). The outer circle displays the mechanisms applied for treatment (with different textures). The data was collected from the Web of Science considering the last 5 years (2016–2021).

significantly increased the surface area-normalized degradation rate constant of TCE to around 50-fold higher than pristine nZVI, by improving electron transport efficiency (**Xu *et al*., 2020**). In addition, a recent study found that applying nZVI under an alternating current electromagnetic field can reduce 100% of TCE within 30 min (**Phenrat *et al*., 2016**). Other studies that used Me/MeO for halogenated organics removal were listed in **Table 3**.

Use of nanohybrids/nanocomposites

Nanohybrids/nanocomposites are mainly used to improve the adsorption or degradation efficiency of halogenated organics by a single nanomaterial (**Fig. 3**(a)). Given the relatively weak performance of nZVI for TCE, (**Meng *et al*., 2021**) nanocomposites have been developed with different modification approaches, such as doping nZVI with rGO, double-layer hydroxyl (LDH), or polyethyleimine (PEI), respectively. The nanocomposites have improved reactivity and TCE removal efficiency (more details were shown in **Table 3**) (Lin *et al*., 2018; Wang *et al*., 2020b; Gu *et al*., 2018). For instance, depositing nZVI onto CNTs membranes increased adsorption and reduction of TCE, and ultimately increased removal efficiency from 74% (for CNT membranes) to 97% (for Fe-CNT membranes) (**Yanez *et al*., 2017**).

Non-halogenated organics

Use of carbonaceous nanomaterials (C-ENMs)

Existing studies have shown that C-ENMs are used for adsorbing non-halogenated organic compounds such as naphthalene, methyl orange, methylene blue, among others (**Fig. 3**(b)). The adsorption efficiency depends strongly on the contaminant (**Table 3**). For example, the adsorption capacity of MWCNT for naphthalene was only 0.38 mg/g, but it was 106.3 for methyl orange and 185.1 mg/g for methylene (Akinpelu *et al*., 2019; Ahlawat *et al*., 2020). Furthermore, a composite of MWCNT and activated carbon had an even higher adsorption capacity for methyl orange and methylene—196.1 and 232.5 mg/g, respectively (**Ahlawat *et al*., 2020**). Hydrophobic interactions plan an important role in the adsorption of organic compounds by C-ENMs. As an example, the exposure of GO to light increased its ability to adsorb phenanthrene due to increased hydrophobicity of GO upon light exposure (**Du *et al*., 2018**).

Use of metal and metal oxides (Me/MeO)

The mechanisms for removing non-halogenated organics using Me/MeO nanomaterials mainly include adsorption and redox reactions (see **Fig. 3**(b) and some recent examples in **Table 3**). NanoTiO_2 is the most popular nanomaterial used for photocatalytic degradation (Pirsaheb *et al*., 2020; Rashed and El-Amin, 2007; Yogi *et al*., 2008). A recent study found that the removal efficiency of methyl orange (45.9%) by commercial nanoTiO_2 under UV light is higher than that under sunlight (26.7%) (**Pirsaheb *et al*., 2020**). Also, nanoCo_3O_4, nanoMgO_2, and nanoCuO have been used as adsorbents for dyes such as methyl orange and methylene blue (Uddin and Baig, 2019; El-Shamy, 2020; Thakur and Kumar, 2019). Some iron-based nanomaterials, such as nanoFe_3O_4, can also remove methyl orange from water through redox reaction (**Arshad *et al*., 2018**).

Use of nanohybrids/nanocomposites

Nanohybrid/nanocomposite are commonly used to achieve improved adsorption and redox efficiency for non-halogenated organics (see **Fig. 3**(b) and some recent examples in **Table 3**). Hybridizing GO with metals (such as Ag, Co, and Pt) enhanced the GO's methylene blue adsorption capacity from 137.5 mg/g to 171.75–365.0 mg/g for the metal-GO nanohybrids (Nas *et al*., 2019; Rohaizad *et al*., 2020). In addition, hybridization or compositing of some nanomaterials can also improve electron transport efficiency. For example, a scoria-Ni/TiO_2 nanocomposite photodegraded > 90% of methyl orange under UV and sunlight, which was much higher than the using nanoTiO_2 alone (**Pirsaheb *et al*., 2020**). Another study found that the depositing nanoFe_3O_4 onto graphene increased the removal efficiency of methyl orange from 43% (for only nanoFe_3O_4) to 99%, and the spent nanohybrid could be easily removed with a magnetic field (**Arshad *et al*., 2018**).

Additionally, Mag-PCMA has affinity for several polycyclic aromatic hydrocarbons (PAHs) (e.g., acenaphthene, naphthalene, and biphenyl) due to the hydrophobic surfactant coating (Wang *et al*., 2009; Clark and Keller, 2012a). The presence of humic acid had a

limited effect on the adsorption of PAHs, indicating a good performance when treating water with high content of NOM (**Wang *et al*., 2009**). Also, the lower costs of Mag-PCMA compared to current treatment technology make it promising in future applications (**Adeleye *et al*., 2016a**).

Use of organic framework nanostructures

Several recent studies on organic framework nanostructure are related to adsorption by metal-doped MOFs (see **Fig. 3**(b) and **Table 3**). Among them, a UiO-66-NH_2 modified MOF was applied for adsorbing methyl orange from wastewater, and the efficiency could reach 84.5% (**Hashem *et al*., 2019**). In addition, MOFs modified with Ni, Co, and Zn could simultaneously adsorb and photodegrade methyl blue, with a removal efficiency of 90% within 100 min (**Zebardast *et al*., 2018**). Although there are fewer studies on the use of COFs and MOFs for non-halogenated compounds, their high porosity and ease of modification make them promising materials for adsorption of non-halogenated organic compounds.

Disinfection Byproducts

Use of carbonaceous nanomaterials (C-ENMs)

The application of C-ENMs in the removal of disinfection by-products (DBPs) is mainly based on adsorption (see **Fig. 4** and **Table 4**) (Dehghani *et al*., 2016; Liu *et al*., 2020c; Silva *et al*., 2019). The adsorption capacity of unfunctionalized MWCNTs for four trihalomethanes (THMs), trichloromethane (TCM), dibromochloromethane (DBCM), bromodichloromethane (BDCM), and tribromomethane (TBM), was reported as 10.98 mg/g, 6.85 mg/g, 6.57 mg/g, and 5.95 mg/g, respectively (**Dehghani *et al*., 2016**). The higher capacity for TCM compared to other THMs was due to the higher polarity and lower molecular weight of TCM, which led to higher penetration into MWCNTs (**Dehghani *et al*., 2016**). On another note, GO was reported to rapidly adsorb 31.6% of monochloroacetic acid (MCAA), 27.1% of dibromoacetic acid (DCAA), and 30.2% of trichlorocetic acid (TCAA) within 2 min, respectively. The mechanism of adsorption was mainly via formation of hydrogen bonds between GO's functional groups and the contaminants (**Liu *et al*., 2020c**).

Use of metal and metal oxides (Me/MeO)

Metal nanomaterials are another type of nanomaterials commonly considered for removing DBPs. In contrast with C-ENMs, current research is more focused on the degradation of DBPs (see **Fig. 4** and **Table 4**). For example, nano$Fe_{3-x}Co_{x4}$ with H_2O_2 degraded more than 85% of TCM, DBCM, BDCM, and TBM in 5 min through the Fenton reaction (**Silva *et al*., 2019**). The degradation pathway was faster and more effective than adsorption with MWCNTs (**Dehghani *et al*., 2016**). nZVI was also efficient for THMs and chloroform (CF) dichlorination because of its strong reducing ability (Xiao *et al*., 2014; Feng *et al*., 2008; Xiao *et al*., 2015).

Use of nanohybrids/nanocomposites

Studies have reported the application of nanohybrids/nanocomposites in removing DBPs via adsorption and degradation (See **Fig. 4** and **Table 4**). Among them, the reduction of dibromoacetic acid (DCAA) increased from 73% (when treated with nanoTi_4O_7 only) to 96% and 94% within 11 s after hybridizing nanoTi_4O_7 with MWCNT and hybridizing nanoTi_4O_7 with PAC, respectively (**Almassi *et al*., 2020**). The addition of the adsorbents (MWCNTs and PAC) helped to concentrate the DBPs close to the catalyst, which improved the dehalogenation efficiency (Radjenović *et al*., 2012; Fang and Al-Abed, 2007). Similar roles were found in THMs reduction by a nZVI/PAC composite, where the adsorption by activated carbon significantly increased the removal capacity of nZVI for THMs (**Xiao *et al*., 2015**).

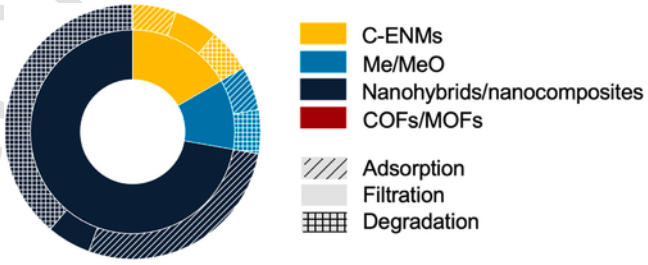

Fig. 4 Studies considering different nanomaterials to remove disinfection byproducts from water based on different mechanisms. The inner circle refers to 4 types of nanomaterials (with different colors). The outer circle displays the mechanisms applied for treatment (with different textures). The data was collected from the Web of Science considering the last 5 years (2016–2021).

Applications of Nanomaterials in Water Treatments

Commercial Considerations

Although the use of nanotechnology for water treatment is promising, some disadvantages have slowed progress towards commercial applications. For example, studies have demonstrated that nZVI has high adsorption capacity and reactivity for several contaminants (Babuponnusami and Muthukumar, 2012; Zha *et al*., 2014; Mikhailov *et al*., 2017; Adeleye *et al*., 2013). However, nZVI reacts very rapidly once it is exposed to oxygen and/or oxygenated water, (Su *et al*., 2020; Adeleye *et al*., 2013, 2016b) releasing Fe^{2+} and losing its reduction potential, which affects its long-term remediation performance (Su *et al*., 2015, 2018b). Several modifications of nZVI have been explored in response to these shortcomings, and the most popular among them is sulfidation. Sulfidation was found to slow down the dissolution and oxidation of zero-valent iron (Su *et al*., 2015, 2020; Huang *et al*., 2015). Many studies have found that the introduction of sulfhydryl groups improves the electron transport efficiency and redox capabilities, resulting in better removal efficiency for certain pollutants (Su *et al*., 2015; Lv *et al*., 2019; Cao *et al*., 2017; Su *et al*., 2020). Since SnZVI is also magnetic, it can be easily separated and recovered from water in real applications.

The cost of many nanomaterials, and the sustainability of the synthesis of many novel nanoparticles are also important considerations, if nanotechnology is going to succeed in the marketplace (Adeleye *et al*., 2016a; Brame *et al*., 2011; T C *et al*., 2018). Nanotechnology also has to demonstrate reliability, ease of use, recoverability of the nanomaterials after they perform their water treatment function, reusability, and wherever possible recyclability (**Qu *et al*., 2013**).

Environmental and Human Health Issues

Another factor that limits the wide application of nanomaterials in water treatment is the potential health and environmental impact of nanomaterials. Although some nanomaterials show high reactivity and could degrade contaminants, formation of byproducts or the reactivity of the nanomaterials themselves may have adverse effects on the environment or organisms (Stevenson *et al*., 2017; Su *et al*., 2018b; Brame *et al*., 2011; Qu *et al*., 2013; Garner *et al*., 2015; Garner and Keller, 2014; Keller *et al*., 2012; Cheng *et al*., 2019a; Chen *et al*., 2013; Saleh, 2020). Some nanomaterials with strong oxidation properties may damage cells or increase oxidative stress by producing reactive oxygen species (ROS) (Stevenson *et al*., 2017; Cheng *et al*., 2019a; Chen *et al*., 2013; Saleh, 2020; Chen *et al*., 2012). However, considerable efforts have made towards understanding the implications of and improving the sustainability of nano-enabled water treatment and nanoremediation (Han *et al*., 2021; Cheng *et al*., 2019a; Saleh, 2020; Thanh, 2013; Phenrat *et al*., 2009). As an example, sulfidation decreases the toxicity of nZVI to several organisms (Han *et al*., 2021; Cheng *et al*., 2019a; Thanh, 2013) due to lower dissolution and oxidative stress (Keller *et al*., 2012; Cheng *et al*., 2019a; Chen *et al*., 2013).

When nanomaterials are used as adsorbents, there is the risk that even a small amount of the nanomaterial loaded with contaminants can be discharged into the environment with treated water (Grassian, 2008; Zhang *et al*., 2008; Weinberg *et al*., 2011). Thus, any such application must guarantee full removal or immobilization of the nanoadsorbents. Similarly, reactive nanomaterials must be completely transformed and/or recovered, to avoid human or ecological exposure to these very active materials.

Combination With Conventional Technology

The combination of nanomaterials and traditional technology is another popular research direction in the application field. This approach can integrate the advantages of multiple treatment technologies and reduce the cost of redesigning and construction of new processes in water treatment. Nanomaterial incorporated with nanofiltration membranes is one of the approaches to improve the performance of filtration. Membrane combined with nano Me/MeO such as nanoTiO_2 and nano-Ag can improve the hydrophilicity of the membrane and anti-fouling properties (Andrade *et al*., 2015; Mollahosseini and Rahimpour, 2014; Anand *et al*., 2018). The C-ENMs-based membrane can enhance the separation performance of the membrane because of easily functionalized. For example, introducing amine-functionalized MWCNTs into the NF membrane could increase the hydrophilicity of the membrane and water permeation. And more functional groups resulted in higher surface charge and salt rejection (**Zarrabi *et al*., 2016**).

Another approach is combining nanoTiO_2 with conventional AOP technologies (Jafarinejad, 2019; Suzuki *et al*., 2015; Bethi *et al*., 2016). Although traditional AOP technology has good removal efficiency for many residual contaminants, it requires a significant amount of energy and other expenses, limiting the application of this technology in water treatment plants (Adeleye *et al*., 2016a; Jafarinejad, 2019; Mahamuni and Adewuyi, 2010). By introducing nanoTiO_2 into the AOP system, the increase rate of photodegradation can improve the efficiency of AOP and save energy required for the treatment (Suzuki *et al*., 2015; Bethi *et al*., 2016).

Additionally, some research explored the combination of nanomaterials with biological treatment (Yang *et al*., 2019a; Almusawy *et al*., 2020; Dixit *et al*., 2011). CNTs were considered a promising material for membrane bioreactor (MBR) because of their high porosity and electron transport efficiency (Hinds *et al*., 2004; Wei *et al*., 2014). A recent study set up a CNTs-based electro-assisted MBR (EMBR) system to treat municipal wastewater (**Yang *et al*., 2019a**). The effluent had less than 40 mg/L of chemical oxygen demand (COD) and 3 mg/L of NH_4^+-N concentration with 4 h hydraulic retention time (HRT), which was significantly lower than that of two traditional PVDF-based MBR systems (over 50 mg/L of COD and 5 mg/L of NH_4^+-N in effluent). Also, electrochemical oxidation could degrade the contaminants on the membrane surface and result in a better anti-fouling property.

Case Studies of Commercial Products Enabled With Nanomaterials

Combination of direct current electrode with nZVI to remove chlorinated ethenes (CEs) from groundwater

Due to its high reactivity, nZVI has become one of the most applied nanomaterials in commercial groundwater treatment. A recent study assessed the performance of commercial nZVI for removal of chlorinated ethenes (CEs) from groundwater (**Černíková *et al*., 2020**). In the study, two different types of commercial nZVIs, TODA and NF 25S, were introduced into multiple wells, and regularly replenished to keep the nZVI concentration at 2–5 kg/m^3. In the injected groundwater, the initial concentration of CEs was 8880 µg/L, dichloroethane (DCE) was the main component (about 7300 µg/L), while vinyl chloride (VC), perchloroethene (PCE), and trichloroethene (TCE) were present at lower amounts. After 25 months of nZVI loading, direct current (DC) electrodes were introduced into the reaction system to test the effect of an electric field on the remediation performance of nZVI. The electrodes were made of stainless steel (because of lower replacement cost), and the distance between the two electrodes was 3 m. The system had a 24 V DC, 7–15 A current, and the maximum output power to the well was 0.24 kW. The anode electrode was regularly replaced due to the adverse effects of aging and formation of oxide layer on electrode after long-term use performance.

Within the 64 months of monitoring, the researchers found that the concentrations of the CEs in groundwater decreased to 50–60% of the initial level after 4-month treatment with nZVI alone. However, due to the consumption of nZVI during the degradation of CEs and the production of byproducts, the concentrations of the pollutants rebounded to the original level or higher after 4 months. The two commercial nZVIs, which were from different manufacturers, had different removal efficiencies on CEs (~46% for TODA and ~60% for NF 25 S) after 4 months of remediation. When the electric field was introduced, the concentration of CEs decreased below 2000 µg/L (about 22% of the initial value) within 4 months. After 50 months and several regular anode replacements, CE concentrations further decreased to 210 µg/L (approximately 2% of the initial value). The concentration rebound was again observed when the electrode failure. The introduction of the electric field modified the degradation mechanisms since oxidation of chlorinated solvents at the anode produced mineralized products, and reduction of the chlorinated solvents at the cathode dechlorinated them into alkanes or a small amount of chlorinated intermediate products. Regarding the processing equipment cost, the study pointed out that when using nZVI alone, the system costs 28.7–34.4 EUR/g of CEs treated. However, introducing DC electrode decreased the cost to 5.2 EUR/g of CEs treated.

Combination of nZVI with biotechnology to treat Cr (VI) and chlorinated solvents in groundwater

In this study, nZVI was combined with biotechnology to remove Cr (VI) and chlorinated solvents in groundwater (**Němeček *et al*., 2016**). The initial concentration of Cr (VI) in groundwater was 4.4–57 mg/L, and CEs were 400–6526 µg/L (where TCE and cis-DCE were the main species). Initially, nZVI was injected into the well to achieve an nZVI concentration of 1 g/L, and again 3 months later to reach a concentration of 2 g/L. Three months after the second nZVI injection, whey was injected and recirculation was started. In the next 10 months, whey was continuously supplemented to maintain the total organic compound (TOC) concentration in the groundwater at 60 mg/L.

When nZVI was initially injected, the concentration of Cr (VI) immediately decreased below the limit of quantitation (LOQ = 0.05 mg/L). However, around one month later, Cr (VI) concentration increased and eventually reached 10%–15% of the initial concentration. A similar decrease and rebound were also found during the second injection, after more nZVI was applied. A low removal efficiency of CEs was also observed during this period because of competition between CEs and Cr (VI). However, after adding whey the concentration of Cr (VI) and CEs decreased rapidly. The concentration of Cr (VI) was lower than the LOQ level, and the reduction product, Cr (III), was immobilized in the soil in oxide and hydroxide forms. CE concentrations after treatment were as low as 0.1–0.2 µg/L. The study indicated that the microorganisms in the whey reduced the oxidized iron (trivalent iron (Fe (III)) to divalent iron (Fe (II))). The Fe (II) acted as a reducing agent for Cr (VI) reduction and extended the service life of nZVI. Additionally, the toxicity of the groundwater was significantly reduced after treatment, indicating that the technology was effective. However, the Cr speciation in soil after the remediation and the possibility of the Cr remobilization in the future were not considered in the study.

Degradation of petroleum hydrocarbons in groundwater with nanoTiO_2 and AOP

Nanosized TiO_2 has a low cost, large surface area, high reactivity, and is considered a promising material for water treatment in the real environment. The small band gap in nanoTiO_2 leads to strong photoreactivity. NanoTiO_2 can generate hydroxyl radicals under solar light (especially UV light) and oxidize residual organic substances. Therefore, nanoTiO_2 is suitable for the AOP-based water purification. In a study, nanoTiO_2 was applied for the treatment of petroleum hydrocarbons in groundwater via sunlight irradiation (**Cho *et al*., 2006**). Two different types of nanoTiO_2 (with a concentration of 1.0% wt.), nanoTiO_2 sludge and nanoTiO_2 immobilized on ceramic beads, were introduced into the photoreactor. The photoreactor unit comprised several quartz columns. The bottom and side of each column were surrounded by aluminum foil with high UV reflectivity. The entire reactor was perpendicular to the incident angle of the noon sun to obtain a high radiation area. The entire system consisted of 4 continuous reactors units (total radiation area was 3 m^2), and the concentrations of benzene, toluene, ethylbenzene, and xylene (BTEX) and total petroleum hydrocarbons (TPH) in the effluent were monitored from noon to 4 pm. In addition, combinations of sunlight + H_2O_2 and sunlight + H_2O_2 + nanoTiO_2 were also used to test the treatment of BTEX and TPH.

Before the treatment, the initial BTEX and TPH concentrations in the groundwater were 46.9–103.0 mg/L and 584.0–954.0 mg/L, respectively. After 4 h of sunlight exposure, the removal of BTEX and TPH in 10 mM H_2O_2-treated group was only 40% and 10%, respectively, due to low generation of hydroxyl radicals from H_2O_2 under sunlight. Higher removal efficiencies were observed in the slurry nanoTiO_2-treated group (80% removal for BTEX and 76% for TPH) than immobilized nanoTiO_2-treated group (35% removal for BTEX and 11% for TPH) in the presence of sunlight. The difference in removal efficiency might be related to higher surface area of nanoTiO_2 in the slurry system than in the immobilized system. The addition of 10 mM H_2O_2 in sunlight + nanoTiO_2 system increased the

removal efficiency to 100% (BTEX) and 88% (TPH) in the slurry nanoTiO_2-treated group, and 66% (BTEX) and 50% (TPH) in the immobilized nanoTiO_2-treated group, indicating the promotion of photo-oxidation by H_2O_2.

Although a better remediation performance was found in the slurry nanoTiO_2-treated group, the recovery of slurry nanoparticles was difficult. Thus, the H_2O_2 + immobilized nanoTiO_2 is a better choice in real-world treatment. Another issue with this system is that the reactor may not work continuously due to the limited daylight time. Therefore, combining solar irradiation with an artificial UV light system may improve the overall efficiency of the system.

Conclusions and Recommendations

With the intensification of water resources issues, it will become more challenging for traditional water treatment technologies to meet increasingly stringent water quality standards, especially for emerging contaminants that most traditional technologies cannot remove efficiently. Although some existing advanced water treatment technologies can remove these hard-to-degrade pollutants, these technologies often consume a large amount of energy, and are not economical, especially when dealing with residual pollutants. There is considerable interest in nanomaterials for water treatment given their high adsorption and/or filtration capacities, and/or reactivity. Also, there is the potential for nanotechnology to be simple to operate and consume less energy. In addition, the performance of nanomaterials can be improved by hybridization or doping with other materials, making them applicable to different environmental conditions and pollutants. However, studies on using nanomaterials to remove DBPs and emerging contaminants (such as MPs and PFASs) are still lacking (**Fig. 5**). Thus, more research should consider the possibility of applying nanomaterials for removing these important persistent contaminants.

Nanomaterials have great potential in water treatment but many issues need to be further investigated and resolved. For example, the fate and transport, and toxic effects of residual nanomaterials after treatment must be fully assessed. Several studies have confirmed that some nanomaterials are toxic to organisms, making it imperative to effectively recover the nanomaterials after their use, or consider further modification to reduce their toxicity. In addition, most of the current studies are lab-scale or pilot-scale, and there is a need to consider how these novel materials can be incorporated into conventional treatment trains. Therefore, future studies should also consider the path to commercial application, including decreasing the cost of nanomaterial synthesis and processing.

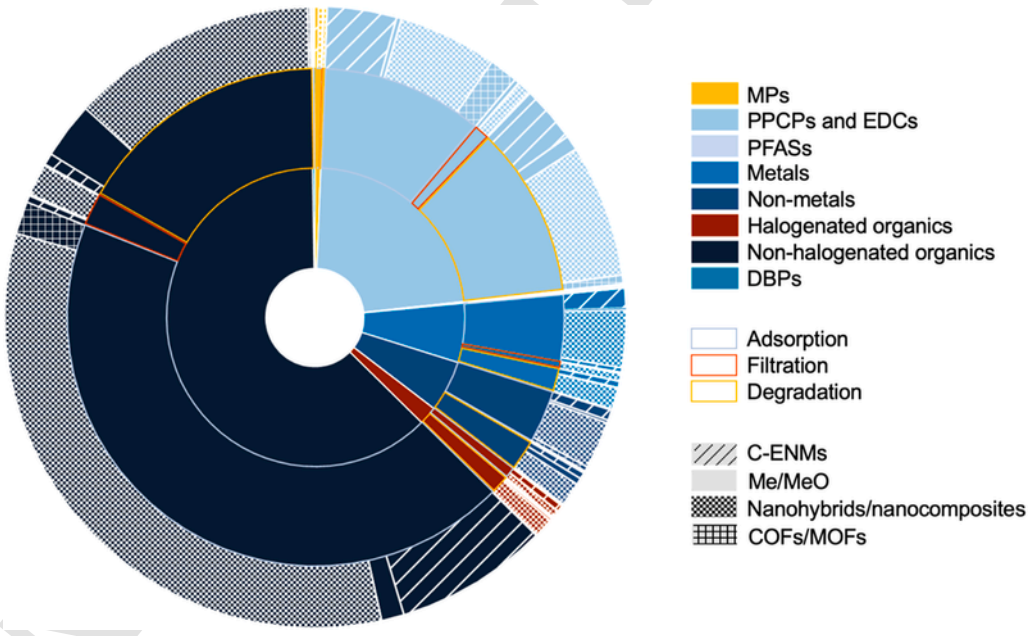

Fig. 5 Studies considering different nanomaterials to remove contaminants from water based on different mechanisms. The inner circle refers to 4 types of nanomaterials (with different colors). The middle circle displays the mechanisms applied for treatment (with different border colors). The outermost circle indicates the nanomaterials applied for treatment (with different textures). The data was collected from the Web of Science considering the last 5 years (2016–2021).

References

Abd-Elhamid, A.I., Kamoun, E.A., El-Shanshory, A.A., Soliman, H.M.A., Aly, H.F., 2019. Evaluation of graphene oxide-activated carbon as effective composite adsorbent toward the removal of cationic dyes: Composite preparation, characterization and adsorption parameters. Journal of Molecular Liquids 279, 530–539.

Abejón, A., Garea, A., Irabien, A., 2015. Arsenic removal from drinking water by reverse osmosis: Minimization of costs and energy consumption. Separation and Purification Technology 144, 46–53.

Adeleye, A.S., Conway, J.R., Garner, K., et al., 2016. Engineered nanomaterials for water treatment and remediation: Costs, benefits, and applicability. Chemical Engineering Journal 286, 640–662.

Adeleye, A.S., Stevenson, L.M., Su, Y., et al., 2016. Influence of phytoplankton on fate and effects of modified zerovalent iron nanoparticles. Environmental Science & Technology 50 (11), 5597–5605.

Adeleye, A.S., Wang, X., Wang, F., et al., 2018. Photoreactivity of graphene oxide in aqueous system: Reactive oxygen species formation and bisphenol A degradation. Chemosphere 195, 344–350.

Adeleye, A.S., Keller, A.A., Miller, R.J., Lenihan, H.S., 2013. Persistence of commercial nanoscaled zero-valent iron (nZVI) and by-products. Journal of Nanoparticle Research 15 (1), 1–18.

Adlnasab, L., Shekari, N., Maghsodi, A., 2019. Optimization of arsenic removal with Fe_3O_4@Al_2O_3@Zn-Fe LDH as a new magnetic nano adsorbent using Box-Behnken design. Journal of Environmental Chemical Engineering 7 (2), 102974.

Ahamad, T., Naushad, M., Al-Maswari, B.M., et al., 2017. Synthesis of a recyclable mesoporous nanocomposite for efficient removal of toxic Hg^{2+} from aqueous medium. Journal of industrial and Engineering Chemistry 53, 268–275.

Ahlawat, W., Kataria, N., Dilbaghi, N., et al., 2020. Carbonaceous nanomaterials as effective and efficient platforms for removal of dyes from aqueous systems. Environmental Research 181, 108904.

Ahmad, M., Ahmad, M., Usman, A.R., et al., 2018. Biochar composites with nano zerovalent iron and eggshell powder for nitrate removal from aqueous solution with coexisting chloride ions. Environmental Science and Pollution Research 25 (26), 25757–25771.

Ahmadzadeh Tofighy, M., Mohammadi, T., 2012. Nitrate removal from water using functionalized carbon nanotube sheets. Chemical Engineering Research and Design 90 (11), 1815–1822.

Ahmed, M.B., Alam, M.M., Zhou, J.L., et al., 2020. Advanced treatment technologies efficacies and mechanism of per- and poly-fluoroalkyl substances removal from water. Process Safety and Environmental Protection 136, 1–14.

Ahsan, M.A., Jabbari, V., Islam, M.T., et al., 2019. Sustainable synthesis and remarkable adsorption capacity of MOF/graphene oxide and MOF/CNT based hybrid nanocomposites for the removal of Bisphenol A from water. Science of the Total Environment 673, 306–317.

Aich, N., Plazas-Tuttle, J., Lead, J.R., Saleh, N.B., 2014. A critical review of nanohybrids: Synthesis, applications and environmental implications. Environmental Chemistry 11 (6), 609–623.

Aigbe, U.O., Osibote, O.A., 2020. A review of hexavalent chromium removal from aqueous solutions by sorption technique using nanomaterials. Journal of Environmental Chemical Engineering 8 (6), 104503.

Akinpelu, A.A., Ali, M.E., Johan, M.R., et al., 2019. Effect of the oxidation process on the molecular interaction of polyaromatic hydrocarbons (PAH) with carbon nanotubes: Adsorption kinetic and isotherm study. Journal of Molecular Liquids 289, 111107.

Al-Anazi, A., Abdelraheem, W.H., Scheckel, K., et al., 2020. Novel franklinite-like synthetic zinc-ferrite redox nanomaterial: Synthesis, and evaluation for degradation of diclofenac in water. Applied Catalysis B: Environmental 275, 119098.

Alavi, S.N., Jozi, S.A., Tahvildar, K., Khoramnezhadian, S., 2021. Advanced oxidation process for haloacetic acid removal in tehranpars water treatment using CuO nanocatalyst. Journal of Applied Chemical Research 15 (1), 36–45.

Ali, I., Peng, C., Naz, I., 2019. Removal of lead and cadmium ions by single and binary systems using phytogenic magnetic nanoparticles functionalized by 3-marcaptopropanic acid. Chinese Journal of Chemical Engineering 27 (4), 949–964.

Ali, S., Rehman, S.A.U., Luan, H.-Y., Farid, M.U., Huang, H., 2019. Challenges and opportunities in functional carbon nanotubes for membrane-based water treatment and desalination. Science of The Total Environment 646, 1126–1139.

Ali, M., Shan, A., Sun, Y., et al., 2020. Trichloroethylene degradation by PVA-coated calcium peroxide nanoparticles in Fe (II)-based catalytic systems: Enhanced performance by citric acid and nanoscale iron sulfide. Environmental Science and Pollution Research 1–15.

Alijani, H., Shariatinia, Z., 2018. Synthesis of high growth rate SWCNTs and their magnetite cobalt sulfide nanohybrid as super-adsorbent for mercury removal. Chemical Engineering Research and Design 129, 132–149.

Alimohammadi, V., Sedighi, M., Jabbari, E., 2016. Response surface modeling and optimization of nitrate removal from aqueous solutions using magnetic multi-walled carbon nanotubes. Journal of Environmental Chemical Engineering 4 (4), 4525–4535.

Almassi, S., Samonte, P.R.V., Li, Z., Xu, W., Chaplin, B.P., 2020. Mechanistic investigation of haloacetic acid reduction using carbon-Ti_4O_7 composite reactive electrochemical membranes. Environmental Science & Technology 54 (3), 1982–1991.

Almusawy, A.M., Al-Anbari, R.H., Alsalhy, Q.F., Al-Najar, A.I., 2020. Carbon nanotubes-sponge modified electro membrane bioreactor (EMBR) and their prospects for wastewater treatment applications. Membranes 10 (12), (433).

Alturki, A.A., Tadkaew, N., McDonald, J.A., et al., 2010. Combining MBR and NF/RO membrane filtration for the removal of trace organics in indirect potable water reuse applications. Journal of Membrane Science 365 (1–2), 206–215.

Amde, M., Yao, J., Liu, J.-F., Tan, Z.-Q., 2020. Nano-selenium functionalized zinc oxide nanorods: A superadsorbent for mercury (II) removal from waters. Journal of Hazardous Materials 392, 122495.

Anand, A., Unnikrishnan, B., Mao, J.-Y., Lin, H.-J., Huang, C.-C., 2018. Graphene-based nanofiltration membranes for improving salt rejection, water flux and antifouling – A review. Desalination 429, 119–133.

Anand, S.R., Aggarwal, R., Saini, D., et al., 2019. Removal of toxic chromium (VI) from the wastewater under the sunlight-illumination by functionalized carbon nano-rods. Solar Energy 193, 774–781.

Andrade, P.F., de Faria, A.F., Oliveira, S.R., Arruda, M.A.Z., do Carmo Gonçalves, M., 2015. Improved antibacterial activity of nanofiltration polysulfone membranes modified with silver nanoparticles. Water Research 81, 333–342.

Angamuthu, M., Satishkumar, G., Landau, M.V., 2017. Precisely controlled encapsulation of Fe_3O_4 nanoparticles in mesoporous carbon nanodisk using iron based MOF precursor for effective dye removal. Microporous and Mesoporous Materials 251, 58–68.

Apopei, P., Orha, C., Popescu, M.I., et al., 2020. Diclofenac removal from water by photocatalysis- assisted filtration using activated carbon modified with N-doped TiO_2. Process Safety and Environmental Protection 138, 324–336.

Arizavi, A., Mirbagheri, N., Hosseini, Z., Chen, P., Sabbaghi, S., 2019. Efficient removal of naphthalene from aqueous solutions using a nanoporous kaolin/Fe_3O_4 composite. International Journal of Environmental Science and Technology 1–12.

Arshad, A., Iqbal, J., Mansoor, Q., 2017. NiO-nanoflakes grafted graphene: An excellent photocatalyst and a novel nanomaterial for achieving complete pathogen control. Nanoscale 9 (42), 16321–16328.
Arshad, A., Iqbal, J., Ahmad, I., Israr, M., 2018. Graphene/Fe_3O_4 nanocomposite: Interplay between photo-Fenton type reaction, and carbon purity for the removal of methyl orange. Ceramics International 44 (3), 2643–2648.
Auset, M., Keller, A.A., 2006. Pore-scale visualization of colloid straining and filtration in saturated porous media using micromodels. Water Resources Research 42 (12).
Babuponnusami, A., Muthukumar, K., 2012. Removal of phenol by heterogenous photo electro Fenton-like process using nano-zero valent iron. Separation and Purification Technology 98, 130–135.
Bae, S., Hanna, K., 2015. Reactivity of nanoscale zero-valent iron in unbuffered systems: Effect of pH and Fe (II) dissolution. Environmental Science & Technology 49 (17), 10536–10543.
Bahnemann, D., 2004. Photocatalytic water treatment: Solar energy applications. Solar Energy 77 (5), 445–459.
Bai, D., Wang, X., Huo, D., et al., 2019. Coprecipitation preparation of Cu/Zn/Al-hydrotalcite-like compound for copper removal from electroplating wastewater. Journal of Chemistry
Balamurugan, K., Subramanian, V., 2013. Adsorption of chlorobenzene onto (5,5) armchair single-walled carbon nanotube and graphene sheet: Toxicity versus adsorption strength. The Journal of Physical Chemistry C 117 (41), 21217–21227.
Balarak, D., Mahdavi, Y., Maleki, A., Daraei, H., Sadeghi, S., 2016. Studies on the removal of amoxicillin by single walled carbon nanotubes. Journal of Pharmaceutical Research International 1–9.
Bandehali, S., Parvizian, F., Moghadassi, A., Hosseini, S., 2019. Copper and lead ions removal from water by new PEI based NF membrane modified by functionalized POSS nanoparticles. Journal of Polymer Research 26 (9), 1–8.
Banks, D., Jun, B.-M., Heo, J., et al., 2020. Selected advanced water treatment technologies for perfluoroalkyl and polyfluoroalkyl substances: A review. Separation and Purification Technology 231, 115929.
Barrejón, M., Syrgiannis, Z., Burian, M., et al., 2019. Cross-linked carbon nanotube adsorbents for water treatment: Tuning the sorption capacity through chemical functionalization. ACS Applied Materials & Interfaces 11 (13), 12920–12930.
Barrera-Díaz, C.E., Lugo-Lugo, V., Bilyeu, B., 2012. A review of chemical, electrochemical and biological methods for aqueous Cr (VI) reduction. Journal of Hazardous Materials 223–224, 1–12.
Behjati, M., Baghdadi, M., Karbassi, A., 2018. Removal of mercury from contaminated saline wasters using dithiocarbamate functionalized-magnetic nanocomposite. Journal of Environmental Management 213, 66–78.
Bethi, B., Sonawane, S.H., Rohit, G.S., et al., 2016. Investigation of TiO2 photocatalyst performance for decolorization in the presence of hydrodynamic cavitation as hybrid AOP. Ultrasonics Sonochemistry 28, 150–160.
Boller, M., 1997. Small wastewater treatment plants – A challenge to wastewater engineers. Water Science and Technology 35 (6), 1–12.
Brame, J., Li, Q., Alvarez, P.J.J., 2011. Nanotechnology-enabled water treatment and reuse: Emerging opportunities and challenges for developing countries. Trends in Food Science & Technology 22 (11), 618–624.
Brandes, R., Belosinschi, D., Brouillette, F., Chabot, B., 2019. A new electrospun chitosan/phosphorylated nanocellulose biosorbent for the removal of cadmium ions from aqueous solutions. Journal of Environmental Chemical Engineering 7 (6), 103477.
Brienza, M., Katsoyiannis, I.A., 2017. Sulfate radical technologies as tertiary treatment for the removal of emerging contaminants from wastewater. Sustainability 9 (9), (1604).
Cao, Y., Hu, X., Zhu, C., et al., 2020. Sulfhydryl functionalized covalent organic framework as an efficient adsorbent for selective Pb (II) removal. Colloids and Surfaces A: Physicochemical and Engineering Aspects 600, 125004.
Cao, Z., Liu, X., Xu, J., et al., 2017. Removal of antibiotic florfenicol by sulfide-modified nanoscale zero-valent iron. Environmental Science & Technology 51 (19), 11269–11277.
Černíková, M., Nosek, J., Černík, M., 2020. Combination of nZVI and DC for the in-situ remediation of chlorinated ethenes: An environmental and economic case study. Chemosphere 245, 125576.
Chang, Y., Cho, Y.-C., Lin, Y.-P., 2020. Degradation of PFOS by a MnO_2/H_2O_2 process. Environmental Science: Water Research & Technology 6 (12), 3476–3487.
Chen, C., Hu, J., Shao, D., Li, J., Wang, X., 2009. Adsorption behavior of multiwall carbon nanotube/iron oxide magnetic composites for Ni (II) and Sr (II). Journal of Hazardous Materials 164 (2–3), 923–928.
Chen, H., Cao, Y., Wei, E., Gong, T., Xian, Q., 2016. Facile synthesis of graphene nano zero-valent iron composites and their efficient removal of trichloronitromethane from drinking water. Chemosphere 146, 32–39.
Chen, Y.J., Chen, Y.F., Miao, C., et al., 2020. Metal-organic framework-based foams for efficient microplastics removal. Journal of Materials Chemistry A 8 (29), 14644–14652.
Chen, H., Huang, M., Liu, Y., Meng, L., Ma, M., 2020. Functionalized electrospun nanofiber membranes for water treatment: A review. Science of the Total Environment 739, 139944.
Chen, J., Meng, X., Tian, Y., et al., 2020. Fabrication of a superhydrophilic PVDF-g-PAA@ FeOOH ultrafiltration membrane with visible light photo-fenton self-cleaning performance. Journal of Membrane Science 616, 118587.
Chen, M.-J., Lo, S.-L., Lee, Y.-C., Huang, C.-C., 2015. Photocatalytic decomposition of perfluorooctanoic acid by transition-metal modified titanium dioxide. Journal of Hazardous Materials 288, 168–175.
Chen, P.-J., Tan, S.-W., Wu, W.-L., 2012. Stabilization or oxidation of nanoscale zerovalent iron at environmentally relevant exposure changes bioavailability and toxicity in Medaka Fish. Environmental Science & Technology 46 (15), 8431–8439.
Chen, P.-J., Wu, W.-L., Wu, K.C.-W., 2013. The zerovalent iron nanoparticle causes higher developmental toxicity than its oxidation products in early life stages of medaka fish. Water Research 47 (12), 3899–3909.
Chen, W., Parette, R., Zou, J., Cannon, F.S., Dempsey, B.A., 2007. Arsenic removal by iron-modified activated carbon. Water Research 41 (9), 1851–1858.
Cheng, Y., Dong, H., Lu, Y., et al., 2019. Toxicity of sulfide-modified nanoscale zero-valent iron to Escherichia coli in aqueous solutions. Chemosphere 220, 523–530.
Cheng, X., Zhou, W., Li, P., et al., 2019. Improving ultrafiltration membrane performance with pre-deposited carbon nanotubes/nanofibers layers for drinking water treatment. Chemosphere 234, 545–557.
Cho, I.H., Kim, L.H., Zoh, K.D., Park, J.H., Kim, H.Y., 2006. Solar photocatalytic degradation of groundwater contaminated with petroleum hydrocarbons. Environmental progress 25 (2), 99–109.
Chong, M.N., Jin, B., Chow, C.W.K., Saint, C., 2010. Recent developments in photocatalytic water treatment technology: A review. Water Research 44 (10), 2997–3027.
Clark, C.A., Heck, K.N., Powell, C.D., Wong, M.S., 2019. Highly defective UiO-66 materials for the adsorptive removal of perfluorooctanesulfonate. ACS Sustainable Chemistry & Engineering 7 (7), 6619–6628.
Clark, K.K., Keller, A.A., 2012. Investigation of two magnetic permanently confined micelle array sorbents using nonionic and cationic surfactants for the removal of PAHs and pesticides from aqueous media. Water, Air, & Soil Pollution 223 (7), 3647–3655.

Clark, K.K., Keller, A.A., 2012. Adsorption of perchlorate and other oxyanions onto magnetic permanently confined micelle arrays (Mag-PCMAs). Water Research 46 (3), 635–644.
Cui, F.Z., Liang, R.R., Qi, Q.Y., Jiang, G.F., Zhao, X., 2019. Efficient removal of Cr (VI) from aqueous solutions by a dual-pore covalent organic framework. Advanced Sustainable Systems 3 (4), 1800150.
Cui, W.-R., Jiang, W., Zhang, C.-R., et al., 2020. Regenerable carbohydrazide-linked fluorescent covalent organic frameworks for ultrasensitive detection and removal of mercury. ACS Sustainable Chemistry & Engineering 8 (1), 445–451.
Cui, J., Zhang, Y., Zheng, Y., et al., 2020. Catalytic degradation of carbamazepine by a novel granular visible-light-driven photocatalyst activating the peroxydisulfate system. Chemical Engineering Journal127867.
Das, R., Abd Hamid, S., Ali, S.B., et al., 2014. Multifunctional carbon nanotubes in water treatment: The present, past and future. Desalination 354, 160–179.
Daud, Z., Awang, H., Latif, A.A.A., et al., 2015. Suspended solid, color, COD and oil and grease removal from biodiesel wastewater by coagulation and flocculation processes. Procedia - Social and Behavioral Sciences 195, 2407–2411.
Davood Abadi Farahani, M.H., Borghei, S.M., Vatanpour, V., 2016. Recovery of cooling tower blowdown water for reuse: The investigation of different types of pretreatment prior nanofiltration and reverse osmosis. Journal of Water Process Engineering 10, 188–199.
de S. Furtado, R.X., Sabatini, C.A., Zaiat, M., Azevedo, E.B., 2021. Perfluorooctane sulfonic acid (PFOS) degradation by optimized heterogeneous photocatalysis (TiO_2/UV) using the response surface methodology (RSM). Journal of Water Process Engineering 41, 101986.
Dehghani, M.H., Mohammadi, M., Mohammadi, M.A., et al., 2016. Equilibrium and kinetic studies of trihalomethanes adsorption onto multi-walled carbon nanotubes. Water, Air, & Soil Pollution 227 (9), 1–17.
Deng, J., Dong, H., Zhang, C., et al., 2018. Nanoscale zero-valent iron/biochar composite as an activator for Fenton-like removal of sulfamethazine. Separation and Purification Technology 202, 130–137.
Diagboya, P.N., Olu-Owolabi, B.I., Adebowale, K.O., 2015. Synthesis of covalently bonded graphene oxide–iron magnetic nanoparticles and the kinetics of mercury removal. RSC Advances 5 (4), 2536–2542.
Ding, B., Huang, S., Pang, K., Duan, Y., Zhang, J., 2018. Nitrogen-enriched carbon nanofiber aerogels derived from marine chitin for energy storage and environmental remediation. ACS Sustainable Chemistry & Engineering 6 (1), 177–185.
Ding, Y., Hu, Y., Peng, X., Xiao, Y., Huang, J., 2020. Micro-nano structured CoS: An efficient catalyst for peroxymonosulfate activation for removal of bisphenol A. Separation and Purification Technology 233, 116022.
Dixit, A., Tirpude, A.J., Mungray, A.K., Chakraborty, M., 2011. Degradation of 2, 4 DCP by sequential biological–advanced oxidation process using UASB and UV/TiO2/H2O2. Desalination 272 (1), 265–269.
Dolar, D., Košutić, K., Ašperger, D., 2013. Influence of adsorption of pharmaceuticals onto RO/NF membranes on their removal from water. Water, Air, & Soil Pollution 224 (1), 1–13.
Dos Santos, S., Adams, E.A., Neville, G., et al., 2017. Urban growth and water access in sub-Saharan Africa: Progress, challenges, and emerging research directions. Science of the Total Environment 607–608, 497–508.
Dou, J., Gan, D., Huang, Q., et al., 2019. Functionalization of carbon nanotubes with chitosan based on MALI multicomponent reaction for Cu2+ removal. International Journal of Biological Macromolecules 136, 476–485.
Du, T., Adeleye, A.S., Zhang, T., et al., 2018. Influence of light wavelength on the photoactivity, physicochemical transformation, and fate of graphene oxide in aqueous media. Environmental Science: Nano 5 (11), 2590–2603.
Du, Y., Lv, X.-T., Wu, Q.-Y., et al., 2017. Formation and control of disinfection byproducts and toxicity during reclaimed water chlorination: A review. Journal of Environmental Sciences 58, 51–63.
Du, Z., Deng, S., Bei, Y., et al., 2014. Adsorption behavior and mechanism of perfluorinated compounds on various adsorbents – A review. Journal of hazardous materials 274, 443–454.
Ekambaram, N., Varjani, S., Goswami, S., Singh, U., Kapoor, T., 2020. Chitosan-based silver nanocomposite for hexavalent-chromium removal from tannery industry effluent using a packed-bed reactor. Journal of Environmental Engineering 146 (6), 04020032.
Eke, J., Banks, L., Mottaleb, M.A., et al., 2021. Dual-functional phosphorene nanocomposite membranes for the treatment of perfluorinated water: An investigation of perfluorooctanoic acid removal via filtration combined with ultraviolet irradiation or oxygenation. Membranes 11 (1), (18).
Elanchezhiyan, S.S., Muthu Prabhu, S., Han, J., et al., 2020. , Synthesis and characterization of novel magnetic Zr-MnFe2O4@rGO nanohybrid for efficient removal of PFOA and PFOS from aqueous solutions. Applied Surface Science 528, 146579.
ElHussein, E.A.A., Şahin, S., Bayazit, Ş.S., 2020. Removal of carbamazepine using UiO-66 and UiO-66/graphene nanoplatelet composite. Journal of Environmental Chemical Engineering 8 (4), 103898.
Elmaci, G., 2020. Microwave-assisted rapid synthesis of C@ Fe_3O_4 composite for removal of microplastics from drinking water. Adıyaman Üniversitesi Fen Bilimleri Dergisi 10 (1), 207–217.
El-Shamy, A.G., 2020. Synthesis of new magnesium peroxide (MgO2) nano-rods for pollutant dye removal and antibacterial applications. Materials Chemistry and Physics 243, 122640.
Fan, W., Gao, W., Zhang, C., et al., 2012. Hybridization of graphene sheets and carbon-coated Fe_3O_4 nanoparticles as a synergistic adsorbent of organic dyes. Journal of Materials Chemistry 22 (48), 25108–25115.
Fang, Y., Al-Abed, S.R., 2007. Modeling the electrolytic dechlorination of trichloroethylene in a granular graphite-packed reactor. Environmental Engineering Science 24 (5), 581–594.
Fang, Y., Wen, J., Zhang, H., Wang, Q., Hu, X., 2020. Enhancing Cr (VI) reduction and immobilization by magnetic core-shell structured NZVI@MOF derivative hybrids. Environmental Pollution 260, 114021.
Fausey, C.L., Zucker, I., Lee, D.E., et al., 2020. Tunable molybdenum disulfide-enabled fiber mats for high-efficiency removal of mercury from water. ACS Applied Materials & Interfaces 12 (16), 18446–18456.
Feng, C., Khulbe, K.C., Matsuura, T., Tabe, S., Ismail, A.F., 2013. Preparation and characterization of electro-spun nanofiber membranes and their possible applications in water treatment. Separation and Purification Technology 102, 118–135.
Feng, J., Zhu, B.-W., Lim, T.-T., 2008. Reduction of chlorinated methanes with nano-scale Fe particles: Effects of amphiphiles on the dechlorination reaction and two-parameter regression for kinetic prediction. Chemosphere 73 (11), 1817–1823.
Franz, S., Falletta, E., Arab, H., et al., 2020. Degradation of carbamazepine by photo (electro)catalysis on nanostructured TiO_2 Meshes: Transformation products and reaction pathways. Catalysts 10 (2), (169).
Ganiyu, S.O., Van Hullebusch, E.D., Cretin, M., Esposito, G., Oturan, M.A., 2015. Coupling of membrane filtration and advanced oxidation processes for removal of pharmaceutical residues: A critical review. Separation and Purification Technology 156, 891–914.
Garner, K.L., Keller, A.A., 2014. Emerging patterns for engineered nanomaterials in the environment: A review of fate and toxicity studies. Journal of Nanoparticle Research 16 (8), (2503).
Garner, K.L., Suh, S., Lenihan, H.S., Keller, A.A., 2015. Species sensitivity distributions for engineered nanomaterials. Environmental Science & Technology 49 (9), 5753–5759.

Ghaemi, N., Daraei, P., Akhlaghi, F.S., 2018. Polyethersulfone nanofiltration membrane embedded by chitosan nanoparticles: Fabrication, characterization and performance in nitrate removal from water. Carbohydrate Polymers 191, 142–151.
Ghernaout, D., 2017. Water treatment chlorination: An updated mechanistic insight review. Chemistry Research Journal 2, 125–138.
Ghernaout, D., 2020. Towards enhancing ozone diffusion for water disinfection – Short notes. Open Access Library Journal 7 (4), (1).
Goetjen, T.A., Liu, J., Wu, Y., et al., 2020. Metal–organic framework (MOF) materials as polymerization catalysts: A review and recent advances. Chemical Communications 56 (72), 10409–10418.
Goodwin, D.G., Adeleye, A.S., Sung, L., et al., 2018. Detection and quantification of graphene-family nanomaterials in the environment. Environmental Science & Technology 52 (8), 4491–4513.
Grassian, V.H., 2008. Nanoscience and Nanotechnology: Environmental and Health Impacts. John Wiley & Sons.
Gu, M., Farooq, U., Lu, S., et al., 2018. Degradation of trichloroethylene in aqueous solution by rGO supported nZVI catalyst under several oxic environments. Journal of Hazardous Materials 349, 35–44.
Gu, M., Hao, L., Wang, Y., et al., 2020. The selective heavy metal ions adsorption of zinc oxide nanoparticles from dental wastewater. Chemical Physics 534, 110750.
Gude, V.G., 2015. Energy and water autarky of wastewater treatment and power generation systems. Renewable and Sustainable Energy Reviews 45, 52–68.
Guo, Z., Liu, J., Li, Y., et al., 2020. Biocatalytic metal–organic framework nanomotors for active water decontamination. Chemical Communications 56 (94), 14837–14840.
Guo, B., Xu, T., Zhang, L., Li, S., 2020. A heterogeneous fenton-like system with green iron nanoparticles for the removal of bisphenol A: Performance, kinetics and transformation mechanism. Journal of Environmental Management 272, 111047.
Guo, S., Xu, H., Zhang, F., Zhu, X., Li, X., 2018. Preparation and adsorption properties of nano magnetite silica gel for methylene blue from aqueous solution. Colloids and Surfaces A: Physicochemical and Engineering Aspects 546, 244–253.
Guo, S., Zhang, J., Li, X., Zhang, F., Zhu, X., 2018. Fe3O4-CS-L: a magnetic core-shell nano adsorbent for highly efficient methyl orange adsorption. Water Science and Technology 77 (3), 628–637.
Gupta, V.K., Kumar, R., Nayak, A., Saleh, T.A., Barakat, M.A., 2013. Adsorptive removal of dyes from aqueous solution onto carbon nanotubes: A review. Advances in Colloid and Interface Science 193–194, 24–34.
Han, L., Li, B., Tao, S., et al., 2020. Graphene oxide-induced formation of a boron-doped iron oxide shell on the surface of NZVI for enhancing nitrate removal. Chemosphere 252, 126496.
Han, E.D., Park, C.W., Lee, S.H., Kim, B.H., Seo, Y.H., 2020. Polar molecule filtration using charged cellulose nanofiber membrane on the nanoporous alumina support for high rejection efficiency. Cellulose 27 (5), 2685–2694.
Han, Z., Salawu, O.A., Zenobio, J.E., Zhao, Y., Adeleye, A.S., 2021. Emerging investigator series: Immobilization of arsenic in soil by nanoscale zerovalent iron: role of sulfidation and application of machine learning. Environmental Science: Nano 8 (3), 619–633.
Hashem, T., Ibrahim, A.H., Wöll, C., Alkordi, M.H., 2019. Grafting zirconium-based metal–organic framework UiO-66-NH2 nanoparticles on cellulose fibers for the removal of Cr (VI) ions and methyl orange from water. ACS Applied Nano Materials 2 (9), 5804–5808.
He, Q., Liang, J.-J., Chen, L.-X., et al., 2020. Removal of the environmental pollutant carbamazepine using molecular imprinted adsorbents: Molecular simulation, adsorption properties, and mechanisms. Water Research 168, 115164.
Henriques, B., Gonçalves, G., Emami, N., et al., 2016. Optimized graphene oxide foam with enhanced performance and high selectivity for mercury removal from water. Journal of Hazardous Materials 301, 453–461.
Hinds, B.J., Chopra, N., Rantell, T., et al., 2004. Aligned multiwalled carbon nanotube membranes. Science 303 (5654), 62–65.
Hong, J., Xie, J., Mirshahghassemi, S., Lead, J., 2020. Metal (Cd, Cr, Ni, Pb) removal from environmentally relevant waters using polyvinylpyrrolidone-coated magnetite nanoparticles. RSC Advances 10 (6), 3266–3276.
Hong, Y., Zhou, H., Xiong, Z., et al., 2020. Heterogeneous activation of peroxymonosulfate by CoMgFe-LDO for degradation of carbamazepine: Efficiency, mechanism and degradation pathways. Chemical Engineering Journal 391, 123604.
Houtz, E., Wang, M., Park, J.-S., 2018. Identification and fate of aqueous film forming foam derived per- and polyfluoroalkyl substances in a wastewater treatment plant. Environmental Science & Technology 52 (22), 13212–13221.
Huang, W.-Q., Liu, S.-R., Huang, Z.-M., et al., 2015. Magic electron affection in preparation process of silicon nanocrystal. Scientific Reports 5 (1), 1–6.
Huang, Y., Keller, A.A., 2013. Magnetic nanoparticle adsorbents for emerging organic contaminants. ACS Sustainable Chemistry & Engineering 1 (7), 731–736.
Huang, Y., Keller, A.A., 2015. EDTA functionalized magnetic nanoparticle sorbents for cadmium and lead contaminated water treatment. Water Research 80, 159–168.
Huang, Y., Keller, A.A., 2016. Isothermal titration microcalorimetry to determine the thermodynamics of metal ion removal by magnetic nanoparticle sorbents. Environmental Science: Nano 3 (5), 1206–1214.
Huang, Y., Fulton, A.N., Keller, A.A., 2016. Optimization of porous structure of superparamagnetic nanoparticle adsorbents for higher and faster removal of emerging organic contaminants and PAHs. Environmental Science: Water Research & Technology 2 (3), 521–528.
Huang, Y., Fulton, A.N., Keller, A.A., 2016. Simultaneous removal of PAHs and metal contaminants from water using magnetic nanoparticle adsorbents. Science of the Total Environment 571, 1029–1036.
Huang, D., Yin, L., Niu, J., 2016. Photoinduced hydrodefluorination mechanisms of perfluorooctanoic acid by the SiC/graphene catalyst. Environmental Science & Technology 50 (11), 5857–5863.
Huang, Y., Lee, X., Macazo, F.C., et al., 2018. Fast and efficient removal of chromium (VI) anionic species by a reusable chitosan-modified multi-walled carbon nanotube composite. Chemical Engineering Journal 339, 259–267.
Huang, Y., Ruan, G., Ruan, Y., et al., 2018. Hypercrosslinked porous polymers hybridized with graphene oxide for water treatment: dye adsorption and degradation. RSC Advances 8 (24), 13417–13422.
Huo, Z.-Y., Du, Y., Chen, Z., Wu, Y.-H., Hu, H.-Y., 2020. Evaluation and prospects of nanomaterial-enabled innovative processes and devices for water disinfection: A state-of-the-art review. Water Research 173, 115581.
Hydari, S., Sharififard, H., Nabavinia, M., Parvizi, M.r., 2012. A comparative investigation on removal performances of commercial activated carbon, chitosan biosorbent and chitosan/activated carbon composite for cadmium. Chemical Engineering Journal 193–194, 276–282.
Ighalo, J.O., Sagboye, P.A., Umenweke, G., et al., 2021. CuO nanoparticles (CuO NPs) for water treatment: A review of recent advances. Environmental Nanotechnology, Monitoring & Management 15, 100443.
Ikhmayies, S.J., 2014. Characterization of Nanomaterials. JOM 66 (1), 28–29.
Ikram, M., Raza, A., Imran, M., et al., 2020. Hydrothermal synthesis of silver decorated reduced graphene oxide (rGO) nanoflakes with effective photocatalytic activity for wastewater treatment. Nanoscale Research Letters 15, 1–11.
Irshad, M.A., Shakoor, M.B., Ali, S., Nawaz, R., Rizwan, M., 2019. Synthesis and application of titanium dioxide nanoparticles for removal of cadmium from wastewater: kinetic and equilibrium study. Water, Air, & Soil Pollution 230 (12), 1–10.
Jabbari, V., Veleta, J.M., Zarei-Chaleshtori, M., Gardea-Torresdey, J., Villagrán, D., 2016. Green synthesis of magnetic MOF@GO and MOF@CNT hybrid nanocomposites with high adsorption capacity towards organic pollutants. Chemical Engineering Journal 304, 774–783.

Jafarinejad, S., 2019. Cost-effective catalytic materials for aop treatment units. In: Gil, A., Galeano, L.A., Vicente, M.Á. (Eds.), Applications of Advanced Oxidation Processes ((AOPs)) in Drinking Water Treatment. Springer International Publishing, Cham, pp. 309–343.
Ji, L., Chen, W., Duan, L., Zhu, D., 2009. Mechanisms for strong adsorption of tetracycline to carbon nanotubes: A comparative study using activated carbon and graphite as adsorbents. Environmental Science & Technology 43 (7), 2322–2327.
Ji, W., Xiao, L., Ling, Y., et al., 2018. Removal of GenX and perfluorinated alkyl substances from water by amine-functionalized covalent organic frameworks. Journal of the American Chemical Society 140 (40), 12677–12681.
Jiang, F., Zhao, H., Chen, H., Xu, C., Chen, J., 2016. Enhancement of photocatalytic decomposition of perfluorooctanoic acid on CeO_2/In_2O_3. RSC advances 6 (76), 72015–72021.
Jiang, Y., Sun, Y., Liu, H., Zhu, F., Yin, H., 2008. Solar photocatalytic decolorization of C.I. Basic Blue 41 in an aqueous suspension of TiO_2–ZnO. Dyes and Pigments 78 (1), 77–83.
Jin, W., Du, H., Zheng, S., Zhang, Y., 2016. Electrochemical processes for the environmental remediation of toxic Cr (VI): A review. Electrochimica Acta 191, 1044–1055.
Joshi, S., Sharma, M., Kumari, A., Shrestha, S., Shrestha, B., 2019. Arsenic removal from water by adsorption onto iron oxide/nano-porous carbon magnetic composite. Applied Sciences 9 (18), (3732).
Jung, C., Son, A., Her, N., et al., 2015. Removal of endocrine disrupting compounds, pharmaceuticals, and personal care products in water using carbon nanotubes: A review. Journal of Industrial and Engineering Chemistry 27, 1–11.
Kallis, G., 2010. Coevolution in water resource development: The vicious cycle of water supply and demand in Athens, Greece. Ecological Economics 69 (4), 796–809.
Kamaraj, M., Srinivasan, N.R., Assefa, G., Adugna, A.T., Kebede, M., 2020. Facile development of sunlit ZnO nanoparticles-activated carbon hybrid from pernicious weed as an operative nano-adsorbent for removal of methylene blue and chromium from aqueous solution: Extended application in tannery industrial wastewater. Environmental Technology & Innovation 17, 100540.
Kanakaraju, D., Glass, B.D., Oelgemöller, M., 2018. Advanced oxidation process-mediated removal of pharmaceuticals from water: A review. Journal of Environmental Management 219, 189–207.
Karim, M.R., Aijaz, M.O., Alharth, N.H., et al., 2019. Composite nanofibers membranes of poly (vinyl alcohol)/chitosan for selective lead (II) and cadmium (II) ions removal from wastewater. Ecotoxicology and Environmental Safety 169, 479–486.
Keller, A.A., Garner, K., Miller, R.J., Lenihan, H.S., 2012. Toxicity of nano-zero valent iron to freshwater and marine organisms. PLOS One 7 (8), e43983.
Khalil, A., Gondal, M.A., Dastageer, M.A., 2011. Augmented photocatalytic activity of palladium incorporated ZnO nanoparticles in the disinfection of Escherichia coli microorganism from water. Applied Catalysis A: General 402 (1), 162–167.
Khan, M., Lo, I.M.C., 2017. Removal of ionizable aromatic pollutants from contaminated water using nano γ-Fe_2O_3 based magnetic cationic hydrogel: Sorptive performance, magnetic separation and reusability. Journal of Hazardous Materials 322, 195–204.
Kim, E.-S., Liu, Y., Gamal El-Din, M., 2011. The effects of pretreatment on nanofiltration and reverse osmosis membrane filtration for desalination of oil sands process-affected water. Separation and Purification Technology 81 (3), 418–428.
Kim, H., Hwang, Y.S., Sharma, V.K., 2014. Adsorption of antibiotics and iopromide onto single-walled and multi-walled carbon nanotubes. Chemical Engineering Journal 255, 23–27.
Kim, K.Y., Ekpe, O.D., Lee, H.-J., Oh, J.-E., 2020. Perfluoroalkyl substances and pharmaceuticals removal in full-scale drinking water treatment plants. Journal of Hazardous Materials 400, 123235.
Kim, S.J., Nam, Y.S., Rhee, D.M., Park, H.-S., Park, W.H., 2007. Preparation and characterization of antimicrobial polycarbonate nanofibrous membrane. European Polymer Journal 43 (8), 3146–3152.
Kończyk, J., Żarska, S., Ciesielski, W., 2019. Adsorptive removal of Pb (II) ions from aqueous solutions by multi-walled carbon nanotubes functionalised by selenophosphoryl groups: Kinetic, mechanism, and thermodynamic studies. Colloids and Surfaces A: Physicochemical and Engineering Aspects 575, 271–282.
Kuganathan, N., Selvanantharajah, N., Iyngaran, P., Abiman, P., Chroneos, A., 2019. Cadmium trapping by C60 and B-, Si-, and N-doped C60. Journal of Applied Physics 125 (5).
Kumar, A., Joshi, H., Kumar, A., 2021. Remediation of arsenic by metal/ metal oxide based nanocomposites/ nanohybrids: Contamination scenario in groundwater, practical challenges, and future perspectives. Separation & Purification Reviews 50 (3), 283–314.
Kumar, R., Khan, M.A., Haq, N., 2014. Application of carbon nanotubes in heavy metals remediation. Critical Reviews in Environmental Science and Technology 44 (9), 1000–1035.
Lal, S., Singhal, A., Kumari, P., 2020. Exploring carbonaceous nanomaterials for arsenic and chromium removal from wastewater. Journal of Water Process Engineering 36, 101276.
Lee, J., Ye, Y., Ward, A.J., et al., 2016. High flux and high selectivity carbon nanotube composite membranes for natural organic matter removal. Separation and Purification Technology 163, 109–119.
Lee, M., Keller, A.A., Chiang, P.-C., et al., 2017. Water-energy nexus for urban water systems: A comparative review on energy intensity and environmental impacts in relation to global water risks. Applied energy 205, 589–601.
Lee, S.-Y., Park, S.-J., 2013. TiO_2 photocatalyst for water treatment applications. Journal of Industrial and Engineering Chemistry 19 (6), 1761–1769.
Li, R., Deng, H., Zhang, X., et al., 2019. High-efficiency removal of Pb (II) and humate by a CeO_2–MoS_2 hybrid magnetic biochar. Bioresource Technology 273, 335–340.
Li, L., Lai, C., Huang, F., et al., 2019. Degradation of naphthalene with magnetic bio-char activate hydrogen peroxide: Synergism of bio-char and Fe–Mn binary oxides. Water Research 160, 238–248.
Li, J., Li, M., Yang, X., et al., 2019. Morphology-controlled synthesis of boehmite with enhanced efficiency for the removal of aqueous Cr (VI) and nitrates. Nanotechnology 30 (19), 195702.
Li, G., Ye, J., Fang, Q., Liu, F., 2019. Amide-based covalent organic frameworks materials for efficient and recyclable removal of heavy metal lead (II). Chemical Engineering Journal 370, 822–830.
Li, J., Zhou, X., Wang, J., Li, X., 2019. Two-dimensional covalent organic frameworks (COFs) for membrane separation: A mini review. Industrial & Engineering Chemistry Research 58 (34), 15394–15406.
Li, M., Yu, Z., Liu, Q., Sun, L., Huang, W., 2016. Photocatalytic decomposition of perfluorooctanoic acid by noble metallic nanoparticles modified TiO_2. Chemical Engineering Journal 286, 232–238.
Li, S., Zhang, G., Zhang, W., et al., 2017. Microwave enhanced Fenton-like process for degradation of perfluorooctanoic acid (PFOA) using Pb-BiFeO3/rGO as heterogeneous catalyst. Chemical Engineering Journal 326, 756–764.
Li, W.-T., Shi, W., Hu, Z.-J., et al., 2020. Fabrication of magnetic Fe_3O_4@metal organic framework@covalent organic framework composite and its selective separation of trace copper. Applied Surface Science 530, 147254.
Li, Z., Zhang, P., Li, J., Shao, T., Jin, L., 2013. Synthesis of In2O3-graphene composites and their photocatalytic performance towards perfluorooctanoic acid decomposition. Journal of Photochemistry and Photobiology A: Chemistry 271, 111–116.

Liang, G., Hu, Z., Wang, Z., et al., 2020. Effective removal of carbamazepine and diclofenac by CuO/Cu_2O/Cu-biochar composite with different adsorption mechanisms. Environmental Science and Pollution Research 27 (36), 45435–45446.
Liang, L., Li, X., Lin, Z., Tian, C., Guo, Y., 2020. The removal of Cd by sulfidated nanoscale zero-valent iron: The structural, chemical bonding evolution and the reaction kinetics. Chemical Engineering Journal 382, 122933.
Liang, L., Li, X., Guo, Y., et al., 2021. The removal of heavy metal cations by sulfidated nanoscale zero-valent iron (S-nZVI): The reaction mechanisms and the role of sulfur. Journal of Hazardous Materials 404, 124057.
Lin, D., Xing, B., 2008. Adsorption of phenolic compounds by carbon nanotubes: Role of aromaticity and substitution of hydroxyl groups. Environmental Science & Technology 42 (19), 7254–7259.
Lin, J., Sun, M., Liu, X., Chen, Z., 2017. Functional kaolin supported nanoscale zero-valent iron as a Fenton-like catalyst for the degradation of direct black G. Chemosphere 184, 664–672.
Lin, K.-S., Mdlovu, N.V., Chen, C.-Y., Chiang, C.-L., Dehvari, K., 2018. Degradation of TCE, PCE, and 1,2–DCE DNAPLs in contaminated groundwater using polyethylenimine-modified zero-valent iron nanoparticles. Journal of Cleaner Production 175, 456–466.
Lin, Y.-T., Weng, C.-H., Chen, F.-Y., 2008. Effective removal of AB24 dye by nano/micro-size zero-valent iron. Separation and Purification Technology 64 (1), 26–30.
Lingamdinne, L.P., Lee, S., Choi, J.-S., et al., 2021. Potential of the magnetic hollow sphere nanocomposite (graphene oxide-gadolinium oxide) for arsenic removal from real field water and antimicrobial applications. Journal of Hazardous Materials 402, 123882.
Liu, X., Lai, D., Wang, Y., 2019. Performance of Pb (II) removal by an activated carbon supported nanoscale zero-valent iron composite at ultralow iron content. Journal of Hazardous Materials 361, 37–48.
Liu, C., Wang, P., Liu, X., et al., 2019. Ultrafast removal of cadmium (II) by green cyclodextrin metal–organic-framework-based nanoporous carbon: Adsorption mechanism and application. Chemistry–An Asian Journal 14 (2), 261–268.
Liu, F., Zhou, K., Chen, Q., Wang, A., Chen, W., 2019. Application of magnetic ferrite nanoparticles for removal of Cu (II) from copper-ammonia wastewater. Journal of Alloys and Compounds 773, 140–149.
Liu, L., Liu, Y., Gao, B., et al., 2020. Removal of perfluorooctanoic acid (PFOA) and perfluorooctane sulfonate (PFOS) from water by carbonaceous nanomaterials: A review. Critical Reviews in Environmental Science and Technology 50 (22), 2379–2414.
Liu, N., Shi, L., Han, X., et al., 2020. A heteropore covalent organic framework for adsorptive removal of Cd (II) from aqueous solutions with high efficiency. Chinese Chemical Letters 31 (2), 386–390.
Liu, Z., Zhang, Z., Peng, J., Wu, J., Huo, Y., 2020. Rapid removal of trace haloacetic acids from drinking water by a continuous adsorption process using graphene oxide. Environmental Technology1–7.
Liu, X., Wei, J., Hou, L., et al., 2021. Feasibility of nanoscale zerovalent iron-loaded sediment-based biochar (nZVI-SBC) for simultaneous removal of nitrate and phosphate: High selectivity toward dinitrogen and synergistic mechanism. Environmental Science and Pollution Research
Liu, X., Wang, M., Zhang, S., Pan, B., 2013. Application potential of carbon nanotubes in water treatment: A review. Journal of Environmental Sciences 25 (7), 1263–1280.
Liu, Z., Wang, H., Ou, J., Chen, L., Ye, M., 2018. Construction of hierarchically porous monoliths from covalent organic frameworks (COFs) and their application for bisphenol A removal. Journal of Hazardous Materials 355, 145–153.
Long, X., Yang, S., Qiu, X., et al., 2021. Heterogeneous activation of peroxymonosulfate for bisphenol A degradation using $CoFe_2O_4$ derived by hybrid cobalt-ion hexacyanoferrate nanoparticles. Chemical Engineering Journal 404, 127052.
Luo, Q., Li, G., Chen, M., et al., 2020. Effect factor of arsenite and arsenate removal by a manufactured material: Activated carbon-supported nano-TiO_2. Journal of Chemistry
Lv, D., Zhou, J., Cao, Z., et al., 2019. Mechanism and influence factors of chromium (VI) removal by sulfide-modified nanoscale zerovalent iron. Chemosphere 224, 306–315.
Lv, Y., Zhang, C., He, A., et al., 2017. Photocatalytic nanofiltration membranes with self-cleaning property for wastewater treatment. Advanced Functional Materials 27 (27), 1700251.
Ma, H., Burger, C., Hsiao, B.S., Chu, B., 2014. Fabrication and characterization of cellulose nanofiber based thin-film nanofibrous composite membranes. Journal of Membrane Science 454, 272–282.
Ma, L., Dong, X., Chen, M., et al., 2017. Fabrication and water treatment application of carbon nanotubes (CNTs)-based composite membranes: A review. Membranes 7 (1), (16).
Ma, M.-D., Wu, H., Deng, Z.-Y., Zhao, X., 2018. Arsenic removal from water by nanometer iron oxide coated single-wall carbon nanotubes. Journal of Molecular Liquids 259, 369–375.
Mahamuni, N.N., Adewuyi, Y.G., 2010. Advanced oxidation processes (AOPs) involving ultrasound for waste water treatment: A review with emphasis on cost estimation. Ultrasonics Sonochemistry 17 (6), 990–1003.
Mahdavi, S., Jalali, M., Afkhami, A., 2014. Removal of heavy metals from aqueous solutions using Fe_3O_4, ZnO, and CuO nanoparticles. In: Diallo, M.S., Fromer, N.A., Jhon, M.S. (Eds.), Nanotechnology for Sustainable Development. Springer International Publishing, Cham, pp. 171–188.
Mardikar, S.P., Doss, V.R., Jolhe, P.D., Gaikwad, R.W., Barkade, S.S., 2021. Chapter 28 – Nanocomposite adsorbent-based wastewater treatment processes: Special emphasis on surface-engineered iron oxide nanohybrids. In: Bhanvase, B., Sonawane, S., Pawade, V., Pandit, A. (Eds.), Handbook of Nanomaterials for Wastewater Treatment. Elsevier, pp. 867–897.
Mastropietro, T., Bruno, R., Pardo, E., Armentano, D., 2021. Reverse osmosis and nanofiltration membranes for highly efficient PFASs removal: Overview, challenges and future perspectives. Dalton Transactions
Masud, A., Guardian, M.G.E., Travis, S.C., et al., 2021. Redox-active rGO-nZVI nanohybrid-catalyzed chain shortening of perfluorooctanoic acid (PFOA) and perfluorooctane sulfonic acid (PFOS). Journal of Hazardous Materials Letters 2, 100007.
Masud, A., Chavez Soria, N.G., Aga, D.S., Aich, N., 2020. Adsorption and advanced oxidation of diverse pharmaceuticals and personal care products (PPCPs) from water using highly efficient rGO–nZVI nanohybrids. Environmental Science: Water Research & Technology 6 (8), 2223–2238.
Matharu, R.K., Porwal, H., Chen, B., Ciric, L., Edirisinghe, M., 2020. Viral filtration using carbon-based materials. Medical Devices & Sensors 3 (4), e10107.
Mehrabi, N., Masud, A., Afolabi, M., et al., 2019. Magnetic graphene oxide-nano zero valent iron (GO–nZVI) nanohybrids synthesized using biocompatible cross-linkers for methylene blue removal. RSC Advances 9 (2), 963–973.
Mekonnen, M.M., Hoekstra, A.Y., 2016. Four billion people facing severe water scarcity. Science Advances 2 (2), e1500323.
Meng, F., Li, Z., Lei, C., Yang, K., Lin, D., 2021. Removal of trichloroethene by iron-based biochar from anaerobic water: Key roles of Fe/C ratio and iron carbides. Chemical Engineering Journal 413, 127391.
Miculescu, M., Thakur, V.K., Miculescu, F., Voicu, S.I., 2016. Graphene-based polymer nanocomposite membranes: A review. Polymers for Advanced Technologies 27 (7), 844–859.
Mikhailov, I., Komarov, S., Levina, V., et al., 2017. Nanosized zero-valent iron as Fenton-like reagent for ultrasonic-assisted leaching of zinc from blast furnace sludge. Journal of Hazardous Materials 321, 557–565.

Mirbagheri, N.S., Sabbaghi, S., 2018. A natural kaolin/γ-Fe2O3 composite as an efficient nano-adsorbent for removal of phenol from aqueous solutions. Microporous and Mesoporous Materials 259, 134–141.
Mohagheghian, A., Ayagh, K., Godini, K., Shirzad-Siboni, M., 2018. Photocatalytic reduction of Cr (VI) from synthetic, real drinking waters and electroplating wastewater by synthesized amino-functionalized Fe3O4–WO3 nanoparticles by visible light. Journal of Industrial and Engineering Chemistry 59, 169–183.
Mollahosseini, A., Rahimpour, A., 2014. Interfacially polymerized thin film nanofiltration membranes on TiO_2 coated polysulfone substrate. Journal of Industrial and Engineering Chemistry 20 (4), 1261–1268.
Mon, M., Bruno, R., Ferrando-Soria, J., Armentano, D., Pardo, E., 2018. Metal–organic framework technologies for water remediation: towards a sustainable ecosystem. Journal of Materials Chemistry A 6 (12), 4912–4947.
Monteoliva-García, A., Martín-Pascual, J., Muñío, M.M., Poyatos, J.M., 2020. Effects of carrier addition on water quality and pharmaceutical removal capacity of a membrane bioreactor – Advanced oxidation process combined treatment. Science of the Total Environment 708, 135104.
Motamedi, E., Talebi Atouei, M., Kassaee, M.Z., 2014. Comparison of nitrate removal from water via graphene oxide coated Fe, Ni and Co nanoparticles. Materials Research Bulletin 54, 34–40.
Mukwevho, N., Gusain, R., Fosso-Kankeu, E., et al., 2020. Removal of naphthalene from simulated wastewater through adsorption-photodegradation by ZnO/Ag/GO nanocomposite. Journal of Industrial and Engineering Chemistry 81, 393–404.
Nabi, I., Bacha, A.-U.-R., Li, K., et al., 2020. Complete photocatalytic mineralization of microplastic on TiO_2 nanoparticle film. iScience 23 (7), 101326.
Nalbandian, M.J., Greenstein, K.E., Shuai, D., et al., 2015. Tailored synthesis of photoactive TiO_2 nanofibers and Au/TiO_2 nanofiber composites: Structure and reactivity optimization for water treatment applications. Environmental Science & Technology 49 (3), 1654–1663.
Nas, M.S., Calimli, M.H., Burhan, H., et al., 2019. Synthesis, characterization, kinetics and adsorption properties of Pt-Co@GO nano-adsorbent for methylene blue removal in the aquatic mediums using ultrasonic process systems. Journal of Molecular Liquids 296, 112100.
Nasiri, E.F., Kebria, D.Y., Qaderi, F., 2018. An experimental study on the simultaneous phenol and chromium removal from water using titanium dioxide photocatalyst. Civil Engineering Journal 4 (3), 585–593.
Nasrollahzadeh, M., Sajjadi, M., Iravani, S., Varma, R.S., 2021. Carbon-based sustainable nanomaterials for water treatment: State-of-art and future perspectives. Chemosphere 263, 128005.
Nasseri, S., Ebrahimi, S., Abtahi, M., Saeedi, R., 2018. Synthesis and characterization of polysulfone/graphene oxide nano-composite membranes for removal of bisphenol A from water. Journal of Environmental Management 205, 174–182.
Nawaz, M., Miran, W., Jang, J., Lee, D.S., 2017. One-step hydrothermal synthesis of porous 3D reduced graphene oxide/TiO_2 aerogel for carbamazepine photodegradation in aqueous solution. Applied Catalysis B: Environmental 203, 85–95.
Němeček, J., Pokorný, P., Lhotský, O., et al., 2016. Combined nano-biotechnology for in-situ remediation of mixed contamination of groundwater by hexavalent chromium and chlorinated solvents. Science of the Total Environment 563–564, 822–834.
Nghiem, L.D., Hawkes, S., 2009. Effects of membrane fouling on the nanofiltration of trace organic contaminants. Desalination 236 (1), 273–281.
Nghiem, L.D., Schäfer, A.I., Elimelech, M., 2006. Role of electrostatic interactions in the retention of pharmaceutically active contaminants by a loose nanofiltration membrane. Journal of Membrane Science 286 (1–2), 52–59.
Nguyen, C.H., Tran, M.L., Van Tran, T.T., Juang, R.-S., 2021. Efficient removal of antibiotic oxytetracycline from water by Fenton-like reactions using reduced graphene oxide-supported bimetallic Pd/nZVI nanocomposites. Journal of the Taiwan Institute of Chemical Engineers 119, 80–89.
Niu, C., Zhang, N., Hu, C., et al., 2021. Preparation of a novel citric acid-crosslinked Zn-MOF/chitosan composite and application in adsorption of chromium (VI) and methyl orange from aqueous solution. Carbohydrate Polymers 258, 117644.
Nödler, K., Scheurer, M., 2019. Substances from multiple sources (SMS): The presence of multiple primary and secondary sources of persistent and mobile organic contaminants is an upcoming challenge for the drinking water sector and regulatory frameworks. Environmental Science & Technology 53 (19), 11061–11062.
Nogueira, V., Lopes, I., Rocha-Santos, T., Gonçalves, F., Pereira, R., 2018. Treatment of real industrial wastewaters through nano-TiO_2 and nano-Fe_2O_3 photocatalysis: Case study of mining and kraft pulp mill effluents. Environmental Technology 39 (12), 1586–1596.
Norzilah, A., Fakhruʹl-Razi, A., Choong, T.S., Chuah, A.L., 2011. Surface modification effects on CNTs adsorption of methylene blue and phenol. Journal of Nanomaterials
Novakovic, M., Strbac, G., Petrovic, M., Strbac, D., Mihajlovic, I., 2020. Decomposition of pharmaceutical micropollutant–diclofenac by photocatalytic nanopowder mixtures in aqueous media: Effect of optimization parameters, identification of intermediates and economic considerations. Journal of Environmental Science and Health, Part A 55 (4), 483–497.
Nzeribe, B.N., Crimi, M., Mededovic Thagard, S., Holsen, T.M., 2019. Physico-chemical processes for the treatment of per- and polyfluoroalkyl substances (PFAS): A review. Critical Reviews in Environmental Science and Technology 49 (10), 866–915.
Ojha, A., 2020. Chapter 19 – Nanomaterials for removal of waterborne pathogens: Opportunities and challenges. In: Vara Prasad, M.N., Grobelak, A. (Eds.), Waterborne Pathogens. Butterworth-Heinemann, pp. 385–432.
Okonji, S.O., Dominic, J.A., Pernitsky, D., Achari, G., 2020. Removal and recovery of selenium species from wastewater: Adsorption kinetics and co-precipitation mechanisms. Journal of Water Process Engineering 38, 101666.
Omo-Okoro, P.N., Curtis, C.J., Marco, A.M., Melymuk, L., Okonkwo, J.O., 2021. Removal of per-and polyfluoroalkyl substances from aqueous media using synthesized silver nanocomposite-activated carbons. Journal of Environmental Health Science and Engineering 1–20.
Onyancha, R.B., Aigbe, U.O., Ukhurebor, K.E., Muchiri, P.W., 2021. Facile synthesis and applications of carbon nanotubes in heavy-metal remediation and biomedical fields: A comprehensive review. Journal of Molecular Structure 1238, 130462.
Ou, J.-H., Sheu, Y.-T., Tsang, D.C.W., Sun, Y.-J., Kao, C.-M., 2020. Application of iron/aluminum bimetallic nanoparticle system for chromium-contaminated groundwater remediation. Chemosphere 256, 127158.
Oyekunle, D.T., Zhou, X., Shahzad, A., Chen, Z., 2021. Review on carbonaceous materials as persulfate activators: Structure–performance relationship, mechanism and future perspectives on water treatment. Journal of Materials Chemistry A 9 (13), 8012–8050.
Oyewo, O.A., Mutesse, B., Leswifi, T.Y., Onyango, M.S., 2019. Highly efficient removal of nickel and cadmium from water using sawdust-derived cellulose nanocrystals. Journal of Environmental Chemical Engineering 7 (4), 103251.
Ozaki, H., Ikejima, N., Shimizu, Y., et al., 2008. Rejection of pharmaceuticals and personal care products (PPCPs) and endocrine disrupting chemicals (EDCs) by low pressure reverse osmosis membranes. Water Science and Technology 58 (1), 73–81.
Painuli, R., Yadav, P.K., Raghav, S., Kumar, D., 2021. Synthesis of carbon nanofibers and its application in environmental remediation. In: Jawaid, M., Ahmad, A., Ismail, N., Rafatullah, M. (Eds.), Environmental Remediation Through Carbon Based Nano Composites. Springer Singapore, Singapore, pp. 325–342.
Pan, X., Ji, J., Zhang, N., Xing, M., 2020. Research progress of graphene-based nanomaterials for the environmental remediation. Chinese Chemical Letters 31 (6), 1462–1473.
Panchal, P., Paul, D.R., Sharma, A., et al., 2020. Biogenic mediated Ag/ZnO nanocomposites for photocatalytic and antibacterial activities towards disinfection of water. Journal of Colloid and Interface Science 563, 370–380.

Panda, A., Yang, Y., Venkateswarlu, S., et al., 2020. Highly durable covalent organic framework for the simultaneous ultrasensitive detection and removal of noxious Hg2. Microporous and Mesoporous Materials 306, 110399.
Pandi, K., Choi, J., 2021. Selective removal of anionic ions from aqueous environment using iron-based metal-organic frameworks and their mechanistic investigations. Journal of Molecular Liquids 329, 115367.
Park, S., Zenobio, J.E., Lee, L.S., 2018. Perfluorooctane sulfonate (PFOS) removal with Pd0/nFe0 nanoparticles: Adsorption or aqueous Fe-complexation, not transformation?. Journal of Hazardous Materials 342, 20–28.
Pendolino, F., Armata, N., 2017. Graphene Oxide in Environmental Remediation Process. Springer.
Phenrat, T., Thongboot, T., Lowry, G.V., 2016. Electromagnetic induction of zerovalent iron (ZVI) powder and nanoscale zerovalent iron (NZVI) particles enhances dechlorination of trichloroethylene in contaminated groundwater and soil: Proof of concept. Environmental Science & Technology 50 (2), 872–880.
Phenrat, T., Long, T.C., Lowry, G.V., Veronesi, B., 2009. Partial oxidation ("Aging") and surface modification decrease the toxicity of nanosized zerovalent iron. Environmental Science & Technology 43 (1), 195–200.
Piao, L., Liu, Q., Li, Y., Wang, C., 2008. Adsorption of L-phenylalanine on single-walled carbon nanotubes. The Journal of Physical Chemistry C 112 (8), 2857–2863.
Pichel, N., Vivar, M., Fuentes, M., 2019. The problem of drinking water access: A review of disinfection technologies with an emphasis on solar treatment methods. Chemosphere 218, 1014–1030.
Pirsaheb, M., Hossaini, H., Nasseri, S., et al., 2020. Optimization of photocatalytic degradation of methyl orange using immobilized scoria-Ni/TiO_2 nanoparticles. Journal of Nanostructure in Chemistry 1–17.
Pourzamani, H., Hajizadeh, Y., Mengelizadeh, N., 2018. Application of three-dimensional electrofenton process using MWCNTs-Fe_3O_4 nanocomposite for removal of diclofenac. Process Safety and Environmental Protection 119, 271–284.
Pradeep, T., 2009. Anshup, Noble metal nanoparticles for water purification: A critical review. Thin Solid Films 517 (24), 6441–6478.
Qin, W., Song, Y., Dai, Y., et al., 2015. Treatment of berberine hydrochloride pharmaceutical wastewater by O_3/UV/H_2O_2 advanced oxidation process. Environmental Earth Sciences 73 (9), 4939–4946.
Qu, J., Wang, H., Wang, K., et al., 2019. Municipal wastewater treatment in China: Development history and future perspectives. Frontiers of Environmental Science & Engineering 13 (6), (88).
Qu, X., Brame, J., Li, Q., Alvarez, P.J.J., 2013. Nanotechnology for a safe and sustainable water supply: Enabling integrated water treatment and reuse. Accounts of Chemical Research 46 (3), 834–843.
Radjenovic, J., Petrovic, M., Barceló, D., 2007. Analysis of pharmaceuticals in wastewater and removal using a membrane bioreactor. Analytical and Bioanalytical Chemistry 387 (4), 1365–1377.
Radjenović, J., Petrović, M., Barceló, D., 2009. Fate and distribution of pharmaceuticals in wastewater and sewage sludge of the conventional activated sludge (CAS) and advanced membrane bioreactor (MBR) treatment. Water Research 43 (3), 831–841.
Radjenović, J., Farré, M.J., Mu, Y., Gernjak, W., Keller, J., 2012. Reductive electrochemical remediation of emerging and regulated disinfection byproducts. Water Research 46 (6), 1705–1714.
Rahdar, S., Pal, K., Mohammadi, L., et al., 2021. Response surface methodology for the removal of nitrate ions by adsorption onto copper oxide nanoparticles. Journal of Molecular Structure 1231, 129686.
Rahmani, A., Ghaffari, H., Samadi, M., 2011. A comparative study on arsenic (III) removal from aqueous solution using nano and micro sized zero-valent iron. Journal of Environmental Health Science & Engineering 8 (2), 157–166.
Ran, Z., Fang, Y., Sun, J., Ma, C., Li, S., 2020. Photocatalytic oxidative degradation of carbamazepine by TiO_2 irradiated by UV light emitting diode. Catalysts 10 (5), (540).
Rashed, M., El-Amin, A., 2007. Photocatalytic degradation of methyl orange in aqueous TiO_2 under different solar irradiation sources. International Journal of Physical Sciences 2 (3), 73–81.
Rego, R.M., Kuriya, G., Kurkuri, M.D., Kigga, M., 2021. MOF based engineered materials in water remediation: Recent trends. Journal of Hazardous Materials 403, 123605.
Regulska, E., Rivera-Nazario, D.M., Karpinska, J., Plonska-Brzezinska, M.E., Echegoyen, L., 2019. Zinc porphyrin-functionalized fullerenes for the sensitization of titania as a visible-light active photocatalyst: River waters and wastewaters remediation. Molecules 24 (6), (1118).
Ren, H.-S., Cao, Z.-F., Wen, X., et al., 2019. Preparation of a novel nano-Fe_3O_4/triethanolamine/GO composites to enhance Pb 2+/Cu 2+ ions removal. Environmental Science and Pollution Research 26 (10), 10174–10187.
Roberson, J.A., 2011. What's next after 40 years of drinking water regulations?. Environmental Science & Technology 45 (1), 154–160.
Rohaizad, A., Shahabuddin, S., Shahid, M.M., et al., 2020. Green synthesis of silver nanoparticles from Catharanthus roseus dried bark extract deposited on graphene oxide for effective adsorption of methylene blue dye. Journal of Environmental Chemical Engineering 8 (4), 103955.
Sadeghzadeh, S., Ghobadi Nejad, Z., Ghasemi, S., Khafaji, M., Borghei, S.M., 2020. Removal of bisphenol A in aqueous solution using magnetic cross-linked laccase aggregates from Trametes hirsuta. Bioresource Technology 306, 123169.
Safari, E., Rahemi, N., Kahforoushan, D., Allahyari, S., 2019. Copper adsorptive removal from aqueous solution by orange peel residue carbon nanoparticles synthesized by combustion method using response surface methodology. Journal of Environmental Chemical Engineering 7 (1), 102847.
Sahebi, S., Sheikhi, M., Ramavandi, B., et al., 2020. Sustainable management of saline oily wastewater via forward osmosis using aquaporin membrane. Process Safety and Environmental Protection 138, 199–207.
Salawudeen, A.O., Tawabini, B.S., Al-Shaibani, A.M., Saleh, T.A., 2020. Poly (2-hydroxyethyl methacrylate) grafted graphene oxide for cadmium removal from water with interaction mechanisms. Environmental Nanotechnology, Monitoring & Management 13, 100288.
Saleh, T.A., 2020. Nanomaterials: Classification, properties, and environmental toxicities. Environmental Technology & Innovation 20, 101067.
Samuel, M.S., Subramaniyan, V., Bhattacharya, J., et al., 2018. A. GO-CS@MOF [Zn (BDC) (DMF)] material for the adsorption of chromium (VI) ions from aqueous solution. Composites Part B: Engineering 152, 116–125.
Samuel, M.S., Bhattacharya, J., Raj, S., et al., 2019. Efficient removal of Chromium (VI) from aqueous solution using chitosan grafted graphene oxide (CS-GO) nanocomposite. International Journal of Biological Macromolecules 121, 285–292.
Santhosh, C., Velmurugan, V., Jacob, G., et al., 2016. Role of nanomaterials in water treatment applications: A review. Chemical Engineering Journal 306, 1116–1137.
Sekar, A.D., Muthukumar, H., Chandrasekaran, N.I., Matheswaran, M., 2018. Photocatalytic degradation of naphthalene using calcined FeZnO/ PVA nanofibers. Chemosphere 205, 610–617.
Shahrashoub, M., Bakhtiari, S., 2021. The efficiency of activated carbon/magnetite nanoparticles composites in copper removal: Industrial waste recovery, green synthesis, characterization, and adsorption-desorption studies. Microporous and Mesoporous Materials 311, 110692.
Shahryari, T., Mostafavi, A., Afzali, D., Rahmati, M., 2019. Enhancing cadmium removal by low-cost nanocomposite adsorbents from aqueous solutions; a continuous system. Composites Part B: Engineering 173, 106963.
Shaji, A., Zachariah, A.K., 2017. Chapter 9 – Surface area analysis of nanomaterials. In: Thomas, S., Thomas, R., Zachariah, A.K., Mishra, R.K. (Eds.), Thermal and Rheological Measurement Techniques for Nanomaterials Characterization. Elsevier, pp. 197–231.

Shalaby, N.H., Elsalamony, R.A., El Naggar, A.M., 2018. Mesoporous waste-extracted SiO_2–Al_2O_3-supported Ni and Ni–H 3 PW 12 O 40 nano-catalysts for photo-degradation of methyl orange dye under UV irradiation. New Journal of Chemistry 42 (11), 9177–9186.
Shan, S.J., Zhao, Y., Tang, H., Cui, F.Y., 2017. A mini-review of Carbonaceous nanomaterials for removal of contaminants from wastewater. IOP Conference Series: Earth and Environmental Science 68, 012003.
Shareef, U., Waqas, M., Bisphenol, A., 2020. Removal through low-cost kaolin-based Ag@ TiO_2 photocatalytic hollow fiber membrane from the liquid media under visible light irradiation. Journal of Nanomaterials
Sharma, G., Naushad, M., 2020. Adsorptive removal of noxious cadmium ions from aqueous medium using activated carbon/zirconium oxide composite: Isotherm and kinetic modelling. Journal of Molecular Liquids 310, 113025.
Sharma, M., Joshi, M., Nigam, S., et al., 2019. ZnO tetrapods and activated carbon based hybrid composite: Adsorbents for enhanced decontamination of hexavalent chromium from aqueous solution. Chemical Engineering Journal 358, 540–551.
Shiraishi, Y., Takeda, Y., Sugano, Y., et al., 2011. Highly efficient photocatalytic dehalogenation of organic halides on TiO_2 loaded with bimetallic Pd–Pt alloy nanoparticles. Chemical Communications 47 (27), 7863–7865.
Siddiqui, S.I., Singh, P.N., Tara, N., et al., 2020. Arsenic removal from water by starch functionalized maghemite nano-adsorbents: Thermodynamics and kinetics investigations. Colloid and Interface Science Communications 36, 100263.
Silva, D.F., Mourão, A., Franco, E.S., et al., 2019. A green alternative for degradation of trihalomethanes by nanocompounds and the use of bioassays to monitor genotoxic effects. Environmental Nanotechnology, Monitoring & Management 12, 100247.
Silva, N.H.C.S., Figueira, P., Fabre, E., et al., 2020. Dual nanofibrillar-based bio-sorbent films composed of nanocellulose and lysozyme nanofibrils for mercury removal from spring waters. Carbohydrate Polymers 238, 116210.
Sirivithayapakorn, S., Keller, A., 2003. Transport of colloids in saturated porous media: A pore-scale observation of the size exclusion effect and colloid acceleration. Water Resources Research 39 (4).
Song, C., Chen, P., Wang, C., Zhu, L., 2012. Photodegradation of perfluorooctanoic acid by synthesized TiO_2–MWCNT composites under 365 nm UV irradiation. Chemosphere 86 (8), 853–859.
Song, K., Mohseni, M., Taghipour, F., 2016. Application of ultraviolet light-emitting diodes (UV-LEDs) for water disinfection: A review. Water Research 94, 341–349.
Sonune, A., Ghate, R., 2004. Developments in wastewater treatment methods. Desalination 167, 55–63.
Sridhar, V., Park, H., 2020. Transforming waste poly (Ethylene Terephthalate) into nitrogen doped carbon nanotubes and its utility in oxygen reduction reaction and bisphenol-A removal from contaminated water. Materials 13 (18), (4144).
Stanley-Wood, N.G., Lines, R.W., 2007. Particle Size Analysis. Royal society of chemistry.
Stefaniuk, M., Oleszczuk, P., Ok, Y.S., 2016. Review on nano zerovalent iron (nZVI): From synthesis to environmental applications. Chemical Engineering Journal 287, 618–632.
Stevenson, L.M., Adeleye, A.S., Su, Y., et al., 2017. Remediation of cadmium toxicity by sulfidized nano-iron: The importance of organic material. ACS Nano 11 (10), 10558–10567.
Su, Y., Adeleye, A.S., Huang, Y., et al., 2014. Simultaneous removal of cadmium and nitrate in aqueous media by nanoscale zerovalent iron (nZVI) and Au doped nZVI particles. Water research 63 (0), 102–111.
Su, Y., Adeleye, A.S., Zhou, X., et al., 2014. Effects of nitrate on the treatment of lead contaminated groundwater by nanoscale zerovalent iron. Journal of Hazardous Materials 280, 504–513.
Su, Y., Adeleye, A.S., Keller, A.A., et al., 2015. Magnetic sulfide-modified nanoscale zerovalent iron (S-nZVI) for dissolved metal ion removal. Water Research 74, 47–57.
Su, Y., Adeleye, A.S., Huang, Y., et al., 2016. Direct synthesis of novel and reactive sulfide-modified nano iron through nanoparticle seeding for improved cadmium-contaminated water treatment. Scientific Reports 6, 24358.
Su, Y., Jassby, D., Song, S., et al., 2018. Enhanced oxidative and adsorptive removal of diclofenac in heterogeneous Fenton-like reaction with sulfide modified nanoscale zerovalent iron. Environmental Science & Technology 52 (11), 6466–6475.
Su, Y., Qian, D., Adeleye, A.S., et al., 2018. Impact of ageing on the fate of molybdate-zerovalent iron nanohybrid and its subsequent effect on cyanobacteria (Microcystis aeruginosa) growth in aqueous media. Water Research 140, 135–147.
Su, Y., Jassby, D., Zhang, Y., Keller, A.A., Adeleye, A.S., 2020. Comparison of the colloidal stability, mobility, and performance of nanoscale zerovalent iron and sulfidated derivatives. Journal of Hazardous Materials 396, 122691.
Sulaymon, A.H., Abid, B.A., Al-Najar, J.A., 2009. Removal of lead copper chromium and cobalt ions onto granular activated carbon in batch and fixed-bed adsorbers. Chemical Engineering Journal 155 (3), 647–653.
Sun, C., Wang, Z., Chen, L., Li, F., 2020. Fabrication of robust and compressive chitin and graphene oxide sponges for removal of microplastics with different functional groups. Chemical Engineering Journal 393, 124796.
Sun, W., Meng, S., Zhang, S., et al., 2018. Insight into the transfer mechanisms of photogenerated carriers for heterojunction photocatalysts with the analogous positions of valence band and conduction band: A case study of ZnO/TiO_2. The Journal of Physical Chemistry C 122 (27), 15409–15420.
Sustarsic, M., 2009. In Waste water treatment: Understanding the activated sludge process, Safety in ammonia Plants and related facilities symposium. pp 26–29.
Suzuki, H., Araki, S., Yamamoto, H., 2015. Evaluation of advanced oxidation processes (AOP) using O_3, UV, and TiO_2 for the degradation of phenol in water. Journal of Water Process Engineering 7, 54–60.
T C, P., Sharma, S.K., Kennedy, M., 2018. Nanoparticles in household level water treatment: An overview. Separation and Purification Technology 199, 260–270.
Tan, K.B., Vakili, M., Horri, B.A., et al., 2015. Adsorption of dyes by nanomaterials: Recent developments and adsorption mechanisms. Separation and Purification Technology 150, 229–242.
Tang, Y., Zhang, S., Su, Y., et al., 2021. Removal of microplastics from aqueous solutions by magnetic carbon nanotubes. Chemical Engineering Journal 406, 126804.
Thakur, P., Kumar, V., 2019. Kinetics and thermodynamic studies for removal of methylene blue dye by biosynthesize copper oxide nanoparticles and its antibacterial activity. Journal of Environmental Health Science and Engineering 17 (1), 367–376.
Thanh, T., 2013. Synthesis of metal sulfide-coated iron nanoparticles with enhanced surface reactivity and biocompatibility. RSC advances 3 (16), 5338–5340.
Thomas, M.S., Pillai, P.K., Faria, M., et al., 2020. Polylactic acid/nano chitosan composite fibers and their morphological, physical characterization for the removal of cadmium (II) from water. Journal of Applied Polymer Science 137 (34), 48993.
Thy, L.T.M., Thuong, N.H., Tu, T.H., et al., 2019. Synthesis of magnetic iron oxide/graphene oxide nanocomposites for removal of cadmium ions from water. Advances in Natural Sciences: Nanoscience and Nanotechnology 10 (2), 025006.
Tian, S., Gong, Y., Ji, H., Duan, J., Zhao, D., 2020. Efficient removal and long-term sequestration of cadmium from aqueous solution using ferrous sulfide nanoparticles: Performance, mechanisms, and long-term stability. Science of the Total Environment 704, 135402.

Tobaldi, D.M., Tucci, A., Škapin, A.S., Esposito, L., 2010. Effects of SiO_2 addition on TiO_2 crystal structure and photocatalytic activity. Journal of the European Ceramic Society 30 (12), 2481–2490.
Tofa, T.S., Ye, F., Kunjali, K.L., Dutta, J., 2019. Enhanced visible light photodegradation of microplastic fragments with plasmonic platinum/zinc oxide nanorod photocatalysts. Catalysts 9 (10), (819).
Tran, T.V., Nguyen, D.T.C., Le, H.T.N., et al., 2020. Optimization, equilibrium, adsorption behavior and role of surface functional groups on graphene oxide-based nanocomposite towards diclofenac drug. Journal of Environmental Sciences 93, 137–150.
Uddin, M.K., Baig, U., 2019. Synthesis of Co3O4 nanoparticles and their performance towards methyl orange dye removal: Characterisation, adsorption and response surface methodology. Journal of Cleaner Production 211, 1141–1153.
Ulucan-Altuntas, K., Debik, E., Ustundag, C.B., Guven, M.D., Gocen, K.A., 2020. Effect of visible light on the removal of trichloromethane by graphene oxide. Diamond and Related Materials 106, 107814.
Vajedi, F., Dehghani, H., 2019. The characterization of TiO_2-reduced graphene oxide nanocomposites and their performance in electrochemical determination for removing heavy metals ions of cadmium (II), lead (II) and copper (II). Materials Science and Engineering: B 243, 189–198.
Verliefde, A.R., Heijman, S., Cornelissen, E., et al., 2007. Influence of electrostatic interactions on the rejection with NF and assessment of the removal efficiency during NF/GAC treatment of pharmaceutically active compounds in surface water. Water Research 41 (15), 3227–3240.
Verma, B., Balomajumder, C., 2020. Magnetic magnesium ferrite–doped multi-walled carbon nanotubes: An advanced treatment of chromium-containing wastewater. Environmental Science and Pollution Research 1–11.
Virkutyte, J., Varma, R.S., 2014. Greener and sustainable remediation using iron nanomaterials. In: In: Sharma, V.K., Chang, S.-M., Doong, R.-A., Wu, C.-H. (Eds.), Green Catalysts for Energy Transformation and Emission Control, vol. 1184, American Chemical Society, pp. 1–21.
Vörösmarty, C.J., Green, P., Salisbury, J., Lammers, R.B., 2000. Global water resources: Vulnerability from climate change and population growth. Science 289 (5477), 284–288.
Wang, C., Xu, B.-Q., Wang, X., Zhao, J., 2005. Preparation and photocatalytic activity of $ZnO/TiO_2/SnO_2$ mixture. Journal of Solid State Chemistry 178 (11), 3500–3506.
Wang, H., Keller, A.A., Li, F., 2010. Natural organic matter removal by adsorption onto carbonaceous nanoparticles and coagulation. Journal of Environmental Engineering 136 (10), 1075–1081.
Wang, H., Keller, A.A., Clark, K.K., 2011. Natural organic matter removal by adsorption onto magnetic permanently confined micelle arrays. Journal of Hazardous Materials 194, 156–161.
Wang, Z., Lin, T., Chen, W., 2020. Occurrence and removal of microplastics in an advanced drinking water treatment plant (ADWTP). Science of the Total Environment 700, 134520.
Wang, Q., Song, X., Tang, S., Yu, L., 2020. Enhanced removal of tetrachloroethylene from aqueous solutions by biodegradation coupled with nZVI modified by layered double hydroxide. Chemosphere 243, 125260.
Wang, M., Xu, Z., Hou, Y., et al., 2020. Photo-Fenton assisted self-cleaning hybrid ultrafiltration membranes with high-efficient flux recovery for wastewater remediation. Separation and Purification Technology 249, 117159.
Wang, L., Xu, H., Qiu, Y., et al., 2020. Utilization of Ag nanoparticles anchored in covalent organic frameworks for mercury removal from acidic waste water. Journal of Hazardous Materials 389, 121824.
Wang, D., Zeng, F., Hu, X., Li, C., Su, Z., 2020. Synthesis of a magnetic 2D Co@NC-600 material by designing a MOF precursor for efficient catalytic reduction of water pollutants. Inorganic Chemistry 59 (17), 12672–12680.
Wang, P., Shi, Q., Shi, Y., et al., 2009. Magnetic permanently confined micelle arrays for treating hydrophobic organic compound contamination. Journal of the American Chemical Society 131 (1), 182–188.
Wang, S., Sun, H., Ang, H.M., Tadé, M.O., 2013. Adsorptive remediation of environmental pollutants using novel graphene-based nanomaterials. Chemical Engineering Journal 226, 336–347.
Wang, W., Hua, Y., Li, S., Yan, W.;, Zhang, W.-x., 2016. Removal of Pb (II) and Zn (II) using lime and nanoscale zero-valent iron (nZVI): A comparative study. Chemical Engineering Journal 304, 79–88.
Wang, Y., Ma, J., Zhu, J., et al., 2016. Multi-walled carbon nanotubes with selected properties for dynamic filtration of pharmaceuticals and personal care products. Water Research 92, 104–112.
Wang, J., Zhang, P., Liang, B., et al., 2016. Graphene oxide as an effective barrier on a porous nanofibrous membrane for water treatment. ACS Applied Materials & Interfaces 8 (9), 6211–6218.
Wang, Y., Pan, C., Chu, W., Vipin, A.K., Sun, L., 2019. Environmental remediation applications of carbon nanotubes and graphene oxide: Adsorption and catalysis. Nanomaterials 9 (3), (439).
Wei, A., Ma, J., Chen, J., et al., 2018. Enhanced nitrate removal and high selectivity towards dinitrogen for groundwater remediation using biochar-supported nano zero-valent iron. Chemical Engineering Journal 353, 595–605.
Wei, G., Yu, H., Quan, X., et al., 2014. Constructing all carbon nanotube hollow fiber membranes with improved performance in separation and antifouling for water treatment. Environmental Science & Technology 48 (14), 8062–8068.
Weinberg, H., Galyean, A., Leopold, M., 2011. Evaluating engineered nanoparticles in natural waters. Trends in Analytical Chemistry 30 (1), 72–83.
Wen, Z., Zhang, Y., Dai, C., 2014. Removal of phosphate from aqueous solution using nanoscale zerovalent iron (nZVI). Colloids and Surfaces A: Physicochemical and Engineering Aspects 457, 433–440.
World Health Organization, 2019. Progress on Household Drinking Water, Sanitation and Hygiene 2000-2017: Special Focus on Inequalities. World Health Organization.
Wu, L.-K., Wu, H., Zhang, H.-B., et al., 2018. Graphene oxide/$CuFe_2O_4$ foam as an efficient absorbent for arsenic removal from water. Chemical Engineering Journal 334, 1808–1819.
Xia, Z., Zhao, Y., Darling, S.B., 2021. Covalent organic frameworks for water treatment. Advanced Materials Interfaces 8 (1), 2001507.
Xian, G., Zhang, G., Chang, H., et al., 2019. Heterogeneous activation of persulfate by Co_3O_4-CeO_2 catalyst for diclofenac removal. Journal of Environmental Management 234, 265–272.
Xiao, C., Lin, J., 2020. PAMPS-graft-Ni 3 Si 2 O 5 (OH) 4 multiwalled nanotubes as a novel nano-sorbent for the effective removal of Pb (II) ions. RSC Advances 10 (13), 7619–7627.
Xiao, J., Yue, Q., Gao, B., et al., 2014. Performance of activated carbon/nanoscale zero-valent iron for removal of trihalomethanes (THMs) at infinitesimal concentration in drinking water. Chemical Engineering Journal 253, 63–72.
Xiao, J., Gao, B., Yue, Q., Gao, Y., Li, Q., 2015. Removal of trihalomethanes from reclaimed-water by original and modified nanoscale zero-valent iron: Characterization, kinetics and mechanism. Chemical Engineering Journal 262, 1226–1236.
Xiao, Y., Ma, C., Jin, Z., et al., 2021. Functional covalent organic framework illuminate rapid and efficient capture of Cu (II) and reutilization to reduce fire hazards of epoxy resin. Separation and Purification Technology 259, 118119.
Xu, J., Avellan, A., Li, H., et al., 2020. Sulfur loading and speciation control the hydrophobicity, electron transfer, reactivity, and selectivity of sulfidized nanoscale zerovalent iron. Advanced Materials 32 (17), 1906910.

Xu, L., Gao, X., Li, Z., Gao, C., 2015. Removal of fluoride by nature diatomite from high-fluorine water: An appropriate pretreatment for nanofiltration process. Desalination 369, 97–104.
Xu, L., Yang, L., Johansson, E.M.J., Wang, Y., Jin, P., 2018. Photocatalytic activity and mechanism of bisphenol a removal over TiO2−x/rGO nanocomposite driven by visible light. Chemical Engineering Journal 350, 1043–1055.
Xu, R., Zhang, P., Wang, Q., et al., 2019. Influences of multi influent matrices on the retention of PPCPs by nanofiltration membranes. Separation and Purification Technology 212, 299–306.
Xu, Y., Liu, T., Zhang, Y., et al., 2017. Advances in technologies for pharmaceuticals and personal care products removal. Journal of Materials Chemistry A 5 (24), 12001–12014.
Xu, Z., Yu, Y., Liu, H., Niu, J., 2017. Highly efficient and stable Zr-doped nanocrystalline PbO2 electrode for mineralization of perfluorooctanoic acid in a sequential treatment system. Science of the Total Environment 579, 1600–1607.
Xue, A., Yuan, Z.-W., Sun, Y., Cao, A.-Y., Zhao, H.-Z., 2015. Electro-oxidation of perfluorooctanoic acid by carbon nanotube sponge anode and the mechanism. Chemosphere 141, 120–126.
Yanez, H., Wang, J.E., Lege, Z., et al., 2017. Application and characterization of electroactive membranes based on carbon nanotubes and zerovalent iron nanoparticles. Water Research 108, 78–85.
Yang, C.-H., Chang, J.-S., Lee, D.-J., 2020. Covalent organic framework EB-COF:Br as adsorbent for phosphorus (V) or arsenic (V) removal from nearly neutral waters. Chemosphere 253, 126736.
Yang, S., Shao, D., Wang, X., et al., 2015. Design of chitosan-grafted carbon nanotubes: Evaluation of how the–OH functional group affects Cs+ adsorption. Marine Drugs 13 (5), 3116–3131.
Yang, Y., Qiao, S., Jin, R., Zhou, J., Quan, X., 2019. A novel aerobic electrochemical membrane bioreactor with CNTs hollow fiber membrane by electrochemical oxidation to improve water quality and mitigate membrane fouling. Water Research 151, 54–63.
Yang, S.Y., Vecitis, C.D., Park, H., 2019. Electrocatalytic water treatment using carbon nanotube filters modified with metal oxides. Environmental Science and Pollution Research 26 (2), 1036–1043.
Yang, X., Huang, G., An, C., et al., 2021. Removal of arsenic from water through ceramic filter modified by nano-CeO2: A cost-effective approach for remote areas. Science of the Total Environment 750, 141510.
Yazdi, F., Anbia, M., Salehi, S., 2019. Characterization of functionalized chitosan-clinoptilolite nanocomposites for nitrate removal from aqueous media. International Journal of Biological Macromolecules 130, 545–555.
Yentür, G., Dükkancı, M., 2020. Synthesis of visible-light heterostructured photocatalyst of Ag/AgCl deposited on (040) facet of monoclinic BiVO4 for efficient carbamazepine photocatalytic removal. Applied Surface Science 531, 147322.
Yogi, C., Kojima, K., Wada, N., et al., 2008. Photocatalytic degradation of methylene blue by TiO_2 film and Au particles-TiO_2 composite film. Thin Solid Films 516 (17), 5881–5884.
Yu, W., Luo, M., Yang, Y., et al., 2019. Metal-organic framework (MOF) showing both ultrahigh As (V) and As (III) removal from aqueous solution. Journal of Solid State Chemistry 269, 264–270.
Yuan, S., Li, X., Zhu, J., et al., 2019. Covalent organic frameworks for membrane separation. Chemical Society Reviews 48 (10), 2665–2681.
Zarrabi, H., Yekavalangi, M.E., Vatanpour, V., Shockravi, A., Safarpour, M., 2016. Improvement in desalination performance of thin film nanocomposite nanofiltration membrane using amine-functionalized multiwalled carbon nanotube. Desalination 394, 83–90.
Zebardast, M., Fallah Shojaei, A., Tabatabaeian, K., 2018. Enhanced removal of methylene blue dye by bimetallic nano-sized MOF-5s. Iranian Journal of Catalysis 8 (4), 297–309.
Zeng, X., Wang, G., Liu, Y., Zhang, X., 2017. Graphene-based antimicrobial nanomaterials: Rational design and applications for water disinfection and microbial control. Environmental Science: Nano 4 (12), 2248–2266.
Zenobio, J.E., Modiri-Gharehveran, M., de Perre, C., Vecitis, C.D., Lee, L.S., 2020. Reductive transformation of perfluorooctanesulfonate by nNiFe0-Activated carbon. Journal of Hazardous Materials 397, 122782.
Zha, S., Cheng, Y., Gao, Y., et al., 2014. Nanoscale zero-valent iron as a catalyst for heterogeneous Fenton oxidation of amoxicillin. Chemical Engineering Journal 255, 141–148.
Zhang, W., Liu, C., Wang, L., et al., 2019. A novel nanostructured Fe-Ti-Mn composite oxide for highly efficient arsenic removal: Preparation and performance evaluation. Colloids and Surfaces A: Physicochemical and Engineering Aspects 561, 364–372.
Zhang, F., Tang, X., Huang, Y., Keller, A.A., Lan, J., 2019. Competitive removal of Pb2+ and malachite green from water by magnetic phosphate nanocomposites. Water Research 150, 442–451.
Zhang, W., Zhang, D., Liang, Y., 2019. Nanotechnology in remediation of water contaminated by poly-and perfluoroalkyl substances: A review. Environmental pollution 247, 266–276.
Zhang, D.Q., Zhang, W.L., Liang, Y.N., 2019. Adsorption of perfluoroalkyl and polyfluoroalkyl substances (PFASs) from aqueous solution - A review. Science of the Total Environment 694, 133606.
Zhang, Q.-Q., Zhu, Y.-J., Wu, J., Dong, L.-Y., 2019. Nanofiltration filter paper based on ultralong hydroxyapatite nanowires and cellulose fibers/nanofibers. ACS Sustainable Chemistry & Engineering 7 (20), 17198–17209.
Zhang, Y., Chen, Y., Westerhoff, P., Hristovski, K., Crittenden, J.C., 2008. Stability of commercial metal oxide nanoparticles in water. Water Research 42 (8), 2204–2212.
Zhao, C., Xu, Y., Xiao, F., et al., 2021. Perfluorooctane sulfonate removal by metal-organic frameworks (MOFs): Insights into the effect and mechanism of metal nodes and organic ligands. Chemical Engineering Journal 406, 126852.
Zhao, H., Gao, J., Zhao, G., et al., 2013. Fabrication of novel SnO_2-Sb/carbon aerogel electrode for ultrasonic electrochemical oxidation of perfluorooctanoate with high catalytic efficiency. Applied Catalysis B: Environmental 136–137, 278–286.
Zhao, Z., An, H., Lin, J., et al., 2019. Progress on the photocatalytic reduction removal of chromium contamination. The Chemical Record 19 (5), 873–882.
Zhou, T., Liang, Q., Zhou, X., Luo, H., Chen, W., 2021. Enhanced removal of toxic hexavalent chromium from aqueous solution by magnetic Zr-MOF@ polypyrrole: Performance and mechanism. Environmental Science and Pollution Research 1–13.
Zhou, Y., Apul, O.G., Karanfil, T., 2015. Adsorption of halogenated aliphatic contaminants by graphene nanomaterials. Water Research 79, 57–67.
Zhuang, S., Chen, R., Liu, Y., Wang, J., 2020. Magnetic COFs for the adsorptive removal of diclofenac and sulfamethazine from aqueous solution: Adsorption kinetics, isotherms study and DFT calculation. Journal of Hazardous Materials 385, 121596.
Zuo, Q., Jin, R., Ma, J., Cui, G., 2014. China pursues a strict water resources management system. Environmental Earth Sciences 72 (6), 2219–2222.